University of Southampton

Faculty of Engineering and Physical Sciences

School of Civil Engineering and the Environment

Geotechnical Properties of High Organic Content Waste

by

Abdulaziz Ibrahim Almohana

Thesis for the degree of Doctor of Philosophy

June 2019

University of Southampton

Abstract

FACULTY OF ENGINEERING AND PHYSICAL SCIENCES

SCHOOL OF CIVIL ENGINEERING AND THE ENVIRONMENT

Thesis for the degree of Doctor of Philosophy

THE GEOTECHNICAL PROPERTIES OF HIGH ORGANIC CONTENT WASTE

by

Abdulaziz Almohana

High organic content waste has a significant effect on the physical and hydrological properties of waste. Therefore, understanding the properties of waste is considered key for landfill designers, and operators. This study presents the results of laboratory tests with regard to the physical properties, settlement, compressibility and hydraulic conductivity of different high organic synthetic municipal solid waste (MSW) matters under different loads simulating burial in a landfill.

Eight different test samples were tested under compression in saturated and unsaturated conditions using a Rowe cell reactor. The saturated tests were used to examine changes in terms of physical and hydrological properties of MSW in order to obtain an understanding of the effect of organic materials (food waste). The goal of the unsaturated test samples was to investigate leachate produced from waste itself. In this regard, food waste was classified into two different groups: loose bound water (LBW) and strong bound water (SBW).

The results show a significant correlation between organic content and the geotechnical and hydrological properties and compressibility of MSW as the organic fraction of MSW dropped by 20%, 40% and 60%. The results indicated that the amount of water released greatly varied according to moisture content, material structure and type of food waste (LBW and SBW). The relationship between settlement and leachate production has been highlighted in this study.

A conceptual model of the release of bound water in relation to the applied stress of mixed waste run under saturated conditions was developed in this study. The conceptual model spreadsheet consists of two variables, namely, input and calculated variables. The input variables comprise the results obtained from the experimental work using a Rowe cell. Meanwhile, the calculated variables are obtained using equations proposed for the conceptual model to determine the change in food-trapped liquid occurring with increased vertical stress. In this regard, a numerical function of the volume fraction of trapped liquid was proposed; this function can be read by the LDAT model. The results obtained from the conceptual model spreadsheet and the LDAT model were compared. The findings showed that the trapped liquid of different high-organic-content waste types has a critical impact on the water released ratio gradient, which increases with the organic fraction in MSW.

Table of Contents

List of Tables

List of Figures

Research Thesis: Declaration of Authorship

Print name:	Abdulaziz Ibrahim Almohana

Title of thesis:	Geotechnical Properties of High Organic Content Waste

I declare that this thesis and the work presented in it are my own and has been generated by me as the result of my own original research.

I confirm that:

1. This work was done wholly or mainly while in candidature for a research degree at this University;
2. Where any part of this thesis has previously been submitted for a degree or any other qualification at this University or any other institution, this has been clearly stated;
3. Where I have consulted the published work of others, this is always clearly attributed;
4. Where I have quoted from the work of others, the source is always given. With the exception of such quotations, this thesis is entirely my own work;
5. I have acknowledged all main sources of help;
6. Where the thesis is based on work done by myself jointly with others, I have made clear exactly what was done by others and what I have contributed myself;
7. None of this work has been published before submission:

Signature:		Date:	

Acknowledgements

بسم الله الرحمن الرحيم

In the Name of Allah, the Most Gracious, the Most Merciful

First, all praises due to Allah Almighty for giving me help, strength, and patient to complete this thesis.

I would like to express my sincere gratitude to my supervisors Professor David Richard and Dr Anne Stringfellow for their guidance, encouragement, and continues support through the research period. Without their support and patient, this project would never been completed. Both my supervisors were not only supportive but also assisted me in grasping the requirements of scientific research and how to think as a researcher. I should always remember and grateful for their support and time they gave me.

I would like also to thank our technicians Harvey Skinner, and Ms. Pilar Pascual for their assistance in setting up my experimental work and solving the problems regarding my devises and reactors.

I am very grateful to Professor James White for his valuable comments, help, and support for the modelling work.

My indebted appreciation and love go for my parents, brothers, and sisters for their unlimited support, patience and moral support which has had a positive impact to complete this thesis.

My warm thanks to my grandmother who can not see my personal gratitude as she passed away during my journey, hope you know that your son just finished his study, my sincere call to be in a better life now.

Last but not least, the biggest thank and my personal gratitude to my beloved wife Moneera (Tootah) for her patience and support during my difficult journey and my lovely daughter Alia who was born eight months before the end of this journey.

Definitions and Abbreviations

M_{wet}^{0}	Initial weight of wet mass
M_{wet}	Weight of wet mass
M_{dry}	Weight of mass after drying
W_{dry}	Moisture content based on the dry weight
W_{wet}	Moisture content based on the wet weight
PSD	Particle size distribution
V	The total volume of the waste in the reactor
H	The depth of the sample in Rowe cell
ρ_{dry}	Dry density
ρ_C	Density of cellular material
ρ_S	Specific gravity
ρ_{wet}	Bulk density
ρ_{SP}	Density of non-food solid particles
ρ_L	Density of liquid
e	Void ratio
n_0	Initial total porosity
n	Total porosity
C_c	Primary compression index

SBW	Strong bound water
LBW	Loose bound water
VS	Volatile solid
ρ_s	Specific gravity
V_v	Volume of voids
V_s	Volume of solids
BMP	Biochemical methane potential
TS	Total solid
SMC	Saturated moisture content
c_v	Coefficient of consolidation
m_S	Mass of non-food solids
m_T^0	Initial mass of trapped liquid
m_e	Unrecorded mass detected as a result of mass balance
m_C	Mass of cellular material
m_{res}	The mass of liquid remaining in the cell after the sample was unloaded
m_D	Mass of drained liquid
v_p	Volume of particles
v_F	Volume of free liquid occupying the pore space
v_F^0	Initial volume of pore water occupying pore space

v_G	Volume of gas occupying the pore space
m_F^f	Mass of free pore liquid remaining in the sample at the end of the test
M_{wet}^f	Mass of the wet sample after the test
v_C	Volume of cellular material
v_S	Volume of solid particles
v_T^0	Volume of initial trapped liquids within the cellular structure of the food waste
v_T	Volume of trapped liquid
v_F^0	Initial pore-water volume
Δv_F	The change in quantity of free pore space
v_F^f	Final pore-water volume
α_T	Volume fraction of the trapped liquids
$\emptyset_i$	Ratio of initial water released
$\emptyset_f$	Ratio of final water released

Chapter 1 Introduction

1.1 Background

landfill has been and continues to be the primary method and perhaps, the most convenient option for the disposal of municipal solid waste (MSW) in many countries (Abdul et al., 2014; Britz et al., 1990; El-Fadel et al., 1999; Feng et al., 2017; Yigit et al., 2012). However, physical, chemical and biological processes (biodegradation of MSW) inside the landfill may pose significant environmental risks in terms of gas emissions and release of leachate leading to the potential contamination of the ground and receiving groundwater (Abdul et al., 2014; Al-arifi et al., 2013; Baawain and Al-futaisi, 2013; Rastogi et al., 2014).

Landfill settlement should be considered seriously, because it will continue even after the landfill site has been closed, affecting the safety of the landfill and efficiency of the capping system (Benson et al., 2007; Elagroudy et al., 2008; Mehta et al., 2002). The settlement rate is related to the waste stabilisation and plays an important role in predicting the void space and volume reduction influencing the initial landfill levels. The main objective of using the conventional landfill is to contain waste and reduce the environmental impacts, associated with leachate production and gas emissions (Hossain et al., 2009). Thus, conventional landfill techniques aim to minimise the infiltration of water into waste and increase the landfill lifetime and monitoring after-care (Chiemchaisri et al., 2002; Gawande et al., 2003; Hossain et al., 2009).

An understanding of the hydraulic and physical properties, settlement, degree of degradation and compressibility of MSW are critical for the design and operation requirements of a landfill. While there is an extensive body of research into these aspects of MSW, studies on the impact of high organic content of MSW on these properties are relatively rare. MSW contains substantial organic materials which contribute to the complex behaviour and instability of landfills. In less developed countries, the organic content (mainly food waste) are high compared with developed countries. This may be because there is more recycling and inert waste diversion. Thus, the leachate produced from MSW containing high organic material (mainly food waste) is significantly abundant due to the high moisture percentage of organic content. This feature justifies further study, particularly for landfill in semi-arid regions that are engaged in developing modern waste management practices.

A search of available literature revealed that the effects of high organic content on key engineering properties of a landfill have received little attention. There is evidence that regions which are now trying to develop waste management systems, particularly in arid regions such as Riyadh, are experiencing difficulties in managing and treating leachate from these wastes, which have to date not been investigated in the literature. Therefore, the examination of hydraulic and physical properties, settlement, degree of degradation and compressibility is extremely important to help in landfill design in countries which have high organic content wastes. In this study, a comprehensive investigation will be conducted into the hydraulic and physical properties, settlement, biodegradation and compressibility of wastes with a high percentage of organic content, using waste at Alsuly landfill, Riyadh as a case study.

1.2 Objective of the study

The aim of this study is to understand the impact of high organic content waste on physical hydrological properties, with the Alsuly landfill in Riyadh, SA being a case study. The results of this work will be applicable to other arid regions, where waste composition is classified as high organic content waste and leads to the generation of large leachate volumes of high strength. The objectives of this investigation are concerned with the engineering characteristics of MSW, which directly stem from its high organic content and composition. This study addresses the following specific objectives:

1. To establish relationships between waste composition and the water balance, water content, bulk density, dry density, saturated moisture content and bulk leachate quality parameters of high organic MSW under differentially applied stresses

2. To establish relationships between waste composition and the permeability, specific gravity, total porosity and void ratio of high organic MSW under differentially applied stresses

3. To investigate the effect of vertical stresses on the water contained in food waste (known as bound water)

4. To link waste bound water and the mechanism of water release during compression and decomposition processes

5. To investigate the effect of decomposition on the release of bound water from food waste.
6. To consider the implications of leachate control and landfill management at Alsuly landfill
7. To develop a conceptual model that can be used to predict the bound water released from different mixed waste compositions which can be used in a numerical model such as LDAT model.

Chapter 2 Literature review

2.1 Introduction

This literature review contains an evaluation of the hydraulic and physical properties, settlement, biodegradation and compressibility of MSW in the landfill. Despite a wide body of research on the geotechnical properties of MSW landfills, there are still wide gaps in our knowledge of the above-mentioned aspects of MSW with high organic contents under different loads.

2.2 Physical characteristics of MSW

It has been shown that the properties of MSW can be defined by simple parameters and are therefore applied to estimating leachate composition and gas generation potential when landfilled. These properties include waste composition, water content, particle size distribution (PSD), dry density, bulk density and saturated moisture content.

2.3 Waste composition

According to EU Directive (1999), MSW is defined as 'waste from households, as well as other waste which, because of its nature or composition, is similar to waste from households'. Thus, MSW usually contains organic materials (e.g. food and garden waste), plastic, paper and metals. MSW composition varies from country to country because of life habits, degree of recycling and recovery and waste management practices (Hudson, 2007; Karak et al., 2012). Table 2-1 shows the typical MSW characteristics and compares the MSW compositions between the developed and less developed countries.

Table 2-1: MSW composition for Riyadh compared with other countries (expressed as percentage of total wet weight).

Components (%)	Typical MSW (Landva and Clark, 1990)	Upper middle income countries (World Bank, 2012)	Riyadh (Saudi Arabia) (Hoy, 2014)	Africa (World Bank, 2012)	Latin America (World Bank, 2012)	Organisation for Economic Co-operation and Development (OECD)
Organic	5–42	54	57.2	57.0	54.0	27.0
Paper	20–55	14	7	9.0	16.0	32.0
Plastic	2–15	11	13.0	13.0	12.0	11.0
Glass	2–15	5	3.0	4.0	4.0	7.0
Metal	6–15	3	2.4	4.0	2.0	6.0
Other	-	13	16.6	13.0	12.0	17.0

It can be seen from Table 2-1 that the MSW composition in Riyadh is similar to other less developed countries, with high levels of organic materials and low levels of inorganic materials. This finding agrees with that of Ziyang et al. (2015) who identified that the low-income countries normally have higher proportions of organic waste compared with the developed countries.

Liu et al. (2015a) also demonstrated that the MSW in the less developed countries normally has high levels of kitchen waste content (more than 40%).

2.3.1 Water content

Waste moisture characteristics are considered important factors in the long-term behaviour of MSW. Normally, moisture content is reported on the basis of dry weight (Rose et al., 2008). The following points illustrate the importance of studying the moisture characteristics of MSW (Chiemchaisri et al., 2002; Di Bella et al., 2012; Nas et al., 2014); these include

- influencing the amount of leachate produced,
- determining the performance of leachate recirculation system, and
- providing a suitable design of an effective leachate collecting system.

The MSW moisture content in the landfill plays an important role in accelerating the rate of waste biodegradation and thus decreasing the stabilisation period and landfill lifetime (Alkaabi et al., 2009; Benbelkacem et al., 2010). Many factors affect the moisture content in landfilled MSW, such as the climate at the site, the season of the year and the co-disposal of liquid waste (Chu et al., 1994; Sanphoti et al., 2006). Management of the landfill also affects moisture content of the landfilled waste. Ojuri et al. (2012) examined the moisture content of three different waste compositions, classified as high percentage of soil-like materials (36%, 54% and 81%) at different depths (0.8 m, 1.4 m and 2 m, respectively). They found that the moisture content increased to 18%, 32% and 50.6%, respectively, as the depth increased from 0.8 m, 1.4 m and 2 m, respectively. The increase in the moisture content may be related to the soil content and landfill depth.

The moisture content can also be correlated with the type of organic waste (e.g. food or garden waste) (Ahmadifar et al., 2015). Zhao et al. (2009) reported that the moisture content of waste with 57% organic waste fraction was 44%. Staub et al. (2009) found that the initial volumetric moisture content of the different types of waste of varying percentages of organic content (36% and 58% by wet weight) was 21% (v/v) and 39% (v/v), respectively. Gao et al. (2015) claimed that MSW with high kitchen waste content (HKWC) (over 40%) was normally characterised by higher initial water content, as opposed to low kitchen waste content (LKWC) (less than 40%). This finding echoes that reported by Ahmadifar et al. (2015) who announced that the moisture content of high organic fraction waste (78.9%) ranged between 60–65%.

In addition, moisture content within the range of 50–60% is considered the optimum practical range for enhancing the methanogenesis phase in MSW (Gurijala and Suflita, 1993). The moisture content of each waste category is presented in Table 2-2. As Table 2-2 illustrate, the moisture content of food waste is high, which contributes to the high moisture content of waste with high organic content (Chen et al., 2010).

Table 2-2: Moisture content of each waste category (Burnley, 2007)

Components	Moisture content %
Organic	56
Paper	20
Dense plastic	1
Plastic film	3
Ferrous metals	1
Non-ferrous metals	0
Combustibles	10
Non-combustibles	1
Garden waste	55.2
Glass	0
Hazardous household	13.0
Textiles	1

2.3.2 Particle size distribution (PSD)

MSW is a heterogeneous mixture and consists a wide range of particle sizes. There are many factors that affect the particle size of landfill waste, such as the waste composition processing of solid waste (shredding), and the degree of waste decomposition. The reduction of the particle size of MSW might make MSW more homogenous. PSD of waste has a significant impact on the degree of decomposition, permeability and biodegradation (Gavelyte et al., 2015; Reddy et al., 2011; Staub et al., 2009a).

According to Durmusoglu et al., (2006), hydraulic conductivity increase when particle size increases, which is consistent with Gavelyte et al., (2016)and Staub et al.'s (2009) findings. In their study, Gavelyte et al.,(2016) concluded that the highest hydraulic conductivity in waste experiments was likely to occur when the size of the particles was 100 mm, and the hydraulic conductivity near these values was 9.20×10^{-6} m/s. In contrast, the lowest hydraulic conductivity in waste was likely when

particle size was approximately 5 mm; this value is approximately equal to 2.10 x 10^{-6} m/s. Staub et al., (2009) found that the hydraulic conductivity of different particle sizes (70 mm and 40 mm) was 5.61 × 10^{-5} m/s and 3.34 × 10^{-5} m/s, respectively.

It is important to note the PSD changes within the depths of the landfill. Compared with the shallow depth of the landfill, PSD seems to be smaller at the greater depth. The change of PSD within the landfill depth may be attributed to the degree of waste decomposition, which is higher at greater depths. Reddy et al. (2011) studied the PSD of different types of organic content wastes (57.5%, 40.2%, 38.9%, 28.6%, and 15.5%) with varying degrees of decomposition (0%, 50%, 53%, 70%, and 86%, respectively). They found that PSD decreased in tandem with increases in the degrees of waste decomposition (Figure 2-1). Reddy et al. (2009a) also studied the PSD of fresh and landfilled waste (1.5 years old) containing about 78% and 61% organic content, respectively. They found that the percentages of waste particle passing a 20-mm sieve for fresh and landfilled samples were 20 and 35 (by wet weight), respectively.

Gaining insights into the relationship between waste composition, water content and particle distribution is necessary for understanding the factors involved in waste with high organic content. The PSD of fresh waste with high organic content needs further investigation in order to learn about the effects of particle size on physical properties such as settlement, compressibility and hydraulic conductivity.

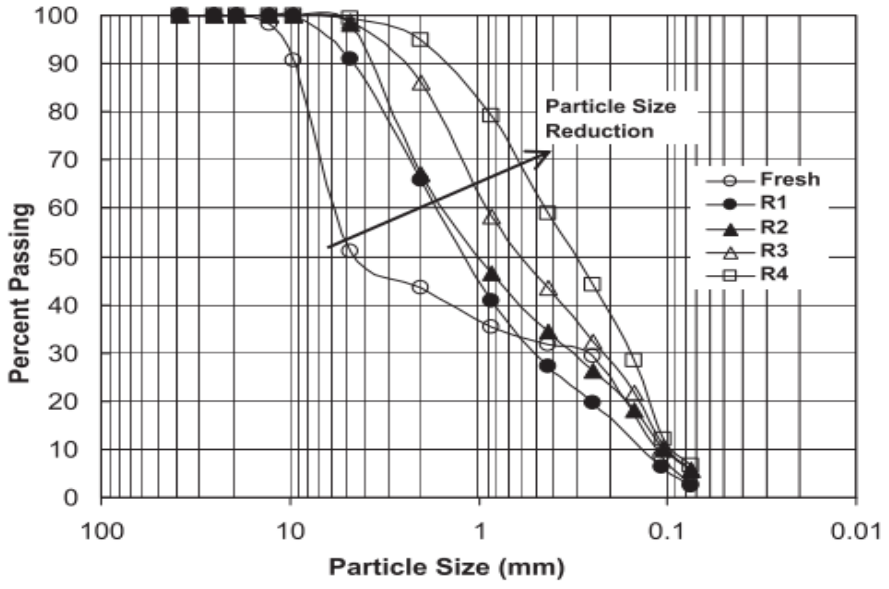

Figure 2-1: Correlation between PSD and the degree of waste decomposition (Reddy et al., 2011).

2.3.3 Dry density (ρ_{dry}) and bulk density (ρ_{wet})

Dry density can be determined by dividing the dry mass of the solid waste (M_{dry}) by the volume of waste (V_i) in the reactor. Bulk density (ρ_{wet}) is defined as the ratio of the total mass of waste ($\mathrm{M_{wet}}$), including moisture content (W_{dry}) to the volume of waste in the reactor.

Tchobanoglous et al. (1993) stated that the dry density of MSW can vary from 180–800 kg/m^3, depending on the degree of waste compaction in the landfill site. Density may also vary based on waste composition, water content and degree of waste compaction. Waste density is a necessary factor to determine the permeability of the organic content and as such determines the relationship between waste composition and water content. In this study where MSW contains high organic content, the relationship between density and hydraulic conductivity needs further investigation to help us determine the impact of high organic content on density and hydraulic conductivity.

2.4 Hydraulic properties

The hydraulic properties of MSW are very important parameters, since they describe the factors that can influence moisture flow within waste. Hydraulic properties include hydraulic conductivity, void ratio and total porosity.

2.4.1 Hydraulic conductivity (permeability)

The hydraulic conductivity of waste describes the movement of fluid and its distribution through waste (Dixon and Jones, 2005; Powrie et al., 2005; Fleming, 2011). The hydraulic conductivity of various porous media is measured using a permeameter (Gavelyte et al., 2015; Reddy et al., 2011; Staub et al., 2009b; Tiwari, 2014). In engineering terms, a permeameter is a simple column that has an inlet and outlet. In a situation where the inlet has a higher hydraulic head relative to the outlet, the flow will be from the inlet to the outlet (Durmusoglu et al., 2006; Gavelyte et al., 2015; Reddy et al., 2011).

It is important to note that several primary factors affect the hydraulic conductivity of MSW, and these include waste composition, moisture content, porosity, degree of compaction, density, overburden pressure and particle size. These influencing factors will be discussed and the relationship between waste composition, water content and permeability (hydraulic conductivity) of different organic contents under different loads will be examined below.

2.4.2 Influence of vertical stress on the hydraulic conductivity of waste

Waste hydraulic conductivity is an important factor in landfill design, as it influences the leachate pressure distribution in the waste body, which is found to affect the existing magnitude and the distribution of the effective stresses and the shear strength (Dixon and Jones, 2005). Powrie and Beaven (1999) found that the quantification of the geotechnical behaviour and hydraulic properties of landfill waste is complex, which is partly due to the variability, degradability and deformability nature of waste constituents; it is also partly because the material is frequently in an unsaturated state with phases of gaseous, solid and liquid present. Powrie et al., (2005) conducted a study into different types of waste and found that the hydraulic properties of waste may change in tandem with effective stress. During the study, they carried out an investigation to determine the influence of vertical stress on hydraulic conductivity of crude, unprocessed household waste; their experimental results revealed that waste hydraulic conductivity tended to decrease by about four order of magnitude with the vertical stress increasing from 30 kPa to 500 kPa (which is equivalent to the 50-m depth of landfill) (Figure 2-2). Reddy et al., (2009a) and Feng et al., (2016) also suggest a similar relationship. Reddy et al. (2009) examined the relationship between hydraulic conductivity and the vertical stress of freshly shredded MSW, using large-scale rigid-wall permeameters. They reported that the hydraulic conductivity was 2×10^{-3} m/s, when the vertically applied stress was zero, and then it decreased to 4.9×10^{-7} m/s under the maximally applied normal stress of 276 kPa. Feng et al. (2016) studied the geotechnical properties of MSW from different depths, ranging from 4 m (21.9% of organic matter) to 16 m (degraded waste and 16% of organic matter). They reported that hydraulic conductivity ranged between 4.6×10^{-4} and 6.7×10^{-3} m/s in these samples. They noted that hydraulic conductivity decreased as the depth increased, where waste material becomes denser, leading to a decreased density and porosity among the deeper layers. Powrie et al., (2005) observed a correlation between the growing effective stress and the diminishing hydraulic conductivity in the first loading. The differences in hydraulic conductivity emanating from waste degradation and the reduction of particle size are basically second order, although they seem to gain more prominence at higher vertically effective stress levels.

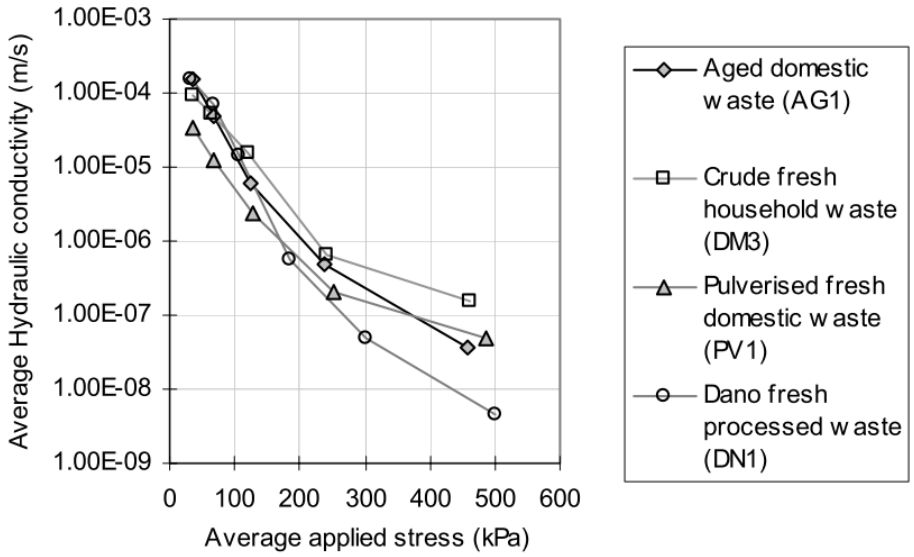

Figure 2-2: Correlation between the average applied stress and average hydraulic conductivity (Powrie et al., 2005).

Based on the above-mentioned studies, it can be shown that increasing waste depth (i.e. increasing the overburdening of stress) can lead to a decrease in waste permeability. Waste that contains high organic content may have a substantial influence on conductivity, because such waste may be more compressible than waste with lower of organic content.

2.4.3 Relationship between hydraulic conductivity and density

Powrie et al. (1999) measured the hydraulic conductivity of unshredded household MSW as a function of both density and stress; they showed that hydraulic conductivity decreased in tandem with an increase in density (Table 2.3). Reddy et al., (2009a) and Stoltz et al., (2010) confirmed the results found by Powrie et al. (1999). Reddy et al. (2009a) used shredded fresh waste, obtained from the Orchard Hills landfill, to study the effect of density on hydraulic conductivity; they showed that, as a result of increase in vertical stress, hydraulic conductivity decreased while density increased. Stoltz et al. (2010) also showed that hydraulic conductivity tended to diminish in tandem with an increase in both compression and waste density. Using a small permeameter device, Tiwari (2014) studied the relationship between hydraulic conductivity and the dry density of fresh waste, obtained from the City of Denton landfill in the United States; they reported that hydraulic conductivity decreased from 2.76×10^{-4} to 2.60×10^{-8} (m/s), when the dry density increased from 374.70 (kg/m^3) to 714.30 (kg/m^3).

Various authors such as Durmusoglu et al. (2006), Gavelyte et al. (2015) and Powrie et al. (1999) collated data from both the laboratory and field-based sites on the hydraulic conductivity of waste. They found that the hydraulic conductivity of waste ranged from 1 x 10^{-3} m/s to 1 x 10^{-9} m/s, although values typically tend to vary between 10^{-3} and 10^{-8} m/s. A summary of the results of hydraulic conductivity and density is shown in Table 2-3.

Table 2-3: MSW hydraulic conductivity from previous studies.

Sources	**Dry density** (kg/m^3)	**Hydraulic conductivity** $(^m/_s)$	**Test type**
Reddy et al. (2009)	410- 1330	$2 \times 10^{-3} \; - \; 4 \times 10^{-7}$	Constant head
Stoltz et al. (2010)	600 – 900	$1 \times 10^{-4} \; - \; 1.1 \times 10^{-5}$	Constant and falling head
Powrie and Beaven (1999)	390 – 720	$1.5 \times 10^{-4} - \; 3.7 \times 10^{-8}$	Constant head
Hossain et al. (2009)	700	$8.8 \times 10^{-5} - \; 1.3 \times 10^{-5}$	Constant head
Tiwari (2014)	374 – 714	$2.76 \times 10^{-4} - \; 2.60 \times 10^{-8}$	Constant head

In a number of large-scale tests on the hydraulic conductivity of waste, performed in Pitsea compression cell, Powrie and Beaven (1999) observed that the relationship between dry density, hydraulic conductivity and average vertical stress appeared to be well defined, although the relationships were different for individual types of waste. They used the Pitsea compression cell (2-m diameter) to test the relationship between the vertical stress and dry density of crude, unprocessed MSW. They reported that the density increased from 0.32 Mg/m^3 at zero average vertical stress to 0.72 Mg/m^3 under average vertical stress of 600 kPa (Figure 2-3). In addition, the hydraulic conductivity decreased from 1.5 × 10^{-5} m/s to 2.7 × 10^{-8} m/s, as the vertically applied stress increased from 40 kPa to 600 kPa, respectively (Figure 2-4). Bleiker et al., (1995) and Stoltz

et al., (2010) indicated that permeability decreases when compression increases, which implies that the density of waste components affects waste permeability.

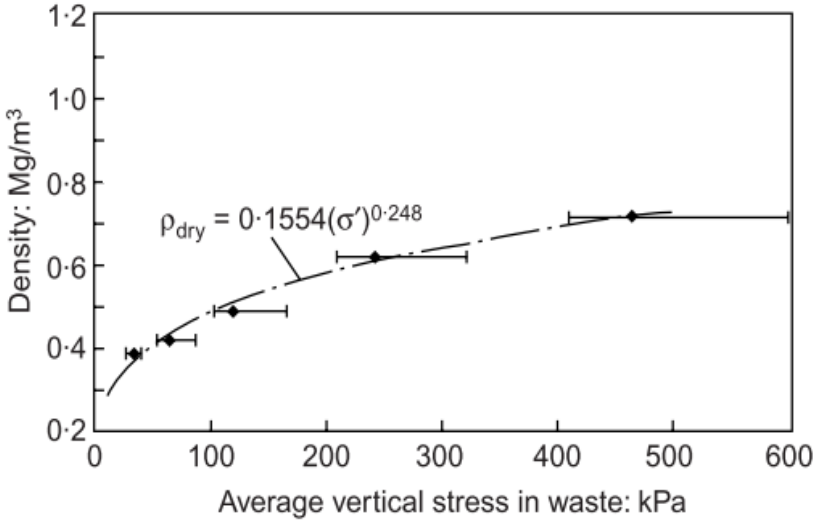

Figure 2-3: The variations of dry density under different average vertical stresses (Powrie and Beaven, 1999).

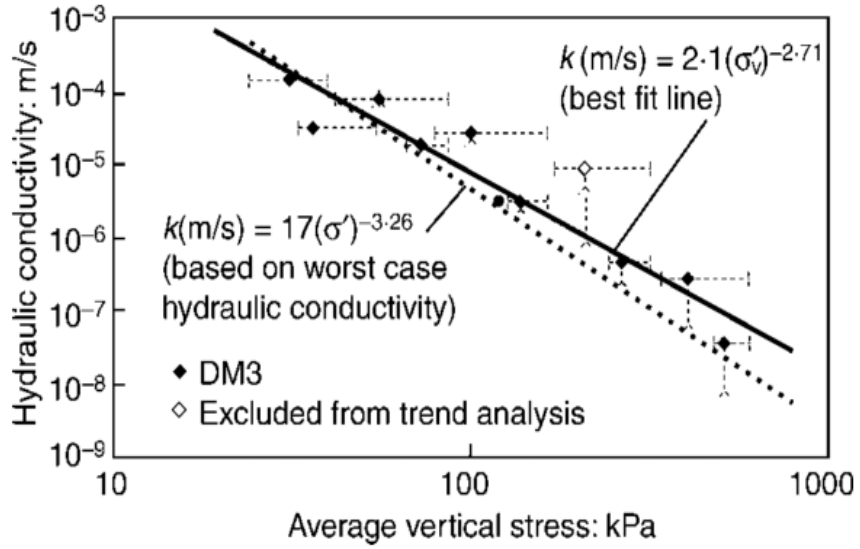

Figure 2-4: The relationship between hydraulic conductivity under different average vertical stresses (Powrie and Beaven, 1999).

2.4.4 Total porosity (n)

Total porosity is defined as the total volume of pores divided by the total volume of solids. Many factors may influence total porosity, such as waste composition, vertical stress and the particle size of MSW. Increased vertical stress increases the dry density and therefore decreases the total porosity of waste, causing a reduction in hydraulic conductivity (Gavelyte et al., 2015; Hudson et al., 2004; Powrie and Beaven, 1999; Staub et al., 2009). The fraction of organic content has a significant influence on the initial total porosity where the high organic content waste has a higher initial total porosity (Zhao et al., 2012). Liu et al. (2015) examined total porosity under 50 kPa of fresh MSW and degraded MSW (30 days and 60 days) comprising organic content of 83.5% (50% of food material), 55.1%, and 22.6%, respectively. They discovered that total porosity decreased from 55.9% to 51.4% and 48.6% for fresh MSW and degraded MSW, respectively.

Powrie and Beaven (1999) also used the Pitsea compression cell (1D compression test) to study the impact of the vertical load on the drainable porosity of crude domestic waste (i.e. unprocessed and undegraded waste) and household waste (obtained direct form the tipping face of a landfill) ; they learnt that the drainable porosity of crude domestic waste decreased from 14.7% to 1.5% when the applied stress (kPa) increased from 40 kPa to 600 kPa, and the drainable porosity of household waste declined from 14.4% to 1.5 % when the applied stress increased from 34 kPa to 463 kPa. Tiwari (2014) also found that drainable porosity was influenced by the increase in dry density. Using a small-scale permeameter device, he reported that the drainable porosity of fresh MSW decreased from 36.20% to 2.90% when the dry density increased from 281.90 to 714.30 (kg/m^3). Staub et al. (2009) used a cell 20 cm in diameter and 30 cm in length to measure the hydraulic conductivity and the effective drainable porosity of two different types of waste (A and B) obtained from two French landfill sites. The main difference between samples A and B is that the organic content was 36.6% and 58.1%, respectively. Also, the average bulk density of samples A and B were 700 and 780 kg/m3. They concluded that as the dry density increased, the effective porosity decreased, which tended to limit the vertical hydraulic conductivity (Figure 2-6). However, the number of tests applied was not sufficient to draw a strong conclusion about the relationship between porosity and hydraulic conductivity.

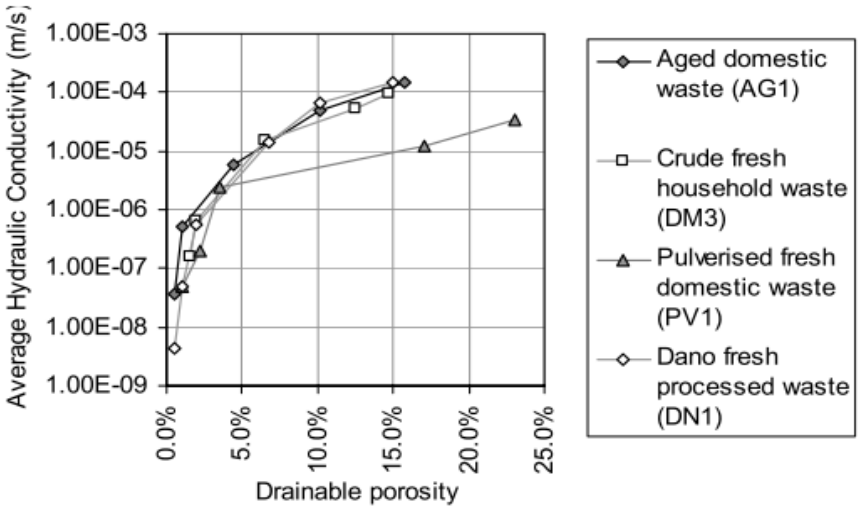

Figure 2-5: Correlation between hydraulic conductivity and drainable porosity (Powrie et al., 2005)

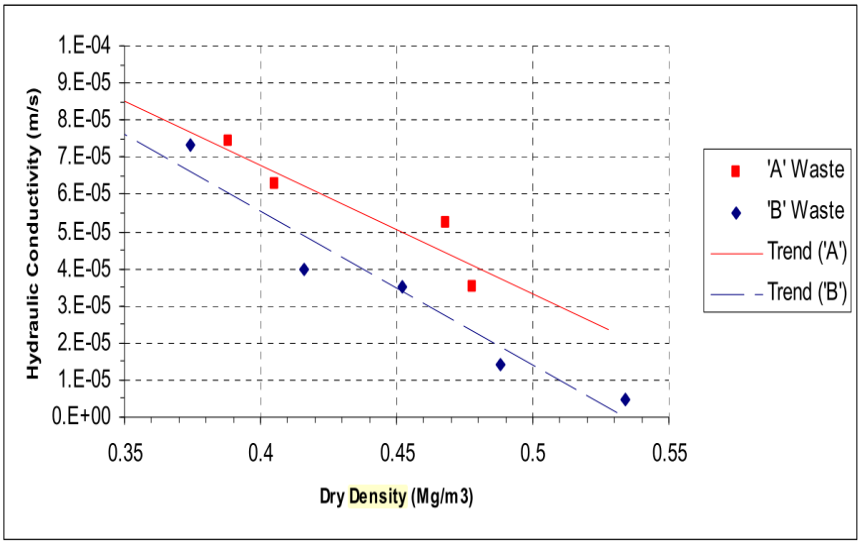

Figure 2-6: Correlation between hydraulic conductivity and dry density (Staub et al., 2009)

2.4.5 Void ratio (e)

The void ratio is an important parameter for evaluating MSW compressibility (Feng et al., 2016). MSW is considered a heterogeneous material that has a considerably high compressibility, depending on waste composition and degradation process (Basha et al., 2016; Feng et al., 2016; Tiwari, 2014). High organic content waste gets easily compressed under vertical stress, which will increase density and lower the void ratio (Dixon and Jones, 2005; Reddy et al., 2009a; Zhao et al.,

2012). Zhao et al. (2012) who studied the impact of stress on the void ratio of different waste compositions with HKWC (i.e. 53.40%, 46.73% and 40.05%). In their research, they found that, at the initial stage (zero kPa), the initial void ratio were 4.26, 3.67 and 3.26, as the food fraction declined from 53.40%, 46.73% and 40.05%, respectively. A high reduction of the void ratio at 400 kPa was also observed for a high organic content waste (53.40%), where the void ratio increased from 0.94, 1.19 and 1.45, as the food portion decreased from 53.40%, 46.73% and 40.05%, respectively.

In their study on the effect of MSW age on the void ratio, Feng et al., (2016) discovered that the void ratio of different samples with organic content of 22.3% , 21.9%, 18.2%, and 16% decreased to 2.41, 2.29, 2.16 and 1.95, as the MSW age increased from 0 , 0.3, 2 and 4 years respectively. The reduction in the void ratio can be attributed to the degradation process, which causes the breakdown of the waste structure, hence, the reduction in particle size resulting in a reduction in the void ratio (Machado et al., 2010). The impact of the varying fractions of high organic content waste on void ratio requires more investigation to deepen our understanding of MSW compressibility.

2.5 Landfill settlement

The prediction of landfill settlement has been considered an important factor in designing and maintaining landfills, helping to estimate landfill capacity as well as designing the gas and leachate extraction system (El-Fadel and Khoury, 2000; Elagroudy et al., 2008). Landfill settlement stems from a decrease in the void ratio of waste, mainly because of the biodegradation processes and load application, leading to a reduction in the volume of refuse (El-Fadel and Khoury, 2000; Siddiqui et al., 2012). Siddiqui (2011) stated that the majority of settlement occurred immediately after applying the vertical load before biodegradation occurred. In addition, the variations in MSW settlement can be related to waste composition, where the settlement of higher organic content waste is considerably greater than low organic content waste (Bae and Kwon, 2017; Elagroudy, 2013); this may be attributed to compressibility, which is considered greater for high organic content waste. In addition, in a high organic content waste, a relatively greater proportion of the waste is removed due to decomposition processes, than in a low organic content waste which results to enhance the settlement rate (Chen et al., 2010; Heshmati R et al., 2014; Swati and Joseph, 2008).

In this study, the water released during primary settlement is considered an important parameter, mainly because of the high moisture content of different types of high organic content waste. In this regard, a distinction is required to be made between the released water and the settlement in MSW with varying fractions of high organic content.

2.5.1 Stages of settlement in MSW landfill

Settlement in MSW landfill may be divided into three distinct stages: (a) initial settlement, (b) primary settlement and (c) secondary settlement (Morris and Woods, 1990). Initial settlement refers to the settlement that occurs after applying an external load to waste; it is the result of compaction between void spaces and particle sizes of waste. Primary settlement occurs when water and gas are withdrawn from the void, mainly because of load application. Secondary settlement happens due to the biological decay of waste and mechanical creep (El-Fadel et al., 1999; Hossain et al., 2003; Ivanova, 2007; Siddiqui, 2011); the time needed to complete the secondary settlement may not be available for several years (El-Fadel et al., 1999; Siddiqui et al., 2012).

2.5.2 Previous studies related to waste settlement

Zeiss et al. (1995) studied the relationship between settlement and waste decomposition by operating six laboratory test cells. Three cells were used as control cells to simulate the dry landfill, and the other three cells were operated as the bioreactor landfill (enhanced cells) over a period of 225 days. The initial settlement after load application was observed to be 17% and 26% for the control and enhanced cells, respectively; further observations were made for the primary settlement of 15% for the enhanced cells and 12% for the control cells and the secondary settlement of 4% for the enhanced cells and 2% for the control cells. Siddiqui et al., (2012) compared mechanically biologically treated (MBT) waste and raw waste, studied by Ivanova (2007) at 50 kPa. They reported that, due to the mechanical creep, total settlement for both MBT and raw waste was 5.09% and 13.9%, respectively. The difference in settlement between these waste types may be attributed to the removal of compressible material from MBT waste during the treatment. Olivier et al. (2007) presented the results of a laboratory experiment, in which MSW was subjected to a vertical stress of 130 kPa. The primary and secondary settlement results reported after a period of two years were found to be 25.4% and 23.9%, respectively. Elagroudy (2013) studied the impact of different waste compositions (100% paper, 100% textile and 100% mixed waste) on settlement. The mixed waste contained 40% paper, 40% textiles, and 20% food waste. The food waste

comprised a mixture of vegetables, rice, chicken bones, and macaroni. In addition, the paper and textiles were shredded to a particle size of 100–150 mm. The author discovered that the percentages reduction on final settlement were 18.5%, 8.3% and 20.9%, respectively; the high reduction observed in 100% mixed waste may be because of the high fraction of organic materials. However, high organic content waste may behave significantly differently, which may be demonstrated by an experimental programme.

Based on the literature review of MSW settlement, the waste composition plays an important role regarding the waste settlement where the high organic content waste is more likely to compress due to the presence of food wastes. In this regard, most of the literature has not deeply characterised the organic waste in terms of types of food wastes. Thus, this study characterised the food waste to understand how this type of waste effects settlement.

2.5.3 Compression index (C_c)

The compression index (C_c) can be used to estimate the primary settlement. The one-dimensional consolidating test (Rowe cell) can be used to determine the compressibility of MSW (Hossain et al., 2003; Landva, Valsangkar, & Pelkey, 2000). As noted above, the compression of MSW leads to reduction in the void ratio and porosity; hence, the reduction will have an impact on the density and permeability of waste. The data obtained from the compression test can be used to estimate the primary settlement of MSW. There is a clear link between the waste organic content and compression index where an increase in the organic content of MSW causes an increase in the compression index (Elagroudy, 2013), which is consistent with the results reported by Zhao et al. (2012). Zhao et al. (2012) used a large oedometer test apparatus (50 cm in diameter and 30 cm in length) to study the compression properties of waste with varying kitchen waste fractions. They observed that the C_c scores were 1.29, 0.96 and 0.47 as the percentage of food waste declined from 53%, 47% and 40%. The differences between the compression results may be attributed to the differences in waste composition as well as the apparatus used. Similarly, Elagroudy, (2013) investigated the C_c of three different waste compositions: R1 (100% paper), R2 (100% textile) and R3 (40% paper, 40% textile and 20% mixed waste). The paper and textiles were shredded to a particle size of 100–150 mm. In addition, the food waste was a mixture of vegetables, rice, chicken bones, and macaroni. They found that the C_c scores were 0.451, 0.309 and 0.625 for R1, R2 and R3, respectively. The high C_c scores for R3 may be linked to the high organic content waste that exists in R3 and different particle size.

Durmusoglu et al. (2006) examined the compression characteristics of MSW by using small and large-scale consolidometer tests of MSW, obtained from the landfills in Brazos country, Texas. In the small-scale consolidation tests, the particles with a size greater than 0.5 cm were excluded from the MSW samples. The particle sizes used in the large-scale consolidometer were smaller than 2.0 cm. They determined that the C_c scores were 0.475 and 0.904 for the small- and large-scale consolidometer test, respectively. The differences in C_c results may be explained by the varying particle sizes between the comparatively small and uniform ones in the small-scale consolidometer test compared with those in the large-scale consolidometer test. The authors did not characterise the waste compositions, mainly because the majority of them were not visually identified; hence, it is difficult to understand the extent to which this may have influenced compressibility. Machado et al. (2002) used triaxial compression tests to study the correlation between the C_c and void ratio of 15-year-old waste (55% paste, comprising soil and organic matter; 17% plastic; 10% stone; 2% paper; 3% textile; 5% metal; 2% glass; 2% rubber and 4% wood. They revealed that C_c is relatively lower for a lower MSW void ratio, ranging between 0.52 and 0.920 at vertical stress between 60 and 640 kPa. Few examples have concentrated on the influence of waste with high organic content. Therefore, further investigation is required to evaluate the compressibility properties of waste compositions with different portions of organic waste, particularly concerning HKWC associated with landfilled wasted in the developing countries. A brief summary of the range of published values of C_c for MSW is presented in Table 2.4.

Table 2-4: Summary of published values of C_c for MSW

Source	**% organic content**	$\boldsymbol{C_c}$
Zhao et al. (2012)	53% - 40%.	1.29 - 0.47
Elagroudy, (2013)	R1 (100% paper), R2(100% textile), R3(40% paper, 40% textile)	0.451- 0.625
Durmusoglu et al. (2006)	Not identified	0.475 - 0.904
Machado et al. (2002)	55%	0.52 - 0.920

2.6 Biological characteristics of MSW

MSW contains organic components, which may be degraded by microbes through biological reactions and converted to biogas under anaerobic conditions (e.g. Alvarez-Vazquez et al., 2004; Kjeldsen et al., 2002a). MSW biodegradation processes in the landfill have been widely studied by numerous researchers who concluded that the biodegradation processes proceed through five distinct phases (L. K. Ivanova, 2007; Kjeldsen et al., 2002b; Rastogi et al., 2014; Sang et al., 2012; Siddiqui et al., 2012; Warith et al., 2005). The characteristics of leachate and landfill gas vary, depending on the landfill age, compositions of the initial waste and the phases of MSW degradation in the landfill. The phases of MSW degradation in the landfill (Figure 2-7) are as follows.

Initial phase (aerobic). This phase occurs immediately after placing MSW in the landfill. In this phase, the biological decomposition initiates in the presence of oxygen in the voids (Rastogi et al., 2014). The organic materials, which are easily degradable by biological decomposition, are converted into carbon dioxide.

Transition phase. In this phase, the landfill converts from aerobic to anaerobic conditions due to the depletion of oxygen. In addition, at the end of this phase, an increase in the concentration of volatile fatty acids (VFAs) and chemical oxygen demand (COD) occurs, mainly because of two major processes, hydrolysis and acidogenesis, which occur at this stage.

Acid formation phase. Acidogenic bacteria dominate this phase, and the biological activities convert the biodegradable organics into volatiles. Furthermore, in this phase, the leachate composition is characterised as VFAs, which reach their peak concentration when pH reaches its lowest value in the leachate (4.5–7.5). The outcome at the end of this stage are high concentrations of VFAs, carbon dioxide and hydrogen as well as a low pH value.

Methane formation phase. Methanogenic bacteria dominate this phase. Around 50–60% of the gas composition in this stage is methane gas (Warith et al., 2005). There is a relationship between methane generation, VFA concentration and pH value. As the methane generation increases, the VFA concentration begins to decrease, and the pH value rises (Rastogi et al., 2014). Moreover, the removal of heavy metals occurs in this phase by precipitation (Warith et al., 2005; Rastogi et al., 2014).

Maturation phase. In this phase, the gas production rate decreases, mainly because of shortages in nutrients and the biodegradation of substrate materials. At this stage, the concentration of leachate remains steady at low concentration values.

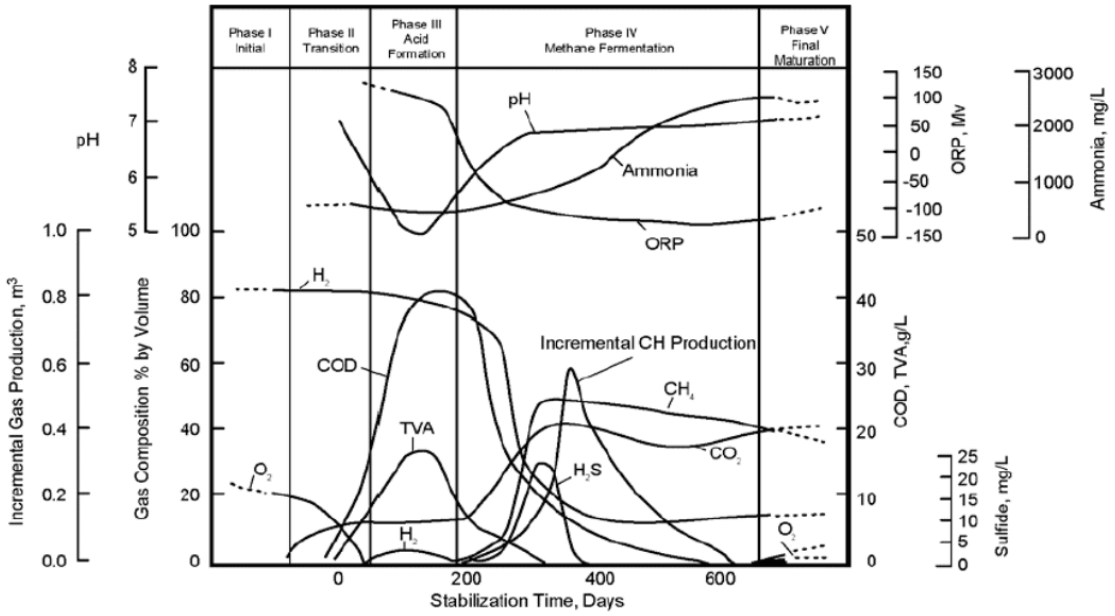

Figure 2-7: Phases of MSW decomposition and stabilisation (Zanetti, 2008)

2.7 Landfill leachate

Leachate is defined as the liquid that is produced through the precipitation of water onto the refuse inside the landfill and the soluble product of the physical, chemical and biological reactions (Myburg and Britz, 1993; Aziz et al., 2010). Landfill leachate usually contains organic materials, inorganic materials, water and heavy metals (Rastogi et al., 2014). A great volume of leachate is produced from high organic content waste, such as food and garden waste (Table 2-2); and in arid regions, this can be the only way to release moisture to form leachate. In the initial stage of decomposition (hydrolysis steps), high organic content (e.g. fruit and vegetables) with lightly bound moisture is easy to be broken down, because they mainly contain sugar, fat, protein and water, which help with moisture release (Eleazer et al., 1997; He et al., 2006). Therefore, the physical and hydrological properties of high organic content waste may differ significantly from low organic content waste especially at the hydrolysis stage. Thus, an in-depth study on the type and fraction of organic waste composition is highly recommended in order to understand the amount of leachate generated from the landfill.

2.8 Bound water of MSW

The leachate generated from the MSW in arid regions due to water ingress might be considered to be low due to the absence of precipitation (Al-Yaqout and Hamoda, 2003; Fourie and Blight, 1999). Thus, the leachate produced from MSW is mainly related to organic materials (e.g. food and garden waste) (Al-Yaqout et al., 2005; Robinson and Grantham, 1988). Safari et al., (2011) stated that the moisture content was about 70% (by dry weight basis) of MSW containing 65% organic material, mainly food waste in the Mashhad landfill, which is considered an arid region. The water content may vary, depending on the type of food waste (e.g. bread or oranges). Water in food materials can exist in two different forms: (a) free water (FW) and (b) bound water (BW) (loose and strong) (Vaclavik, 2008; Kumar et al., 2012; Srikiatden et al., 2017; Caurie, 2011; Khan and Karim, 2017). The amount of bound water released from organic materials mainly depends on the water bond strength within the food material structure(i.e. whether it is FW or BW) (Joardder et al., 2013). FW means that water exists in the intercellular space of food materials. Loosely bound water (LBW) is defined as intracellular and can be extracted by squeezing and pressing, such as tomatoes and oranges. While the strong bound water (SBW) is known as the cell wall water presented in foods, such as bread and cooked rice (SBW) (Figure 2-8) (Devine et al., 2014; Joardder et al., 2013; Khan et al., 2016). The main difference between FW, LBW and SBW is that water migration in FW is less constrained than that in LBW and SBW (Khan et al., 2016).

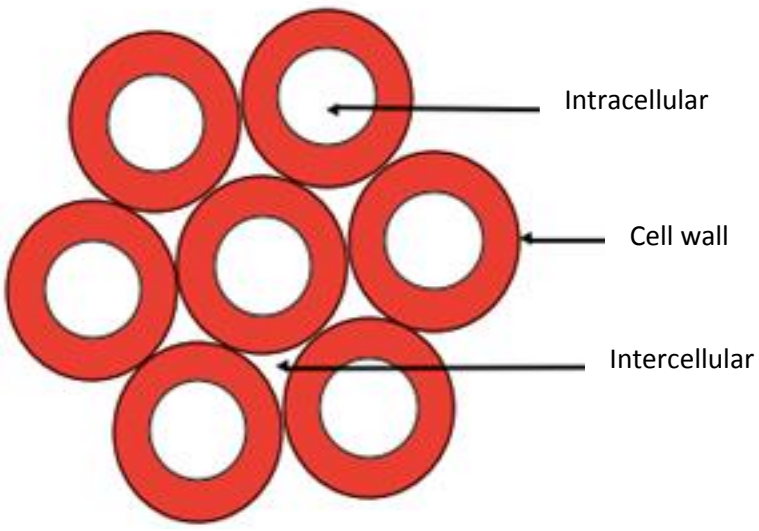

Figure 2-8: Schematic illustration of water distribution inside food materials

The migration of BW (LBW and SBW) can be due to the changes in plant-based food material structure and pore space, while the movement of FW hardly affects the material structure (Joardder et al., 2017; Khan et al., 2018; Raponi et al., 2017). The amount of FW depends on the porosity of the material and how saturated it is, bearing in mind that the porosity of high organic content materials is high. Khan et al. (2016) used proton nuclear magnetic resonance (^{1}H NMR) T2 relaxometry to study the proportions of three types of water (i.e. FW and BW (LWB and SBW)) in different plant-based food materials, such as apples, tomatoes, cucumbers and potatoes. They found that the amount of LBW was about 80–92%, while FW and SBW was 6–16% and 1–6%, respectively. The highest percentage in LBW among these different plant-based food materials was found in cucumbers with a value of about 91.5%. Halder et al. (2011) used the Bioimpedance Analysis Technique and found that the intracellular water content (LBW) of cucumber, tomato, apple and potato was 95.3%, 87.7%, 90.2% and 95.3%, respectively. They studied the SBW of potato under differentially applied pressures, using two different methods: (a) classical pressure plate experiment and (b) liquid extrusion porosimetry (Figure 2-9).

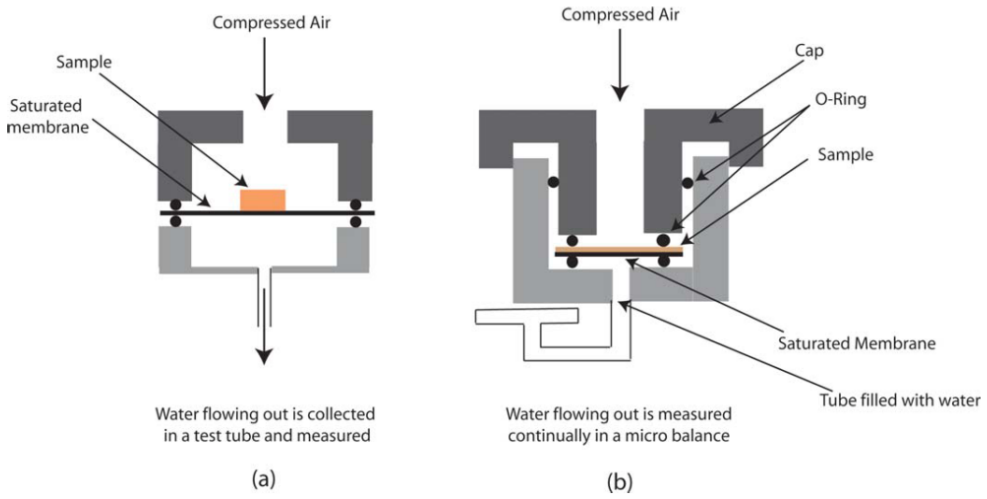

Figure 2-9: A schematic of the experimental setup of different methods: (a) classical pressure plate experiment and (b) liquid extrusion porosimetry (Halder et al. 2011)

The maximum pressure applied for both the classical pressure plate experiment and liquid extrusion porosimetry was 1500 kPa and 700 kPa, respectively. They observed that both these methods only allowed 2% of the water to flow out of the sample at 1500 and 700 kPa for both the classical pressure plate experiment and liquid extrusion porosimetry, respectively. Elsewhere, Prothon et al. (2003) concluded that the migration of LBW (intracellular water) resulted from changes in material

structure, mainly because, during food processing, the water contained in the pore spaces is emptied and filled with air; consequently, the material tissue is no longer capable of maintaining its structure. The principle used for water migration in food processing activities may be applicable to this study, where the moisture content is extracted from the sample through drying or pressing (compaction) (Datta, 2006). A brief summary of the published values of LBW and SBW of different food wastes is presented in Table (2.5).

Table 2-5: A summary of the reported values of different food waste BW

Material	Test	LBW (%)	SBW (%)	Reference
Potato	NMR	81.3 ± 3.8	5.8 ± 2.1	(Khan et al., 2016)
	BIA	95–96		(Halder et al., 2011)
	Classical pressure Plate experiment	—	2	(Halder et al., 2011)
	Liquid extrusion Porosimetry	—	2	(Halder et al., 2011)
Apple	NMR	87.8 ± 4.2	2.5 ± 2.1	(Khan et al., 2016)
	BIA	90–91		(Halder et al., 2011)
Tomato	NMR	87.6 ± 4.6	2.3 ± 4.2	(Khan et al., 2016)
	BIA	95–96		(Halder et al., 2011)
Cucumber	NMR	88.3 ± 3.2		(Khan et al., 2016)
	BIA	95–96		(Halder et al., 2011)

The majority of research on FW and BW has focused on preserving food as well as the amount of water that evaporated during food processing (e.g. drying). There is a lack of information on the correlation between the amount of leachate produced and the composition of organic waste. Therefore, determining the relationship between the production of leachate and types of organic composition is needed, particularly in the less developed modern management practices in landfills such as in Riyadh, where the proportion of organic content appears to be high (Ashebir et al., 2009; Raponi et al., 2017).

2.9 Water release due to organic matter decomposition

The volume of leachate generated from a landfill located in arid region mainly depends on the organic waste fraction, and its production from the landfill is due to two reason: (a) vertical load and (b) decomposition of organic matter. The destruction of food structural tissue is caused by enzyme activity or chemical reactions (Rawat, 2015). Enzymes are the key to degradation and the release of water, particularly from fruit and vegetables (Barth et al., 2009; Holcroft, 2015). The weight loss in fruit and vegetables is attributed to water loss (Holcroft, 2015; Nunes and Emond, 2007).

In addition, the temperature has a direct impact on the weight loss (moisture loss) of fruit and vegetables (Hammond et al., 2015; Nunes and Emond, 2007; Thompson et al., 2008). For instance, Hammond et al. (2015) stated that the food microorganism increases in tandem with an increase in the temperature within the range of 0–40 ^{0}C, while the activity of microbes is zero below the freezing temperature. Thompson et al. (2008) examined the relationship between water loss and the temperature on the market life of products (e.g. cherries). They found that the loss of water after three days was 1.9% and 4.4% as the temperature increased from 0.5 ^{0}C to 20 ^{0}C, respectively, illustrating that the amount of water lost varied depending on temperature generated.

The destruction of food in terms of water loss from fruit and vegetables after harvest has raised concerns about food quality and economic losses (Nunes and Emond, 2007). In addition, the rate of weight loss of fruit and vegetables may vary according to their cellular structure of the materials. For instance, Nunes and Emond (2007) linked some of the weight loss variations in fruit and vegetables to the absence of a natural waxy skin surface. For example, a mushroom is more likely to release water compared with a tomato. They studied the weight loss of fruit and vegetables obtained from a commercial operation in Quebec, Canada or in Gainesville, FL. The researchers

performed the experiments at 20 ^{0}C, with humidity ranging from 85% to 95%, using clamshells or plastic baskets, with 3–18 days' running time depending on the product. The weight loss and quality of fruit and vegetables were evaluated daily until they were considered unacceptable for sale. The results showed that the highest weight loss among the fruit and vegetables selected belonged to mushrooms (after 7 days) and peaches (after 14 days), where the weight loss was 57% and 25%, respectively. In contrast, the lowest weight loss was observed in tomato (2.5%, after 14 days) and blueberry (3%, after 12 days).

Respiration rate plays an important role in shortening the biochemical process (D'Aquino et al., 2016; Fagundes et al., 2015; Valentinuzzi et al., 2018). A high respiration rate of the fruit and vegetables that contain about 90% of water occurs when they are harvested, leading to the growth of microbes, diminished water content, and change in quality (Rickman et al., 2007). The impact of atmospheric packaging on the extended shelf life of food materials has been investigated by many researchers (e.g. Bovi et al., 2018; Chandra et al., 2018; Fagundes et al., 2015). Fagundes et al. (2015) studied the effect of modified atmosphere packing (MAP) on the shelf life of cherry tomatoes. The weight loss of cherry tomatoes (100 grams) under two different atmospheric compositions (i.e. 1–5% O_2 + 5% CO_2 + 90% N_2) modified atmospheric packaging (MAP) and synthetic air (control) was investigated. The experiments ran for 25 days at a temperature of 5 ^{0}C. The results showed that MAP had a positive impact on reducing weight loss compared with the control samples, where the weight loss of cherry tomato for both MAP and control samples were 0.18% and 0.26%, respectively from the initial weight. This confirms the results reported by Chandra et al. (2018) who studied the impact of packaging on radishes, using the following scenarios of packaging treatment: (a) carton paper (control), (b) plastic crates (non-packaging) and (c) packaging with perforated HDPE film. They discovered that after 130 days of storage, the weight loss in the control and non-packaging samples was 10% and 18%, respectively while only 3% a weight loss radishes in packaging with perforated HDPE film. The limited weight loss in packaging with perforated HDPE film might be attributed to high humidity (about 95%).

Elsewhere, Hii et al. (2014) examined the effect of convective air drying on the quality of cooked and raw chicken at different temperatures (i.e. 60, 70 and 80 ^{0}C). They found that the cooked chicken had a lower initial moisture content and dried faster than the raw chicken. The moisture content for both raw and cooked chicken was 2.7 (g water/g dry solid) and 2.0 (g water/g dry solid), respectively. The high moisture content observed in the raw chicken may be connected with the moisture-holding capacity of cooked chicken, which is considered to be lower than that of raw

chicken, mainly because of shrinkage emanating from the loss of inner moisture content during cooking.

To the best of our knowledge, no previous studies have focused on the mechanism of water release from the organic matter, such as fruit and vegetables of landfill MSW. Most of the researches into the weight loss of food waste have been concerned with food preservation in terms of extending the shelf life of the products. Therefore, knowing and understanding the weight loss through moisture loss of organic materials are highly recommended to landfill designers, especially for waste with high organic content, helping them in estimating settlement and the leachate produced.

However, it is important to know that conditions are different in landfill e.g. that higher temperatures and anaerobic degradation may result in different water loss rates to the ambient, aerobic conditions described.

2.10 Models used to predict waste and landfill condition

Numerous studies have been conducted to assess waste condition inside the landfill in a short period (L. K Ivanova, 2007; Siddiqui, 2011). Predicting the physical and hydrological behaviour of waste disposed in the landfill site for a long time seems to be difficult, due to time constraints, the amount of data that needs to be collected and limited availability of resources to collect the data. It is worth noting that knowing the waste condition is necessary in order to adopt the most appropriate remediation. Numerical models (see below) can be important tools for predicting and elucidating the landfill condition. In addition, the use of numerical models provides sufficient analysis to the landfill designer of the physical and hydrological properties of disposed MSW in the landfill site. Nevertheless, these numerical models are very useful for reducing costs and potential errors.

2.10.1 Efficiency of numerical models

Several software programmes are available for landfill modelling. Most of these models assume that users understand landfill behaviour in terms of waste components and period of filling. In 2007, a challenge to the landfill modellers was introduced at the University of Southampton that asked for predicting the performance of laboratory experiments, using two consolidating anaerobic reactors (CARs). The various applications of six groups were compared to assess the performance

in terms of degradation and settlement of MSW (Beaven, 2008). The six different groups of participants facing the challenge were as follows:

1- Golder Associates, UK; GasSim2

2- University of Cantabria, Spain; Moduelo

3- Napier University, UK; HBM

4- Technical University Braunschweig, Germany; POSE

5- University of Southampton, UK; LDAT

6- University of Sao Carlos, Brazil, Gibson and Lo and EPA

Table 2-6: Groups of participants facing the University of Southampton's challenge

Parameters	**GasSim2**	**Moduelo**	**HBM**	**POSE**	**LDAT**	**Gibson and Lo and EPA**
Gas generation	√	√	√	√	√	√
Leachate chemistry	-	√	√	-	√	√
Settlement	-	√	√	√	√	-

GasSim2 is a model that was developed by Golder associates on behalf of the UK Environmental Agency. The model is able to predict the gas produced from laboratory experiments. The drawback of this model is that waste settlement and leachate production can not adjust to the model. The model- based on running Monte Carlo techniques, was aimed at predicting the secondary settlement, where the primary settlement was ignored, while the gas emitted in the related settlement was induced by mechanical creep components (biodegradation and secondary compression).

HBM is a model developed by Napier University. The HBM model aligns biodegradation, mechanical and hydraulic behavior of landfills into a fixed element framework. This pathway is made up of a combination of enzymatic hydrolysis functions which breaks the solid waste substrate down to Monod kinetics and volatile fatty acids to show what the onward conversion into carbon dioxide and methane entails. The waste composition is used to create one single split between inert materials and degradable making them model input parameters. HBM does not need any complicated approach to decide on the material needed for degradation. Wood textiles, paper, combustibles and food are all considered degradable, while yard waste as well as "others" are evenly split between inert and degradable. Every other category is considered inert.

LDAT is a numerical model developed by the University of Southampton. LDAT contains sub-models, which are used to simulate landfill processes in terms of waste degradation, landfill gas production, leachate transport and settlement. LDAT can be used to reproduce the processes occurring in large landfills on a laboratory or field scale with a good degree of accuracy compared with other models in Table 2-6.

These models are not the only models available; many models have been used to predict landfill settlement in order to estimate landfill capacity, leachate collection system, gas extraction and landfill final cover system. A brief discussion of the advantages and disadvantages of these models is presented below.

Edgers et al. (1992). These researchers proposed a waste settlement model, where the settlement in the landfill is characterised by two main stages: (a) mechanical compression and (b) biological processes. The major disadvantage of this model is that the model only deals with the growth kinetics of a single species of bacterial population (methanogens). Another drawback of this model is that it is difficult to determine accurately how the settlement rate increases due to decomposition.

Park and Lee, (2002). These authors proposed a biological model to estimate settlement. They stated that landfill settlement occurs due to the decomposition of biodegradable solid waste, using first-order kinetics. In addition, the model assumed that the settlement of biodegradable refuse was due to the solubilisation from decomposition. The major drawback of this model is that it does not consider the immediate compression after the placement of the waste.

Machado et al. (2002, 2008). These researchers proposed a model to simulate the mechanical behaviour of MSW based on the results from the laboratory, using triaxial compression and the

confined compression of large samples. They assumed that the mechanical behaviour was represented by two different materials: (a) fibrous material and (b) organic paste, according to the coupled elasto-plastic model. Machado et al. (2008) improved the earlier model and considered biodegradation. The loss in mass and fibre changes are caused by organic degradation with time; mass losses are calculated based on the gas produced through a first-order decay model. Although the proposed model covers most of the mechanisms for MSW changes in terms of biodegradation and mechanical behaviours, the large samples required (parameters) make the model difficult to use.

2.11 Landfill degradation model (LDAT)

LDAT is a numerical model that contains sub-models in order to simulate landfill processes in terms of waste degradation, landfill gas production, leachate transport and settlement. LDAT is designed to simulate the anaerobic degradation of solid waste in a saturated condition in order to study the influence of degradation on leachate flow in solid pore spaces. LDAT has been used to support the investigation relating to the physical and hydrological properties of biodegradable solid waste, accelerating landfill stabilisation by using leachate recirculation and aerobic treatment (Hudson et al., 2004; White et al., 2004, ; White, 2008; White and Beaven, 2013; Woodman et al., 2014) . LDAT can be used to simulate the different processes in a large landfill, such as settlement, degradation, hydraulic conductivity, leachate generation and gas production under differentially applied loads. In LDAT, each element has three different boundaries: (a) the upper boundary element, (b) active element and (c) lower boundary element. In the upper boundary element, LDAT allows the user to change the vertical applied stress and measure the gas produced (CH_4 CO_2), while the lower boundary element allows the measurement of leachate produced from waste, opening the lower boundary and allowing leachate to drain out from waste. The active element is responsible for calculating the hydraulic conductivity, dry density, settlement and water content.

The degradation of carbohydrates, fat and protein can be obtained in LDAT by using a chemical pathway. For example, when waste composition is described in LDAT as green waste, food, paper, carton, textile or inert material, LDAT converts these compositions into carbohydrates, fat and protein. In LDAT, the gas produced can be calculated by converting waste to gas through a chemical pathway with a set of stoichiometric equations (White, 2008).

The LDAT model contains three different cases: (a) single element, (b) five-element stack and (c) ten-element stack. These different cases can be used depending on research and laboratory purposes. Furthermore, LDAT allows the user to create their own case. For each case, LDAT allows the user to change and modify the parameters of the active, upper and lower boundary elements; each element has these components (Figure 2-10).

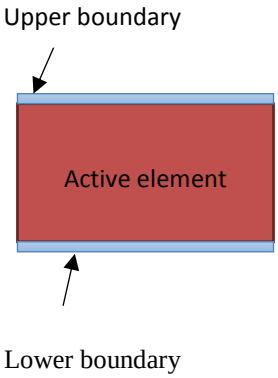

Figure 2-10: A schematic view of the boundaries of a single element in LDAT model

2.12 Summary of the literature review

Hydraulic properties, physical characteristics, settlement, degree of degradation and compressibility of MSW are vital for the design and operation of the landfill. Extensive studies were presented in this chapter concerning the physical properties, hydraulic properties, biodegradation, settlement and compressibility of different types of waste under different loads. The following points capture the essence of this review:

1. Waste composition varies from country to country for many reasons such as life habits, degree of recycling and recovery and waste management.

2. In the less developed countries, the percentage of organic content is much higher than the developed countries.

3. There is a strong correlation between the particle size, waste composition, vertical stress and hydraulic conductivity. Hydraulic conductivity increases when the particle size increases, while high organic content waste has lower hydraulic conductivity than low organic content waste.

4. The relationships discussed do not take into account the effect of waste composition. Waste composition clearly has an important impact on the permeability-density relationship. The previous works do not provide clear indications as what the impact of waste on very high organic waste composition will be in terms of the short- and long-term hydraulic characteristics of waste.

5. The differences in the dry density of MSW depend on many factors, such as waste composition, water content and the degree of waste compaction.

6. The percentage of moisture content of MSW increases significantly with organic content present in MSW.

7. Hydraulic conductivity has a significant impact on the movement of water within waste; it decreases as the vertical stress (overburden pressure) and waste density increases.

8. There is a correlation between total porosity, void ratio and waste composition. This has been shown to apply at organic content up to 53% , but work at higher organic content is needed..

9. Determining landfill settlement is important in landfill design, landfill capacity and leachate extraction systems. It has been shown that the settlement of high organic content waste is high, due to high compressibility, where the materials with high organic content waste are easily compressed compared with low organic content waste.

10. The compression index is directly related to organic content, where the compression index increases in tandem with an increase in the organic content of MSW.

11. The majority of settlement occurs immediately after applying the vertical load and before biodegradation occurs, although high organic content will generate more settlement.

12. FW and BW play important roles in the leachate generated inside the landfill; therefore, understanding how water is released from waste is crucial for the leachate design system. In addition, the linkage between settlement and water released between LBW and SBW needs further investigation.

Chapter 3 Materials and methods

3.1 Introduction

This chapter focuses on the methods used and the experimental work conducted in this study. MSW materials with different organic waste content were analysed to study the effect of high organic content on the hydraulic properties, physical properties, settlement and compressibility of MSW. To accomplish this, the test samples were analysed using one-dimensional compression (Rowe cell test). The samples were tested under saturated and unsaturated conditions depending on the purpose of the experimental study. Each test was done in duplicate to measure the variability of the test results. The composition and characteristics of the test samples in this study were based on waste from Alsuly landfill site, Riyadh, which is described in Section 3.2.

3.2 Site location

The Alsuly landfill is located close to Riyadh city, in the Kingdom of Saudi Arabia (KSA) (

Figure 3-1). The KSA lies in the centre of the Arabian Peninsula. Riyadh is the capital city of the KSA, and has a population of about six million people (General Authority for Statistics, 2010).

Figure 3-1: Overview of the Alsuly landfill in Riyadh city ("Google Maps," 2015).

3.2.1 Riyadh landfill site

Landfill is currently the only way to manage waste in Riyadh city. All waste from different locations in Riyadh is disposed of at the active Alsuly landfill site (Ouda et al., 2013). The landfill is 8 million square metres in area and has been in use since 2006 (HPA, 2015) (Clean.alriyadh.gov.sa). The Alsuly landfill is still using a simple method—dumping waste (Al-Wabel et al., 2011). The daily cover layer (clay) is used to overlay the dumped waste. The base of the Alsuly landfill has a liner (15 cm asphalt) and drainage pipes to collect the leachate produced; there is also a pond to collect the leachate arriving from the drainage pipes. At present, the leachate collected from the bottom of the landfill is pumped again to the top of the landfill, without any treatment or system for maintaining a specific moisture content in the waste.

According to the company responsible for Alsuly landfill, a new landfill has been planned, which is equipped with a gas collection system and leachate treatment plants; high-density polyethylene (HDPE) is going to be placed as a liner at the base of the new landfill. The objective of building a new landfill is to achieve the required wastewater quality standards (Table 3-1). Due to a paucity of information and lack of communication with Alsuly landfill staff regarding the production and concentration of leachate produced from the landfill, this study focuses on the geotechnical properties of high organic content waste.

Table 3-1: Effluent discharge standards of Riyadh MSW after treatment

Parameters[a]	**Effluent discharge standards**
pH	5-9
Colour	Not objectionable
Chemical Oxygen Demand (COD)	< 1000
Biochemical Oxygen Demand (BOD5)	< 50
Chromium	< 0.2
Lead	< 0.2
Copper	< 0.1
Zinc	< 1

Cadmium	< 0.1

[a] All values are in $\frac{mg}{L}$ except pH

3.3 Composition of different types of organic waste

In this research study, eight samples with different waste compositions were tested. For example, the effect of the proportion of non-compressible material, together with organic matter, on the leachate produced was studied in cases 1, 2, 3 and 4. These samples had different percentages of organic matter, in order to understand the effect of organic matter on the geotechnical behaviour and hydraulic properties of landfill waste. The effect of organic waste content on the physical properties, hydraulic conductivity, settlement, and leachate produced and the compressibility of the waste under different loads was examined. Case 5, 6, 7 and 8 were tested to obtain an understanding of the water released from the organic content because, in arid countries, most of the leachate (water) produced inside a landfill is related to the amount of organic content in the waste disposed in a landfill. The type and percentage of waste composition in each sample is described in Table 3-2.

Table 3-2: Percentage and type of waste composition of each sample

Components	Represents the maximum organic content found in Riyadh landfill (%)	Reduced by 20 % from the Riyadh MSW which represents the organic content found in section (3.3.2)	Reduced by 40 % from the Riyadh MSW (intermediate between case 2 and 4)	Reduced by 60 % from the Riyadh MSW (representing a European style waste)	LBW (%)	SBW (%)	50 % SBW and 50 % LBW	45 % SBW and 55 % LBW
Case number	1	2	3	4	5	6	7	8
Organic	73	58	44	29	100	100	100	100
Paper	1	3	4	6	__	__	__	__
Plastic	3	4	6	8	__	__	__	__
Metals	20	22	23	25	__	__	__	__
Glass	2	4	5	7	__	__	__	__
Textile	0.4	2	4	5	__	__	__	__
Carton	1	3	4	6	__	__	__	__

3.3.1 Waste composition of Riyadh MSW

It was not possible to transport Riyadh waste to the UK, so the landfill in Riyadh city was used as the test site to gain a general understanding of the characteristics and composition of the waste found there. Photographs of different types of wastes were taken to characterise the materials because it was difficult to gain access to sort out the waste by hand at the site (Figure 3-2). However, around 20 kg of MSW was collected in order to study the composition, characteristics and particle size distribution (PSD) of the Riyadh MSW. Details of the composition of the waste and mass of each component are shown in Table 3-3.

Figure 3-2: Sample of waste obtained from the Riyadh landfill (04/04/2016)

As illustrated in Table 3-3, the majority of the waste sample by mass was organic materials. This category represents around 73% of the total mass of the waste (wet weight). The second most prevalent category of the sample was metals (19.98%). The percentage of plastic, paper and cartons were 2.77%, 1.06% and 1.05%, respectively.

Table 3-3: MSW components of sample expressed as total weight percentage

Components	(percentage mass content)	Mass of sample from the total mass (grams)
Plastic	2.80	555.00
Carton	1.10	209.00
Paper	1.10	213.00
Metals	20.00	3995.00
Glass	1.90	375.00
Organic materials	73.00	14576.00
Textile	0.40	78.00

3.3.2 Loose bound water (LBW) and Strong bound water (SBW) of Riyadh MSW

Around 570 kg of fresh MSW was obtained and separated to determine the percentage of LBW and SBW in the organic matter (Figure 3-3 and Figure **3-4**). Organic matter comprised around 58% of the total waste. The selection of organic waste with high LBW and SBW was based on the definitions discussed in chapter 2, section 2.8, and the reported values obtained from the literature review (Table 2.5). For example, in organic materials with LBW, such as cucumbers and tomatoes, it is easy to migrate water when vertical stress is applied; however, in food products with SBW, such as rice and bread, water migration is difficult. LBW comprised about 55% of the total organic matter and SBW comprised 45% of the total organic matter. The greater amount of LBW might explain the large volume of leachate that is produced from the landfill, due to it having a high composition of organic waste content. The leachate produced from the LBW and SBW was measured in Rowe Cell tests described in 3.4; results from the tests are discussed in Chapter 4.

Figure 3-3: Photographs taken for the sample of LBW

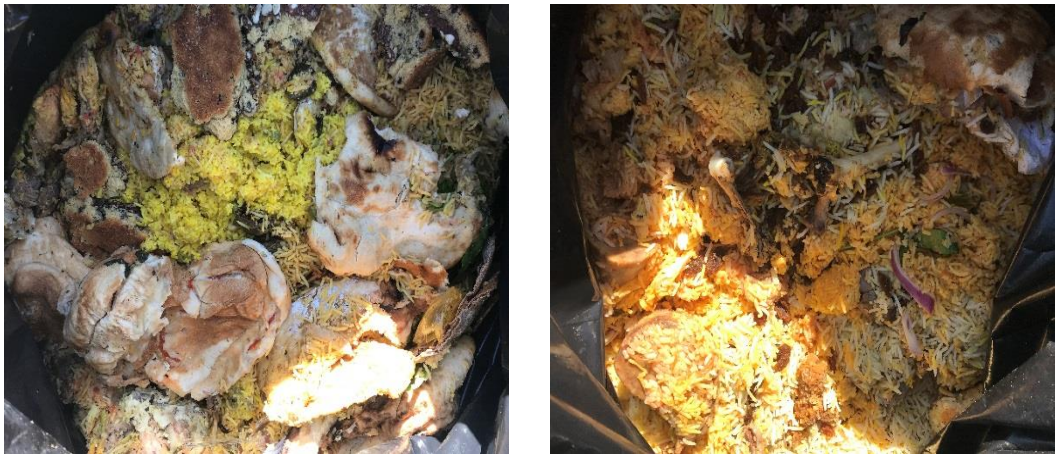

Figure 3-4: Photographs taken for the sample of SBW.

3.4 Apparatus

3.4.1 Rowe cell

In this study, two Rowe cells were used with slightly different diameters. The first Rowe cell (252.3 mm diameter, 100 mm height) manufactured by VJ Technology, an industrial equipment supplier in Reading, England, was used to conduct the tests to analyse water content, settlement, compressibility, and hydrological and physical properties of different high organic wastes (cases 1 - 4). The second Rowe cell (255 mm diameter, 100 mm height) manufactured by the University of Southampton was used to examine the tests investigating the water released from LBW and SBW wastes. The reason of replacing the latter Rowe cell was due to it leaking during the test.

According to British Standard (BS 1377: part 6 [1990]), vertical load can be applied to the test sample using free strain or equal strain. In the free strain method, a flexible rubber diaphragm is used to ensure uniform stress distribution over the surface of the test sample. In the equal strain method, a rigid plate is used to apply pressure to the surface of the test sample to maintain the loaded surface plane during the test. In the current research, one-way vertical load was applied to the sample to measure the effects of vertical load on the permeability, moisture content and settlement of the sample with high organic content. A schematic view of the Rowe cell test is shown in Figure 3-5. The following points summarise the advantages of using a Rowe cell in comparison to the conventional oedometer:

1. Vertical stress can be applied more reliably to the test sample under a different vertical load (up to 1000 kPa).

2. It is easy to measure the drainage and pore water pressure (PWP) at any time during the test.

3. The Rowe cell accommodates a large particle size within the test sample; this improves the reliability of the results.

As shown in Figure 3-5, the Rowe cell apparatus contains the following components: a cover, a base and a Perspex cylinder (255 mm diameter, 100 mm height). A Perspex cylinder allows for visual monitoring during the test. The flexible rubber diaphragm was inserted into the cell cover to deliver the load to the sample by applying water pressure to the top of the flexible rubber diaphragm. To ensure uniform load distribution over the sample, a plastic disc with hole diameters ranging between 5 mm and 3 mm was placed between the sample and the flexible rubber diaphragm. Then, a mesh was placed to prevent the fine particles from escaping through the porous disc. An aluminium spindle was fitted onto the base of the flexible rubber diaphragm by passing it through the centre of the lid and rigid plate. The upper edge of the aluminium was connected to the cover drainage valve. A linear voltage displacement transformer (LVDT) was passed through the centre of the lid to measure the vertical settlement change. The following points describe the three drainage ports (Figure 3-5):

1. The first drainage port is connected to the back pressure valve to measure the liquid volume change.

2. The second drainage port is connected to the PWP transducer to measure the volume of liquid expelled from the outflow valve.

3. The third drainage port is connected to the lower part of diaphragm by the flexible tube passing through the aluminium spindle. Similar to controller two, this controller could indicate changes in the back PWP and the volume of liquid flowing in or out.

4. The fourth drainage port is connected to the flexible diaphragm through the lid and vertical load is applied; the liquid volume used to apply the load is also measured.

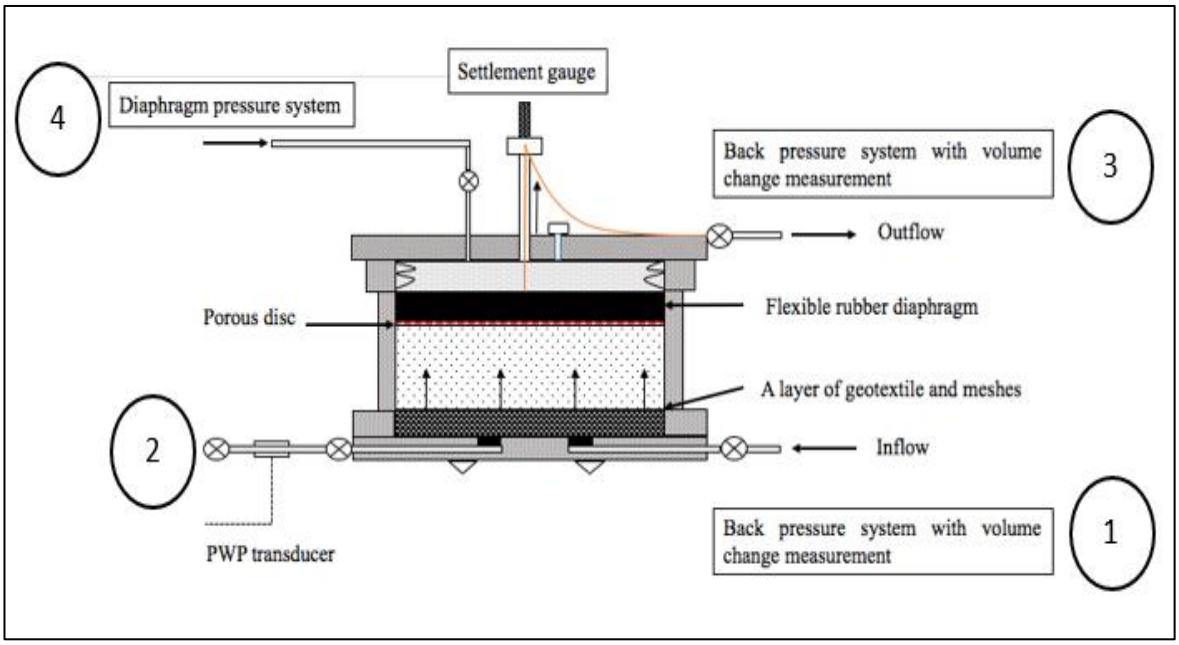

Figure 3-5: Schematic of the Rowe cell test device.

3.4.2 Setting-up the Rowe cell before testing

The following steps were followed to check for and prevent leakage in the Rowe cell before starting the test:

1. The back pressure, base pressure transducer and LVDT were calibrated.

2. The volume/pressure controllers, the pore pressure transducer and the LVDT were connected through a data logger to a computer, running a GDSLAB software consolidation programme (Standard Hydrocon).

3. Silicon grease was applied to the O-rings at the base and lid of the cell.

4. Silicon grease was applied to the base and top of the Perspex cylinder to ensure a good seal between the O-rings and the Perspex cylinder.

5. Deaerator water obtained from a Nold DeAerator was introduced to the Rowe cell. The deaerator water was left for at least 24 hours without any application of pressure to check for any internal or external leaks in the system.

6. The amount of applied pressure was increased to 50 kPa, 150 kPa and 300 kPa, and the same procedure used in the previous step was followed for each applied stress to indicate any possible leaks from the pressure controller pipes and part of the Rowe cell.

7. An incompressible material (metals) (Figure 3.6) was placed below a flexible rubber diaphragm to prove that there were no leaks inside the Rowe cell system. As the vertical applied stress became constant, the volume change of the liquid spent for the application of the vertical stress was stable (constant), which means that the Rowe cell was working well and no leaks were discovered in the system.

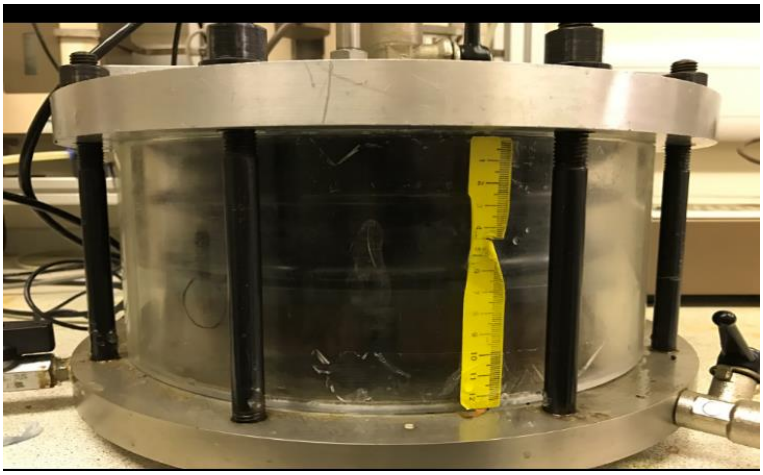

Figure 3-6: Rowe cell with an incompressible material with a flexible rubber diaphragm

3.4.3 Setting up the Rowe cell before beginning the experiment of different wastes with a high organic content

The volume/pressure controllers, the pore pressure transducer and the LVDT were connected through a data logger to a computer running a GDSLAB software consolidation programme (Standard Hydrocon) where the changes in the main parameters (pressure, volume and settlement) were saved at pre-set time intervals (60 seconds). The sample was placed consecutively in the Rowe cell in three layers. The test samples were not dried prior to conducting the test in order to avoid any damage to structure of the material. The wet mass of each layer was 500 g. After placing the last layer, each tested sample was covered by fine mesh followed by a plastic disc to prevent sealing. Then, the lid was placed and the Rowe cell was assembled using eight clamping bolts. The Rowe cell and the pressure controllers were filled with deaerator water obtained from a Nold DeAerator. The deaerated water was stored in a small tank next to the pressure controllers and the Rowe cell. The tested sample was flushed with nitrogen to prevent any air from being trapped during saturation. Additionally, the methanogenesis and sulphate reducing bacteria were inhibited in the waste by dissolving 2.54 g of sodium molybdate and 0.42 g of 2-bromoethanesulfonate (BES) in 3.5 L of deaerated water in the tank (Chae et al., 2009; Ranade et al., 1998).

3.4.4 Steps used to select a sample of synthetic waste with high organic waste for the Rowe cell (1500 g)

MSW was collected separately from the waste bins located at the University of Southampton. The characteristics and composition of the collected waste were adjusted to make them similar to the waste obtained from the Riyadh landfill in Saudi Arabia (Table 3-2).

1. A total of 5 kg of MSW was collected separately from the waste bins located at the University of Southampton. The waste was stored in plastic bags in the fridge .

2. Oversized waste (greater than 40 mm) was shredded so that the proportions of different waste types were distributed (by mass) to the scaled down sieve sizes (37.5, 31.5, 25.0, 22.4, 16.0, 13.2, 11.2, 9.5 and 4 mm) in order to achieve a PSD with the same curve shape as that of the original waste (section 3.6.2).

3. The reduced particle size of the tested sample was achieved manually by shredding the sample using a knife, a scissors or a hammer.

4. A total of 5 kg of the test sample was sieved mechanically using different sieve sizes (37.5, 31.5, 25.0, 22.4, 16.0, 13.2, 11.2, 9.5 and 4mm). The sample in each sieve was collected, characterised and weighed after the mechanical shaker was completed, and then the PSD was plotted. The waste was sieved at its as-received moisture content, and each fraction of the test sample was sorted into various materials depending on the waste composition (Table 4-3).

3.5 Test methodology of different high organic content wastes

This section describes the Rowe cell test method used in this study. The mass of the waste that was used in the Rowe cell is 1500 g. The waste composition of each case (cases 1, 2, 3 and 4) are presented on Section 3.3, Table 3-2. The hydraulic properties, settlement and hydraulic conductivity were measured at different applied vertical stresses. The maximum vertical stress that can be used in the Rowe cell is 300 kPa. During the initial phase in which no load was applied to the test sample, the hydraulic properties and other parameters, such as bulk density, dry density and total porosity (n), were measured. Next, the vertical stress was increased to 25 kPa, and the physical and hydraulic properties and other parameters, such as total porosity (n), dry density (ρ_d) and bulk density, were determined. Then, the vertical stress load was increased to 50 kPa (equal to 15 m depth of the landfill), and the physical and hydraulic properties were determined again to determine how increasing the vertical stress impacted the properties of the waste samples. The same procedures were followed for the next vertical stress test at 75 kPa, with 25 kPa increments. In the last stage, the vertical stress was increased to 300 kPa, which is equivalent to 30 m depth of the landfill; again, the hydraulic properties, settlement and hydraulic conductivity were measured. Waste with different types of organic content was used to examine the effect of dissimilar organic properties on the hydraulic properties, settlement and hydraulic conductivity.

3.6 Physical properties

This section discusses the methods used to determine the physical properties of the initial synthetic waste samples in terms of their particle size distribution, moisture content, saturated moisture content, bulk density and dry density.

3.6.1 Particle size distribution (PSD)

A sample of about 20 kg of Riyadh MSW was obtained from the Riyadh landfill to determine the PSD. The PSD of the samples was not measured at the landfill because there were no sieves at the site and the waste could not be brought back to the UK due to the restrictions on bringing waste from other countries or regions back to the UK. Therefore, the PSD of the sample was determined from photographs of the waste samples. The material in the photographs was identified and then categorised by size, as if sieved through an imaginary set of sieves. The sample was "sieved" through sieves with the following sizes: 375, 315, 250, 224, 160, 132, 112, 95 and 4 mm. The sieve sizes were chosen based on the largest and smallest sized particles of the actual waste of both samples, as well as the conventional sieve sizes in the mechanical sieve shaker located in the Southampton lab. The PSD divides the entire mass into a small number of different size ranges, which makes it easier to characterise the waste based on the type and size of the material. Furthermore, the PSD of the Riyadh sample was used to scale the waste fractions used in the synthetic waste in future tests involving the Rowe cell (section 3.4.4). To make the sieve analysis more realistic for the sample, the second longest length of each component from the photo was used. This approach was used because, during mechanical sieving, there is a higher probability that the second longest length will pass through the sieve openings.

In a mechanical sieve shaker, the waste is fed into the top sieve (large opening) followed by sieves with successively smaller openings. Commonly, waste is not homogenous; it contains different sized particles. During mechanical sieving of the waste, the waste with large particle sizes does not pass through the small sieves. The weight of the waste retained on each sieve was determined and characterised for the PDS curve. In the current situation, where the waste is not physically available, the concept and procedures of the mechanical sieve shaker were followed. Based on the size of each fraction of the waste, the percentage and components of the retained waste on each sieve were determined by determining the total amount of waste on each sieve.

The following technique was employed to justify the methodology used for sieving the synthetic waste. Approximately 300 g of mixed waste (plastic, rubber, paper, cartons) was sieved using a mechanical shaker, and the PSD was obtained (Figure 3.8). Then, photographs of the wastes from different sieve sizes were taken and printed to calculate the average scale between the actual dimensions of the PSDs in those materials and the dimensions of the materials in the photographs. In the photographs, the particle size with the second longest length (mm) was measured using a ruler. The average scale (reference) was calculated by measuring the second longest length (mm)

of one real waste component and one waste component in the photographs. For example, in Figure 3.7.b, the lengths of the second longest component, seen in the red box, in real waste and in the waste in the photograph were 39 mm and 12 mm, respectively. Consequently, each 1-mm length in the photograph is equal to 3.25 mm in real waste. This method was applied for all the components from the different sieve sizes in order to find the average scale (reference) for each photograph. After measuring the particle sizes of each component for all the photographs, the PSD was plotted and compared with the PSD obtained from the mechanical sieve shaker (Figure 3.8). The trend of both PSDs was identical for the sieve sizes of 16 mm, 13.20 mm, 11.20 mm, 9.5 mm, 8mm and 6.70 mm, while there was a slight change in the PSDs for the sieve sizes of 22.40 mm, 31.50 mm and 40 mm. This might be attributable to the mechanical shaker because some of particle sizes can escape the opening of the sieve due to vibration and the type of material.

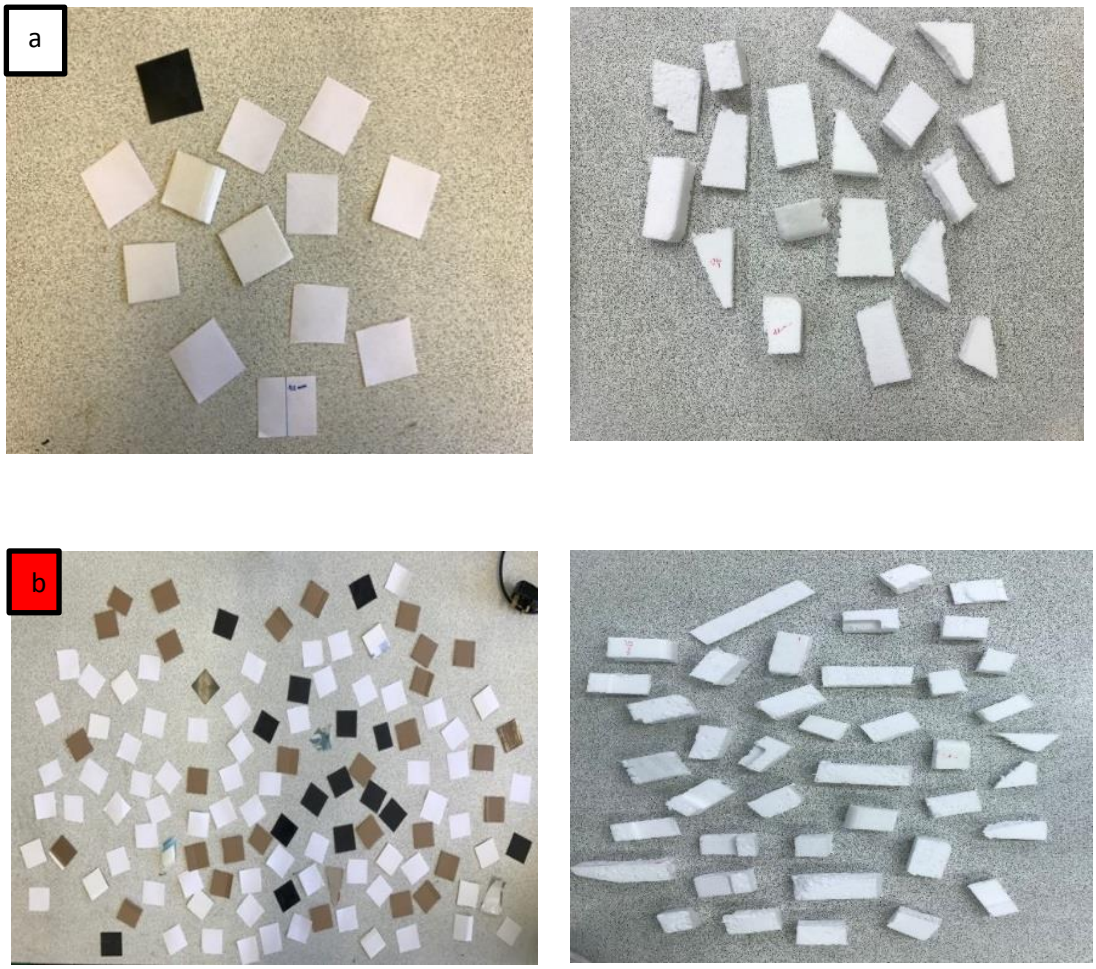

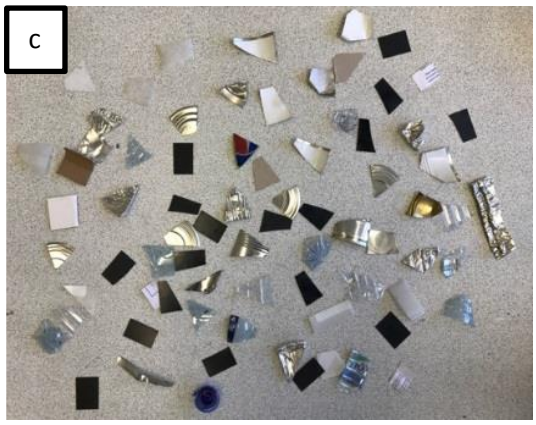
c


d


e


f

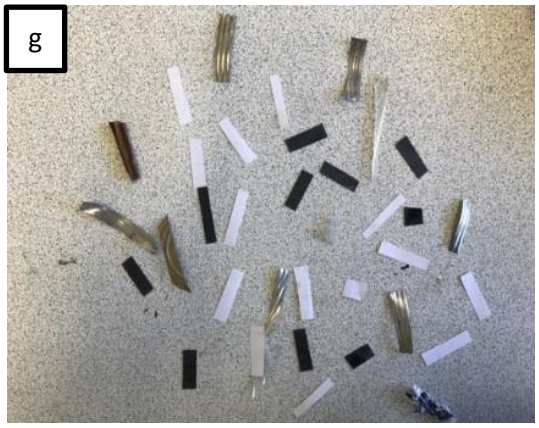
g

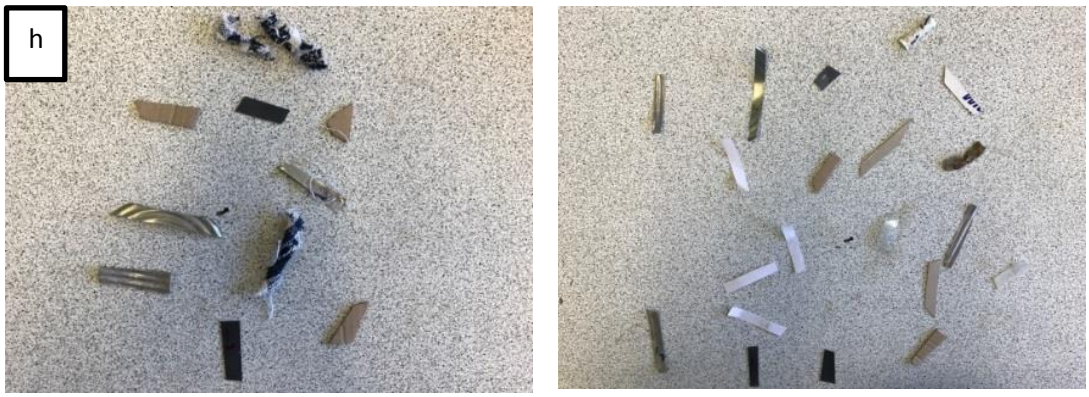

Figure 3-7: Particle size distribution of different sieve sizes: a) >40 mm, b) < 40 mm > 31.5 mm, c) < 31.5 mm > 22.5 mm, d) < 22.5 mm > 16.5 mm, e) < 16.5 mm > 13.20 mm, f) < 13.20 mm > 11.20 mm, g) < 11.20 mm > 9.5 mm, h) < 9.5 mm > 8 mm and i) < 8 mm > 6.70 mm.

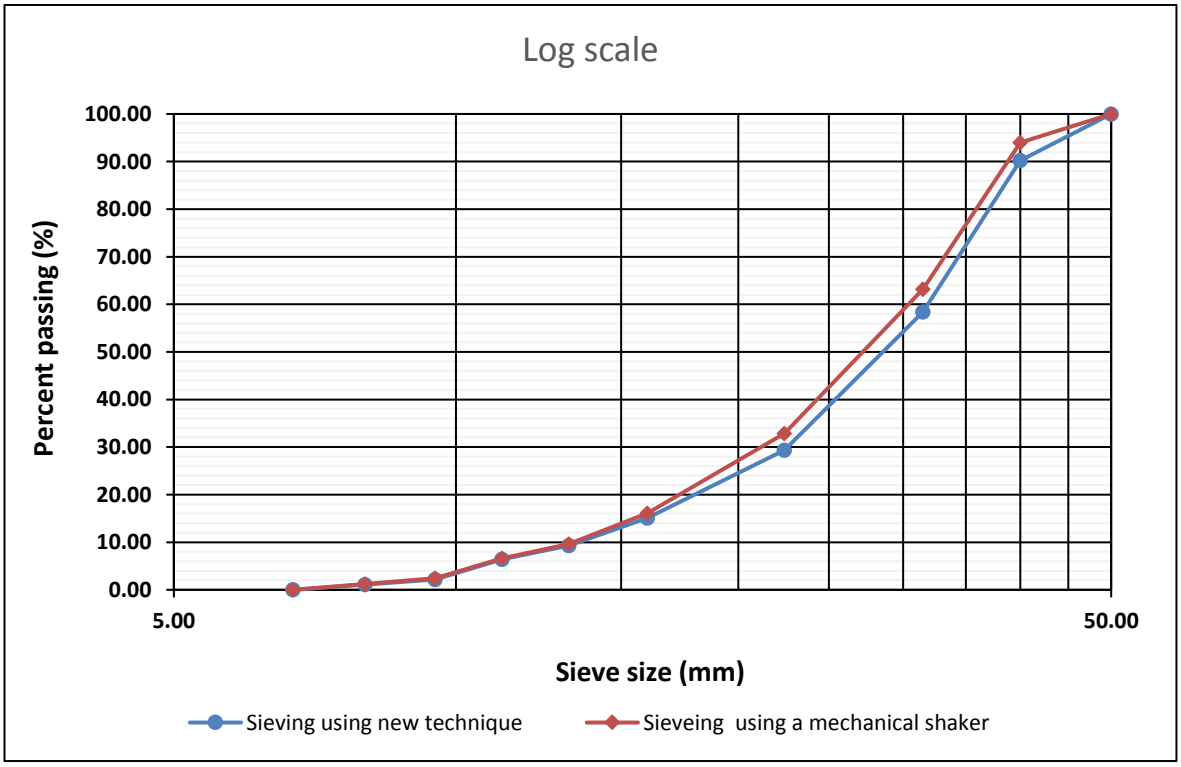

Figure 3-8: PSD assessment of the waste samples using two different methods.

3.6.2 Methods for scaling down the waste for the Rowe cell

According to Beaven (2000), in one-dimensional compression (Rowe cell test) the maximum particle size of a test sample should be at least five-to-ten times smaller than the cell diameter in order to obtain a representative results. Therefore, the test sample was shredded to a maximum size of 40 mm. Based on this information, the original PSD of the waste sample was reduced by shredding the MSW to the required PSD in the Rowe cell (Figure 3-9). To achieve the required PSD with an acceptable particle size range, the size of each sieve was reduced by 90% (Figure 3-9). The shifting of the PSD was completed by considering the consistency of the PSD curve of the sample. The maximum and minimum particle sizes of the waste test sample were 22.4 mm and 4 mm, respectively. The particle size of the sample after shifting was appropriate for use with the Rowe cell. The size of the particles and the percentage weight (by total mass) of each component are described in Chapter 4.

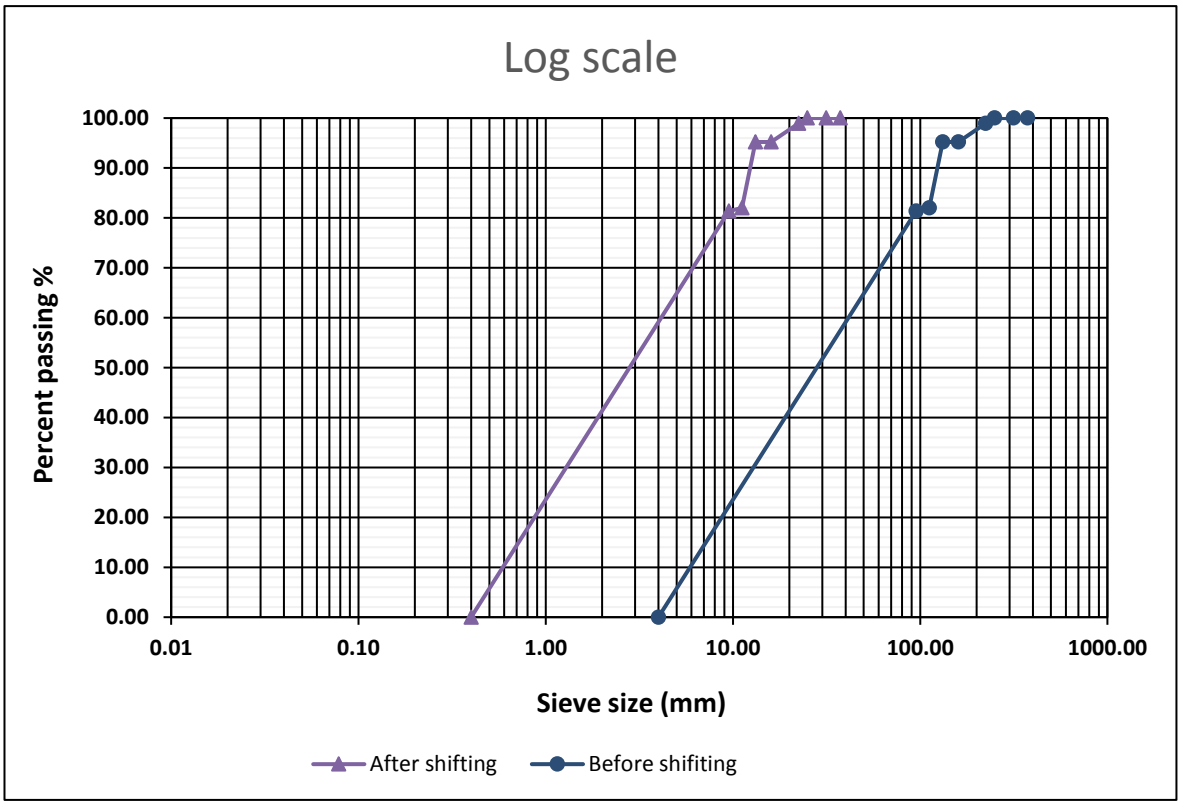

Figure 3-9: Particle size distribution of the waste after shifting to the required particle size.

3.6.3 Moisture content (MC)

The moisture content was determined on two different ways: wet weight basis (W_{wet}) and dry weight basis (W_{dry}). The test samples were drying at 70 ^{0}C until a constant weight has achieved (no further reduction on the weight of the samples). The moisture content was determined using the following equations 3.1 and 3.2:

$$W_{wet} = \frac{M_{wet} - M_{dry}}{M_{dry}} \quad \textbf{(3.1)}$$

$$W_{dry} = \frac{M_{wet} - M_{dry}}{M_{wet}} \quad \textbf{(3.2)}$$

where M_{wet} = the weight of the wet mass, and M_{dry} = the weight of the mass after drying.

3.6.4 Saturated moisture content (SMC)

The SMC of the fresh MSW was determined at different stages of vertical load, ranging from 0 kPa to 300 kPa, with 25 kPa increments. In cases 1 to 4, deaerated water was introduced to saturate the samples at the beginning of the tests, and the volume of added water was recorded. The deaerated water introduced to the samples was left for at least 24 hours to ensure that the test samples had adequate time to absorb the water. Thereafter, the SMC at different applied loads was calculated by measuring the amount of water drained from the samples during the consolidation of the sample. The following equations clarify the procedures that were followed to determine the SMC for each step under different loads:

- At 0 kPa

$$SMC = \frac{M_{tw} - M_{dry}}{M_{dry}} * 100 \quad \textbf{(3.3)}$$

- At 25 kPa

$$SMC = \frac{M_{tw} - M_{d25} - M_{dry}}{M_{dry}} * 100 \quad \textbf{(3.4)}$$

- At 50 kPa

$$SMC = \frac{M_{tw} - M_{d25} - M_{d50} - M_{dry}}{M_{dry}} * 100 \quad \textbf{(3.5)}$$

- At 75 kPa

$$SMC = \frac{M_{tw} - M_{d25} - M_{d50} - M_{d75} - M_{dry}}{M_{dry}} * 100 \quad \textbf{(3.6)}$$

where SMC = the saturated moisture content, M_{tw} = the mass of the solid, including the deaerated water added to the sample, M_{d25} = the mass of the water drained after applying 25 kPa, M_{d50} = the mass of the water drained after applying 50 kPa, M_{d75} = the mass of the drained water after applying 75 kPa and M_{dry} = the mass of the dried waste. The same procedure and equations were followed for the other vertical stresses, ranging from 100 kPa to 300 kPa, with 25 kPa increments.

3.6.5 Bulk density (ρ_{wet})

The initial bulk density (ρ_{wet}) is defined as the ratio of the total mass of the waste, including moisture content, to the volume of the waste in the reactor. Initially, 1500 g of fresh waste was placed consecutively in the Rowe cell in three layers. The mass of each layer was 500 g. In this test, the ρ_{wet} was measured under different stresses. The ρ_{wet} can be determined using Equation 3.7:

$$\rho_{\mathrm{wet}} = M_{wet} / V_i \quad \textbf{(3.7)}$$

where, M_{wet} = the mass of the sample, including the MC of the waste and V_i = the total volume of the waste in the reactor.

3.6.6 Dry density (ρ_{dry})

Dry density (ρ_{dry}) was obtained to assess the degree of waste compaction. This can be computed by dividing the dry mass of the solid waste by the total volume of waste in the reactor. In this study, because the test samples were not dried, the ρ_{dry} was obtained based on ρ_{wet}. Equation 3.8 describes the correlation between these two types of densities.

$$\rho_{dry} = \rho_{wet}/(1 + W_{dry}) \quad \textbf{(3.8)}$$

3.7 Hydraulic properties

The hydraulic properties of the sample in this study were determined using the Rowe cell described in Section 3.4. The following sections describe the method used to determine the hydraulic properties, such as hydraulic conductivity, total porosity, settlement, void ratio and compressibility of different waste materials with high organic content.

3.7.1 Determination of hydraulic conductivity

The basic principle of testing the hydraulic conductivity of a soil can be applied to testing it in waste materials (Hudson, 2007). Additionally, the concept of obtaining the hydraulic conductivity in a constant head test was used to determine the hydraulic conductivity in a Rowe cell. With a Rowe cell, hydraulic conductivity can be measured at various applied pressures using either upward flow or downward flow. The flow was induced in the reactor by the inlet pressure (P_1), which is greater than the outlet pressure (P_2), while the applied stress of the inlet pressure is less than the applied stress of the outlet pressure (Figure 3.10). The head gradient that is used depends on the material being tested. For example, in silt and sand, the required head gradient might be a few centimetres, while in clay the required head difference is up to 2 m in order to have a measurable flow through clay samples (Barnes, 2000 as cited by Hudson, 2007). When the required hydraulic gradients are high, the gradient should be cautiously increased, and the flow rate should be observed to prevent internal erosion of the sample (Hudson, 2007). The method described in BS1377: part 6 (1990) was used to determine the hydraulic conductivity of the tested sample in the Rowe cell. Hydraulic conductivity can be measured using Equation 3.9:

$$\mathrm{k} = \frac{\mathrm{q}}{\mathrm{Ai}} = \frac{qH\gamma_w}{A(P_1 - P_2)} \qquad \textbf{(3.9)}$$

where k = the vertical hydraulic conductivity, q = the steady state flow rate, A = the cross-section area of the tested sample, H= the sample depth, P_1 = the inlet back pressure and P_2 = the outlet back pressure.

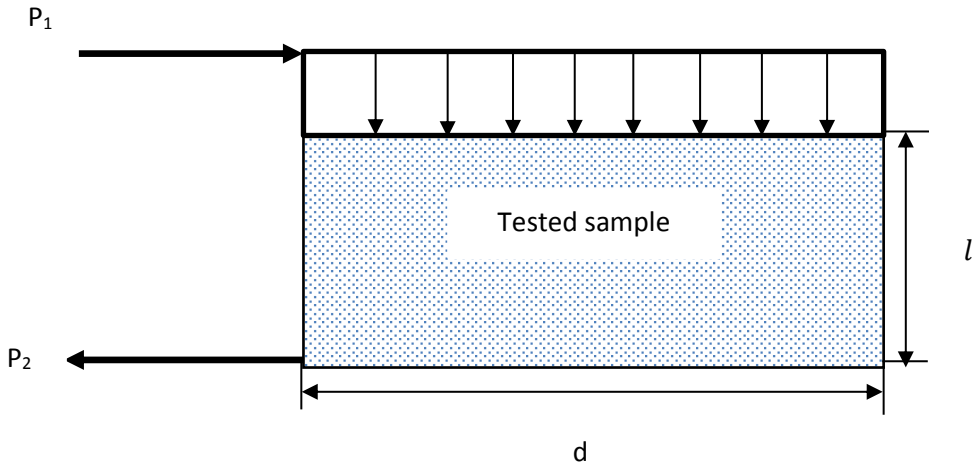

Figure 3-10: Scheme of the saturation measurement of hydraulic conductivity using a Rowe cell.

3.7.2 Specific gravity (ρ_s)

Specific gravity was determined using a standard gas jar method (BS 1377-2, 1990). Specific gravity was computed using Equation 3.10:

$$\rho_s = \frac{m_2 - m_1}{(m_4 - m_1) - (m_3 - m_2)} \quad \textbf{(3.10)}$$

where m_1= the mass of the gas jar and the ground glass plate, m_2 = the mass of the gas jar, plate and waste, m_3 = the mass of the gas jar, plate, waste and water and m_4 = the mass of the gas jar, plate and water.

3.7.3 Total porosity (n)

Total porosity is defined as the volume of the voids to the total volume. The initial total porosity (n_0) was determined using the following equations (3.11 and 3.12):

$$n_0 = V_v / (V_s + V_v) \quad \textbf{(3.11)}$$

where V_v = the volume of the void and V_s = the volume of the solids.

The total porosity at the end of the consolidation phase was determined based on the void ratio:

$$n = e/(1 + e) \quad \textbf{(3.12)}$$

where n and e are the total porosity and the void ratio at the end of the consolidation phase, respectively.

3.7.4 Void ratio (e)

The void ratio (e) of fresh MSW was determined under different applied stress, ranging from 0 kPa to 300 kPa, with 25 kPa increments. The initial e was computed using the Equation 3.13:

$$e_0 = \frac{n_0}{1 - n_0} \quad \textbf{(3.13)}$$

where e_0 = the initial void ratio.

The method used to determine e under different loads was described in BS 1377-6 (1990). The change in e under different applied stresses can be determined by Equation 3.14:

$$\Delta_e = \frac{1+ e_0}{H_0} \times \Delta H \quad \textbf{(3.14)}$$

where Δ_e= is the cumulative change in e at the end of the consolidation phase, H_0 is the initial height of the specimen and ΔH= is the cumulative change in the height of the specimen at the end of a consolidation phase from the initial height.

The e at the end of the consolidation phase is calculated from Equation 3.15:

$$e = e_0 - \Delta_e \quad \textbf{(3.15)}$$

The total porosity at the end of each consolidation case can be calculated by knowing the value of e. The total porosity is related to e. as calculated from Equation 3.16:

$$\mathrm{n} = \frac{\mathrm{e}}{1+ \mathrm{e}} \quad \textbf{(3.16)}$$

where e = the void ratio of the tested sample at the end of each consolidation phase.

3.8 Compressibility of MSW

The compressibility of MSW plays an important role in determining the primary settlement. The cell diaphragm and lid were fitted, and deaerated water was introduced through the base (inflow). The pressure controllers were then connected to the sample, and the saturation process continued by incrementally increasing the back pressure applied to the sample. Once saturated, the required effective stress was applied, and the sample was consolidated to a primary stage of settlement. Volume changes and sample settlement were measured during this stage.

The compression index (C_c) can be used to estimate the primary settlement. The data obtained from the compression test was used to estimate the primary settlement. The compression index (C_c) is defined by Holtz (1981), and written as:

$$C_c = \frac{-\Delta e}{\Delta \log \sigma} \quad \textbf{(3.17)}$$

where, C_c = the primary compression index, Δe = the change of the void ratio and Δσ is the change in the vertical effective stress.

3.9 Determination of the percentage of SBW and LBW of 100% organic content (food waste)

The amount of SBW and LBW in 100% organic waste under load was determined using the Rowe cell (255 mm diameter, 100 mm height) under different applied loads. The same procedures used to set up the Rowe cell prior to starting the experiments were followed (see Section 3.4.2). The particle size of the test samples was shredded to less than 9.5 mm (section 3.4.4). Table 3-4 shows the waste type of each experiment.

The following steps describe the procedure used to determine the water released from these different samples:

1. Around 1500 g of waste with LBW (from a tomato, cucumber, orange, lemon and apple) was placed in the Rowe cell in an unsaturated condition. The waste sample was not saturated so as to determine the amount of water released from the waste itself. After the test sample reached consolidation, which means no more water was coming out of it, the water that was released was collected and measured.

2. About 1500 g of waste with SBW (from rice, pasta and chicken) was placed in the Rowe cell, and the same procedure used in the previous step was followed.

3. A waste mixture of 50% SBW and 50% LBW (1500 g) was tested, and the same procedure used in the previous steps was applied. The LBW and SBW were mixed in order to obtain a reference waste.

4. Then, 1500g of 45% SBW and 55% LBW from the Riyadh MSW was measured using the same procedure that was used in the tests described in the previous steps.

Table 3-4: The proportion of LBW and SBW used for the water release test due to compression

Experiments	Proportion of food wastes on each experiments (%)								
	LBW					SBW			
	Cucumber	Lemon	Tomato	Apple	Orange	Rice	Chicken	Pasta	Bread
Case (5), (100% LBW)	20	20	20	20	20	×	×	×	×
Case (6), (100% SBW)	×	×	×	×	×	25	25	25	25
Case (7), (50%LBW and 50% SBW)	10	10	10	10	10	12.50	12.50	12.50	12.50
Case (8), (55% LBW and 45% LBW)	11	11	11	11	11	11.25	11.25	11.25	11.25

3.10 Determination of water released due to decomposition

The effect of biodegradation on the water released from LBW and SBW for different types of food waste was determined. The main objective of this test was to calculate the amount of water discharged from the food waste due to waste decomposition. Initially, eight reactors with a volume capacity of 1 L were filled using 220 g each of LBW waste and SBW waste. About 400 mL of water was added to each reactor, and the reactors were placed in a water bath at 35℃. The weight changes in each sample were due to water flowing out from the samples. The experiments were conducted in duplicate for each reactor, and the average in weight loss of each sample was taken. The following steps describe the procedure used to calculate the weight loss of each sample:

1. The change in weight of all samples was measured by taking out the samples from the reactors and sieving out solids using a strainer. After all the water flowed out from the strainer, the weight of the solids of all samples was calculated using a weight balance.

2. After weighing, the samples and liquid were put back into the reactors and weighed again. Some water was lost due to evaporation or the decomposition process; the water loss was compensated by adding water equivalent to the added water at the beginning of the test (400 mL)

3. The same procedure and methods were followed for all test samples.

The water migrated from the food waste can be calculated daily by measuring the change in the weight of the food waste. The reduction of food waste weight can be attributed to the water released due to biodegradation. Table 3-5 shows the waste type of each of the reactors. The experiments were completed when no change in the weight of the food waste was observed.

Table 3-5: The type of LBW and SBW organic waste used for the water release test due to decomposition

Reactors	**Type of waste**
R1	Lemon
R2	Cucumber
R3	Tomato
R4	Apple
R5	Orange
R6	Rice
R7	Bread
R8	Pasta

Figure 3-11: Set up of the test reactors used to determine the water losses due to decomposition

3.11 Limitation of the method used in this study

Since the waste of this project is related to the waste of other countries, some difficulties and limitations of using the project's method are discussed in the following point:

1. The methodology used for sieving the synthetic waste is presented in section 3.6.2. The actual waste was not sieved as there was no mechanical sieve shaker on the site of the Riyadh landfill. Thus, the particle size distribution curve might be slightly different if the actual waste components were sieved using a mechanical sieve shaker.
2. The degradation of different types of organic waste was inhibited in this study as the Rowe cell reactor was not made to collect the gas produced during biodegradation processes. In this regard, the waste of test samples presented in this study are considered fresh wastes. Physical and hydraulic properties might be impacted if degraded test samples were tested.
3. The consolidation anaerobic reactor (CAR) used from previous researchers such as Siddiqui (2011) accepts a larger particle size and sample. Also, the biodegradation impacts can be investigated with compression. However, the Rowe cell was the best alterative option to carry out the test as the CAR reactors were not available for this project.

Chapter 4 Result and discussion

4.1 Introduction

An understanding and determining of the hydraulic properties, physical characteristics, and settlement of MSW are critical for the design and operation of a landfill in terms of maintaining the landfill, estimating landfill capacity, and designing the gas and leachate extraction system (Elagroudy et al., 2008; El-Fadel and Khoury, 2000; Staub et al., 2009). Thus, the results presented in this chapter highlight the impact of different high organic content waste (food waste) on the changes of physical and hydraulic properties. In this chapter, the results obtained from the experimental study are presented and analysed.

The characteristics and compositions of waste were adjusted to make it similar to waste with a high organic content, such as the Riyadh MSW. Thereafter, the organic matter (food waste) was reduced by 20%, 40%, and 60% in order to investigate the impact of organic content (food waste) on the physical and hydraulic properties and settlement of MSW. The characteristics of the different types of waste were measured before and after performing the compaction tests. The leachate produced (water release) from different types of organic content was investigated using Rowe cell. Thus, the organic material was classified into two different categories: LBW and SBW. Next, the water content in the food material was analysed and measured. The effect of biodegradation on weight reduction, which is related to the water released, was conducted and analysed. The results of this study are compared with other previously reported studies.

4.2 Results of LBW and SBW of different food wastes run under unsaturated conditions

The main goal of determining LBW and SBW is to evaluate the amount of water released from different types of food waste, where the water released is mainly directed to the leachate produced in the landfill site. LBW and SBW of different waste compositions were determined using Rowe cell. The types of waste and the procedures followed to drain the leachate from each test were described in Chapter 3, Sections 3.9. The experiments of each test were conducted twice to assure the accuracy and reliability of the results.

4.2.1 Water released from 100% LBW

The water released (leachate) from the waste itself has been obtained under different vertical stresses from 0 to 300 kPa with increments of 25 kPa. The moisture content of the sample was 92% (based on wet basis). The objective of obtaining the water released from LBW was to examine the amount of water which was drained from waste without the other components, such as plastic, paper, etc. As shown in Figure 4-1, in the initial stage where the vertical stress is equal to zero, no water is drained from the sample. This may be attributable to the material structure, which was not exposed to change due to zero stress. However, approximately 2.40% of the total volume of water was released when the vertical stress increased to 25 kPa. The slight amount of water released at 25 kPa can be explained as the resistance of the material structure, which may be greater than the applied load. On the other hand, about 91% of the water was drained from the sample between the vertical stresses of 50 kPa, 75 kPa and 100 kPa. The high amount of water released at these rates of stress can be imputed to change in the material structure, as the tissue of the material was no longer able to hold its structure. Therefore, the structure of the material was broken, leading to intracellular water (LBW) inside the pore space, flowing out from the sample. The percentage of LBW from the initial mass of the sample obtained in this study was 87.50%, which is similar to Kan et al.'s (2007) results. They concluded that LBW was about 80–92% for food waste, containing apple, pear, kiwi, nectarine and apricot. There was a slight increase in leachate produced, as the vertical stress increased from 125 kPa to 225 kPa. This may be because most of the LBW was released at the vertical stress rates of 50 kPa, 75 kPa and 100 kPa; consequently, a small amount of water was held in the pore spaces, and this was moved out as the vertical stress increased from 125 kPa to 225 kPa. In addition, no water migrated out from the sample during the last vertical stress steps: 250 kPa, 275 kPa and 300 kPa. This can be explained by the fact that, by then, the pore space within the material structure was completely empty or perhaps the applied stresses were not enough to release the remaining water within the material structure.

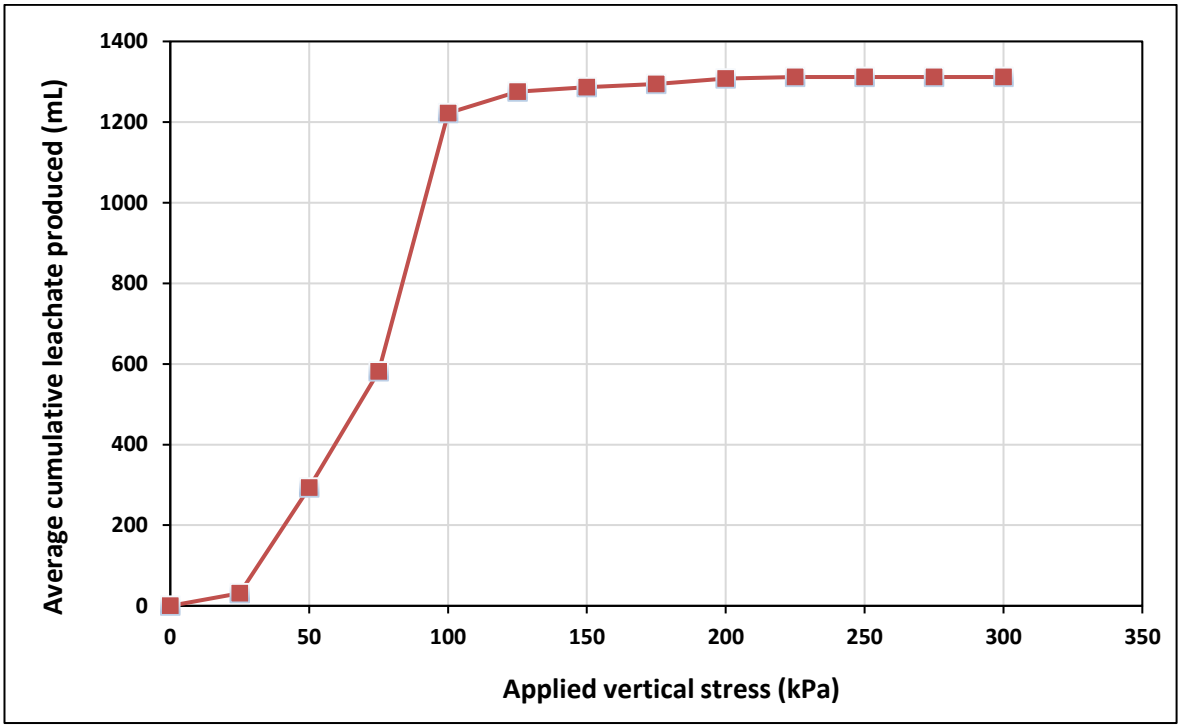

Figure 4-1: Leachate produced from 100% LBW waste

4.2.2 Water released from 100% SBW

The leachate produced from SBW was obtained by following the same procedures and methods as for LBW. The components of the test sample (cooked sample) were rice, chicken, pasta and bread. The moisture content of the sample was 56% (based on wet basis). The total amount of water (mL), drained from the sample, was 177 mL, which constituted about 11.80% of the total weight. As shown in Figure 4-2, the water began to be released when the vertical stress rose to 25 kPa, and it only slightly increased as the vertical stress increased to 300 kPa. The small percentage of water produced from the sample (11.80%) can be explained by the type of waste material used, as its structure was not readily broken down, leading to the production of cell wall water. This is because of the material resistance, which is able to hold the water under differentially applied loads. The results found in this study were different from the results obtained by Khan and Karim (2017) and Halder et al. (2011). Khan and Karim (2017) stated that the percentage of SBW of different waste compositions ranged between 1% and 6%. Halder et al. (2011) also found that only 2% of SBW was released at the pressure of 700 kPa, which may be because of the different materials used in this study, particularly in terms of material tissues; the capillary pressure of the materials used may be lower than the applied pressure and, therefore, the water would be able to flow out from the pores. In addition, the variations between the results found in this study and other related studies can be

attributed to methodological differences: while most of the previous studies investigated weight loss for food processing purposes, in this study the weight loss was due to compression.

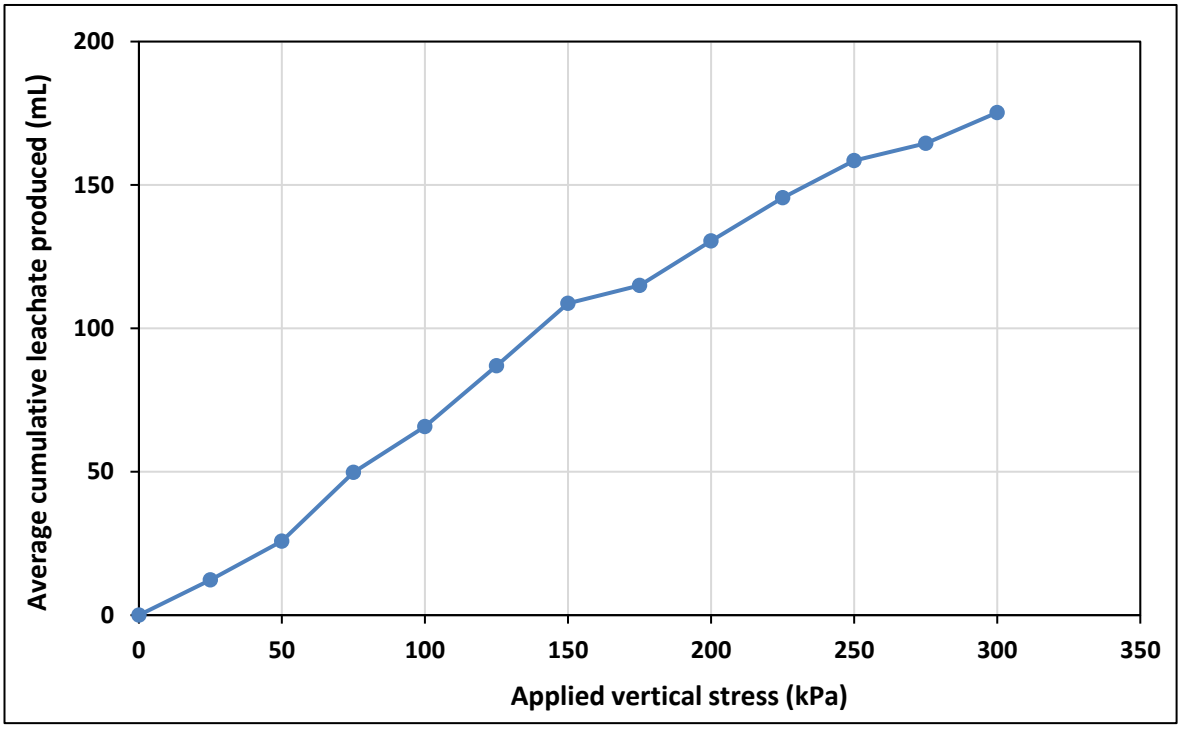

Figure 4-2: Leachate produced from 100% SBW waste

4.2.3 Water released from 50% LBW and 50% SBW and Riyadh organic matter

To make a waste sample similar to the composition of organic content in Riyadh MSW, which could therefore serve as a reference, a sample containing organic matter with 50% LBW and 50% SBW was tested, and the moisture content was 75% (based on wet basis). Thereafter, a sample of Riyadh organic matter, comprising 45% SBW and 55% LBW, was studied in order to evaluate the leachate produced from the fresh MSW, and the moisture content was 77.6% (based on wet basis). Figure 4-3 compares the leachate produced from the reference sample and Riyadh waste with other different waste composition samples. The results of the two samples were as expected, as LBW and SBW both diminished by about 50%, and the curves of the two samples mediated the other curves.

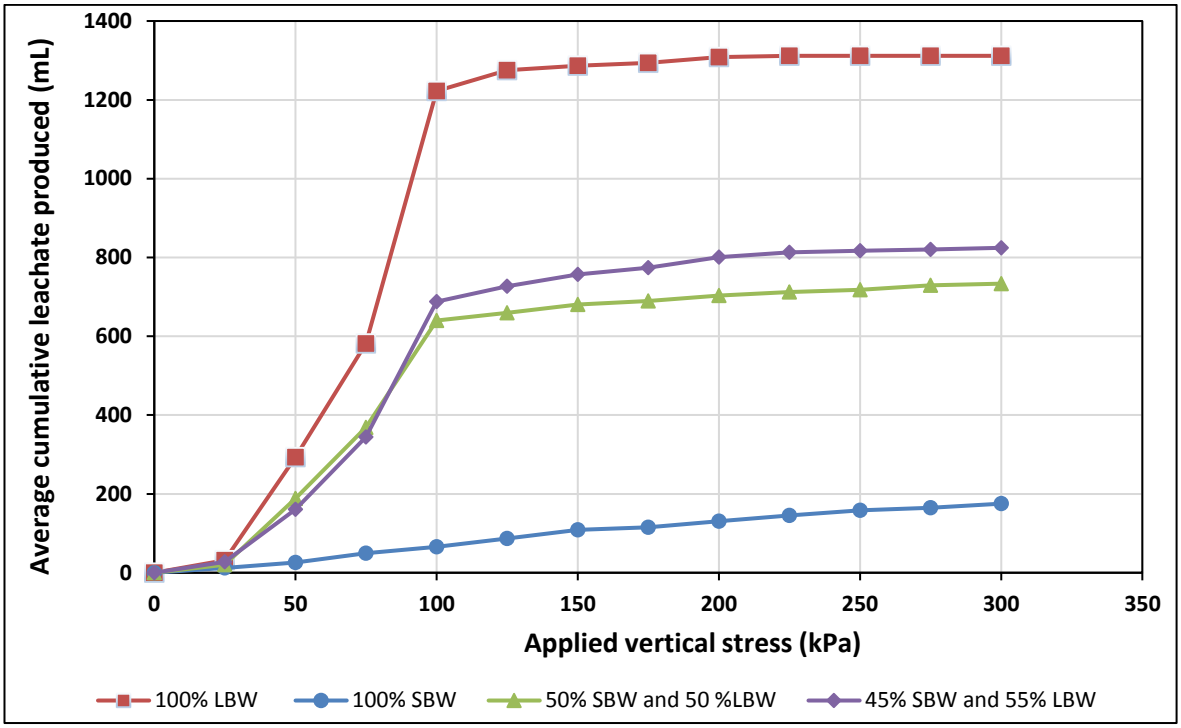

Figure 4-3: Leachate produced from different compositions of organic matter

These figures show clearly that the type of organic material has a significant direct impact on the leachate produced in the landfill. Therefore, knowing the characteristics of organic waste will be valuable when predicting the water draining out from the sample (leachate).

4.2.4 Mass balance of LBW and SBW

The mass balance of the different fractions of LBW and SBW are presented in Table 4-1. The change in sample weight was attributed to the water released from the samples due to compression. There may be a slight difference between the amounts of water released and change in sample weight, which might be due to waste adsorption or water loss during the measurements.

Table 4-1: Mass balance rates different fraction of LBW and SBW

Type of waste (%)	Weight of sample prior the test (g)	Weight of sample after the test (g)	Amount of water released (mL)	Mass balance error (%)
LBW (100)	1500	175	1312	0.89
SBW (100)	1500	1300	175	1.65

LBW (50) and SBW (50)	1500	752	734	0.97
LBW (55) and SBW (45)	1500	650	825	1.70

4.2.5 Settlement of different LBW and SBW composition

The settlement of different LBW and SBW compositions without the incompressible material was obtained in order to learn about the impact of LBW and SBW on the settlement of waste. The initial height of all the samples was 50 mm. As Figure 4-4 illustrates, the settlement of the samples varied under different vertical stresses. The percentage reduction of both 100% LBW and 100% SBW was respectively 73% and 60% from the initial height of the samples. The high percentage reduction in 100% LBW can be attributed to waste type as the water was easily released from the LBW sample (compressible material). A large volume of water drained from the sample when the vertical stress increased from 50 kPa to 100 kPa (see Section 4.2.1). In contrast, the settlement of 100% LBW at 50 kPa was less than the other type of waste. This may be attributed to the material structure of LBW material, where the material tissue was able to resist the vertical stress of 50 kPa. On the other hand, the total settlement of 100% SBW was 29.70 mm, which was equal to about 60% of the initial height. The difference may be due to the samples' tissues, as the tissues inside the SBW waste are less likely to be broken due to the vertically applied stress compared with the material tissues of LBW (Joardder et al., 2017; Khan et al., 2018).

The settlement of the reference waste (50% LBW and 50% SBW) and the bound water of the Riyadh organic matter were compared with other types of waste (Figure 4-4). The results of both waste types were reasonable, as LBW and SBW were reduced in both samples.

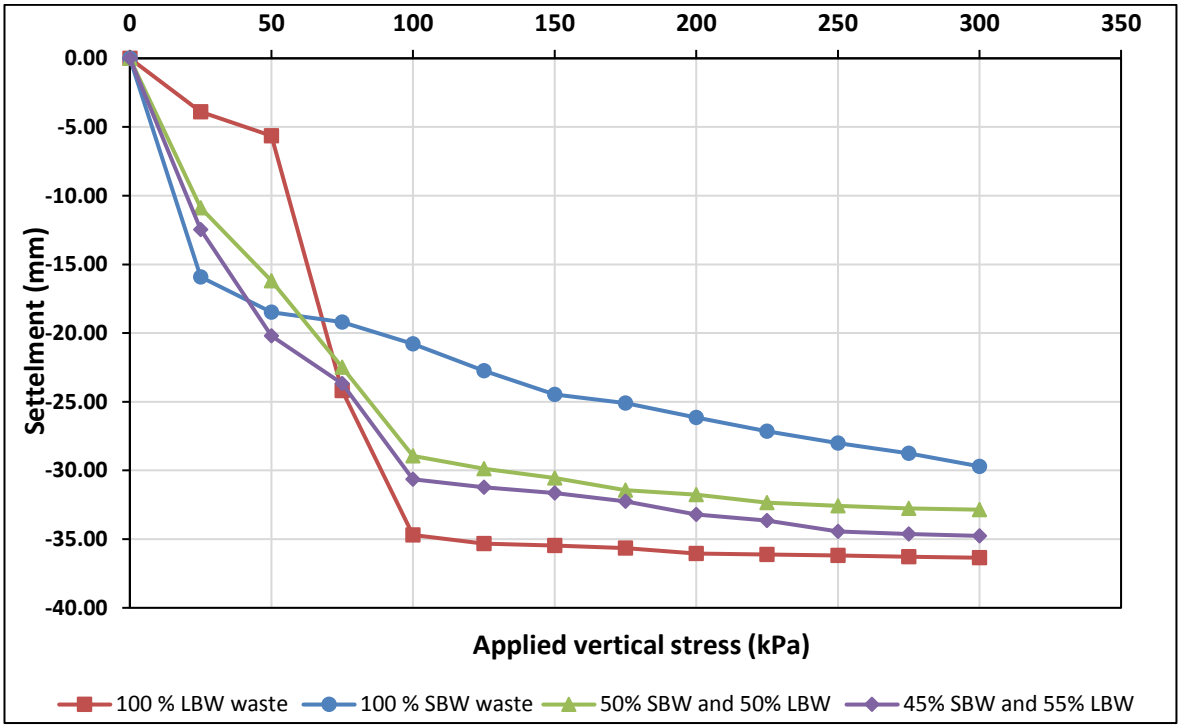

Figure 4-4: Settlement vs verically applied stress of different percentages of LBW and SBW

4.2.6 Water release from LBW due to decomposition

The effect of decomposition on the migration of water from different waste composition has been investigated in this study. The degradation effect of different high organic MSW was inhibited on Rowe cell; thus, the water released from Rowe cell was due to the impact of compression. Therefore, several experiments have been conducted in order to identify the amount of water loss arising from the degradation process. The procedures and methods of this investigation were explained in Chapter 3, Section 3.10. First of all, different waste compositions, including LBW and SBW waste, were studied and analysed in terms of weight loss arising from the decomposition processes. The experiments were conducted in duplicate for each reactor, and the average was taken. The variations in the duplicate samples for all waste types ranged from 1 to 10%. The waste composition and the weight of each reactor are presented in Table 3-5. Figure 4-5 shows weight loss of different LBW waste types over time. A rapid decrease in weight was found in cucumber and tomato, where the reductions from the initial mass were 99.84% and 99.87%, respectively. On the other hand, the least reduction was observed in lemon with a decrease of about 38.30% from the initial mass. The trends in the weight losses of both orange and apple were fairly similar with a decrease of about 53% and 63% from the initial mass. The differences in weight loss among these various fruit and vegetables may be attributed to the material structure and water content.

Rahman (2007) and Rickman et al. (2007) stated that the growth of spoilage microbes is enhanced for the fruit and vegetables which contain about 90% water content. In this regard, the massive weight losses in cucumber and tomato may indicate the high amount of water content with a value of 97.13% and 95.83%, respectively. This finding agrees with that of deMan et al. (2018) who indicated that water activity and moisture content play a critical role in the chemical and microbiological activities, which are responsible for food spoilage. In addition, the temperature is considered an important factor where the microorganism of food material increases with a rise in temperature.

However, the visual inspection of the tested samples after 100 days illustrated that the water in lemon and orange was released (Figure 4-6), while the remaining amount of water within the material tissue and crust could be released by applying compression. In contrast, most of the water in cucumber and tomato flowed out due to weakness in the material structure. This accounts for the considerable amount of water when the vertical stress was applied from 0 kPa to 100 kPa, where the material structure started to destruct, leading to the release of water from the samples (Figure 4-3)

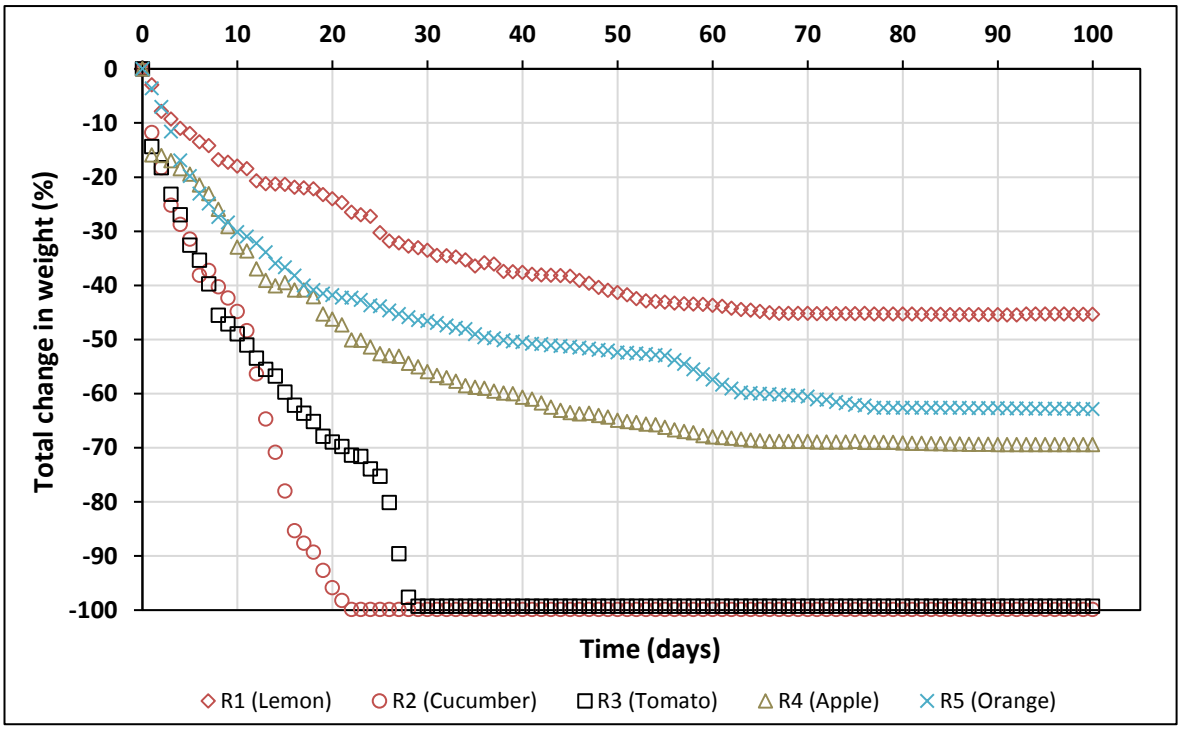

Figure 4-5: Water released from LBW due to degradation.

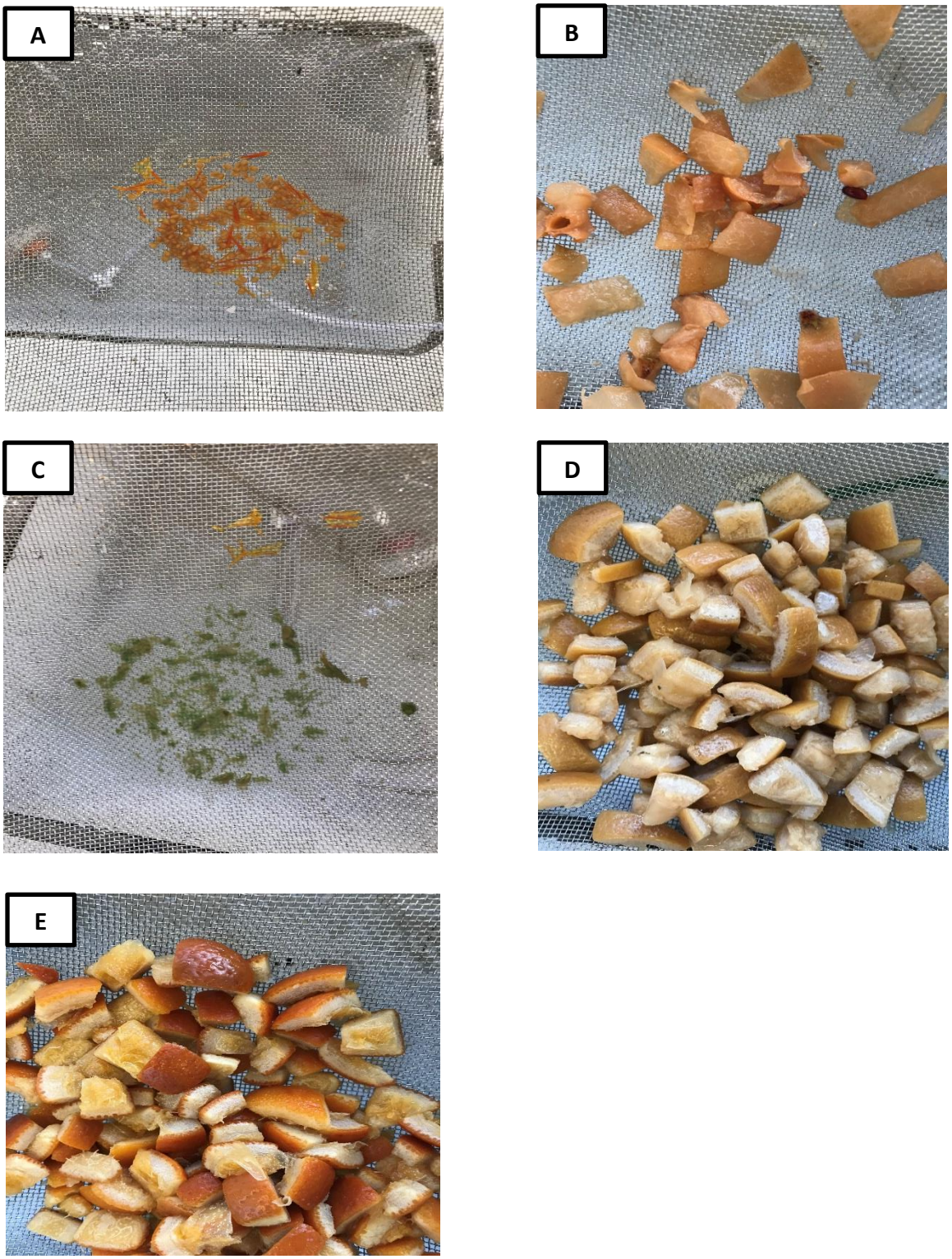

Figure 4-6: Photographs of LBW waste at the end of the test: A: Tomato, B: Apple, C) Cucumber, D) Lemon, E) Orange

4.2.7 Water released from SBW due to decomposition

The effect of decomposition on SBW waste, such as cooked rice, cooked pasta and bread, was investigated according to the same process as LBW (see Section 3.10). The variations in the duplicate samples for all waste types ranged from 1 to 8%. As it can be seen in Figure 4-7, the amount of water released was considerably lower than the water migrated from LBW waste (Figure 4-5). This can be attributed to the material structure, where SBW was less likely to collapse compared with LBW samples. For comparison, after running the experiments for 14 days, the greatest reductions in SBW and LBW were obtained in bread and cucumber with reductions of about 2.67% and 78.83%, respectively. This confirms that SBW or LBW and material structure have a significant impact on the water losses arising from the degradation processes. As shown in Figure 4-7, the least reduction in water losses was observed in pasta, which can be due to the difficulties involved in migrating water with the structure (Altan and Maskan, 2005; Piwińska et al., 2015). On the other hand, it can be noted that the weight of bread and rice keep changing over time. Figure (4-8) shows that bread and rice after 100 days turned into something resembling sponge and broke down into small pieces, which the sieve was unable to hold or filter some components of the material.

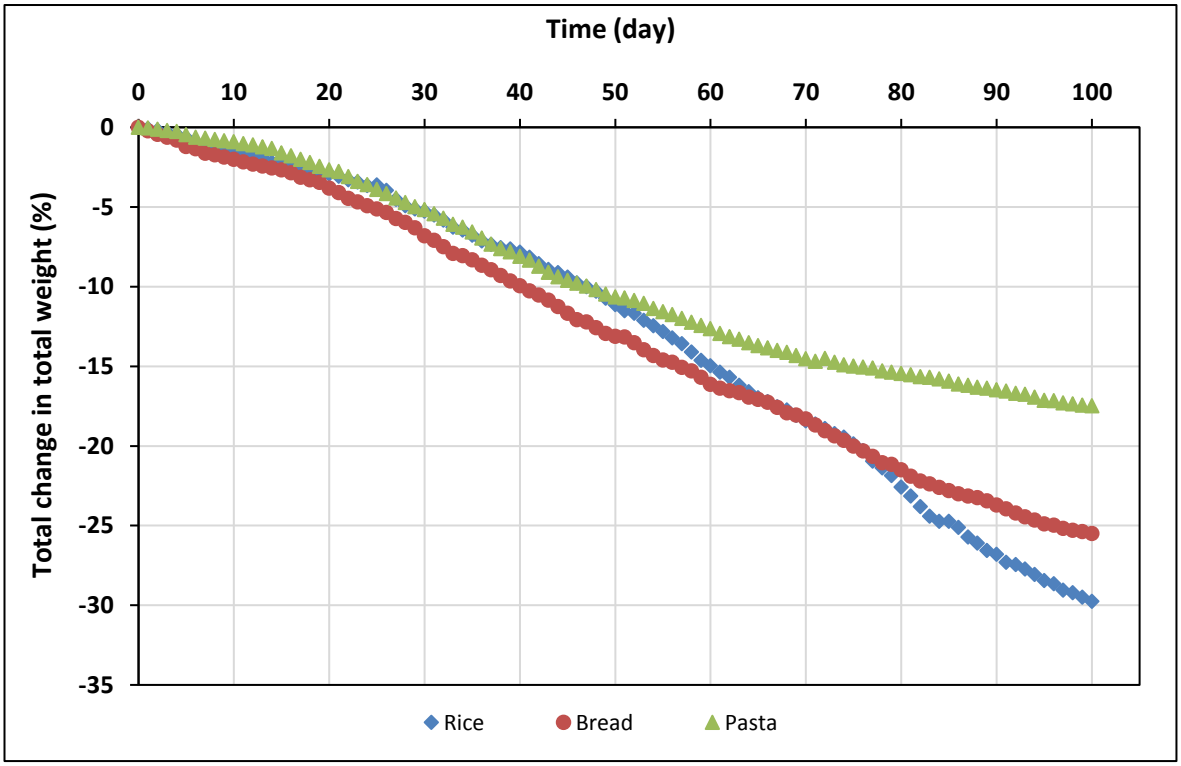

Figure 4-7: Water released from SBW due to degradation

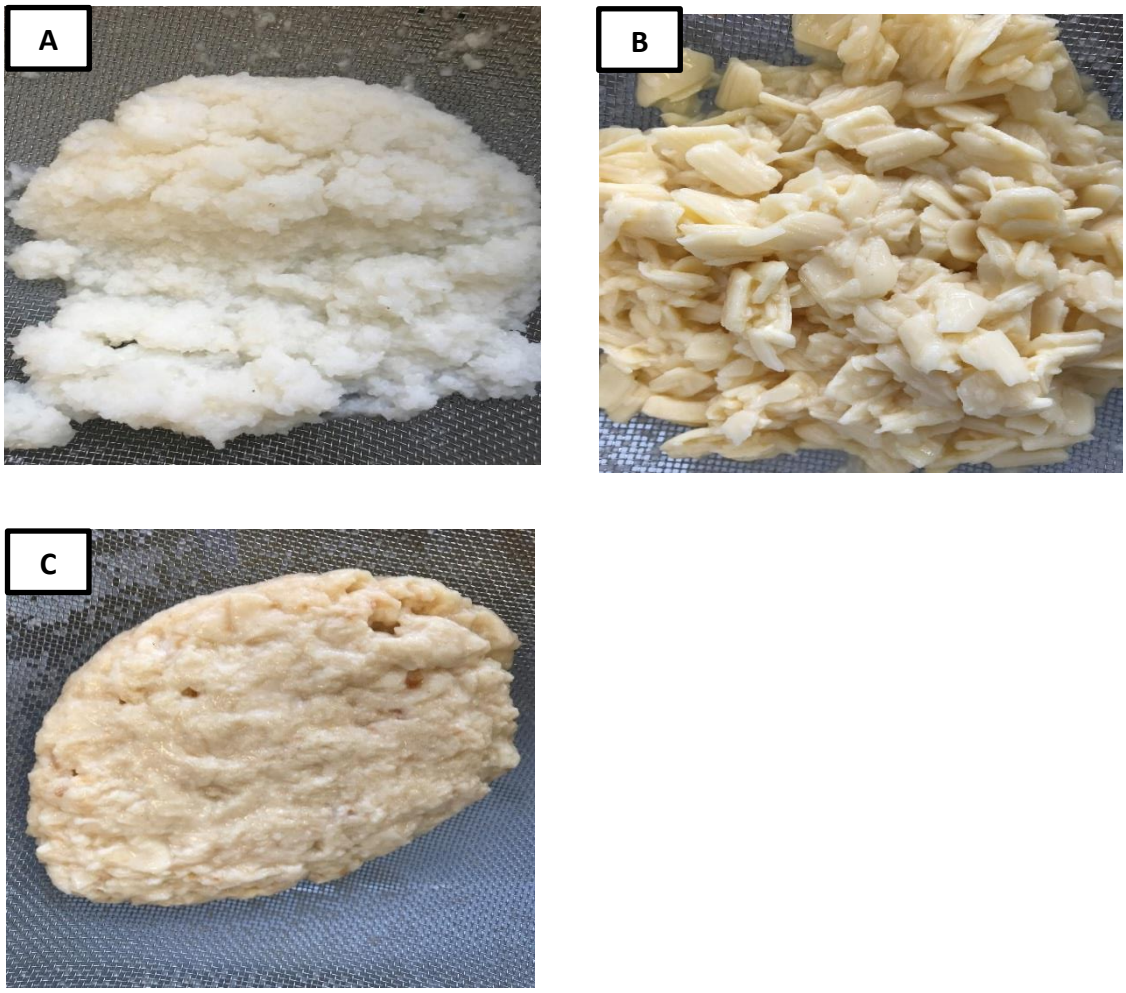

Figure 4-8: Photographs of SBW waste at the end of the test: A) Rice, B) Pasta, C) Bread

4.2.8 The practical application of the results to classify food material

The results in Figure 4-3, obtained from experimental work using a Rowe cell, can be used as a reference by landfill operators and designers to classify the water bound strength of food material (LBW and SBW). As illustrated by Figure 4-9, when food material was compressed at 100 kPa, and the mass of the water released was greater than or equal to 80% of the sample's total mass, then it was classified as LBW waste. In contrast, food waste was classified as SBW when the mass of the water expelled was equal to or less than 4.50%. This concept is applicable to all other types of waste. This procedure can be applied by landfill designers and operators to build an appropriate leachate collection system if a compression cell (e.g. Rowe cell) is available.

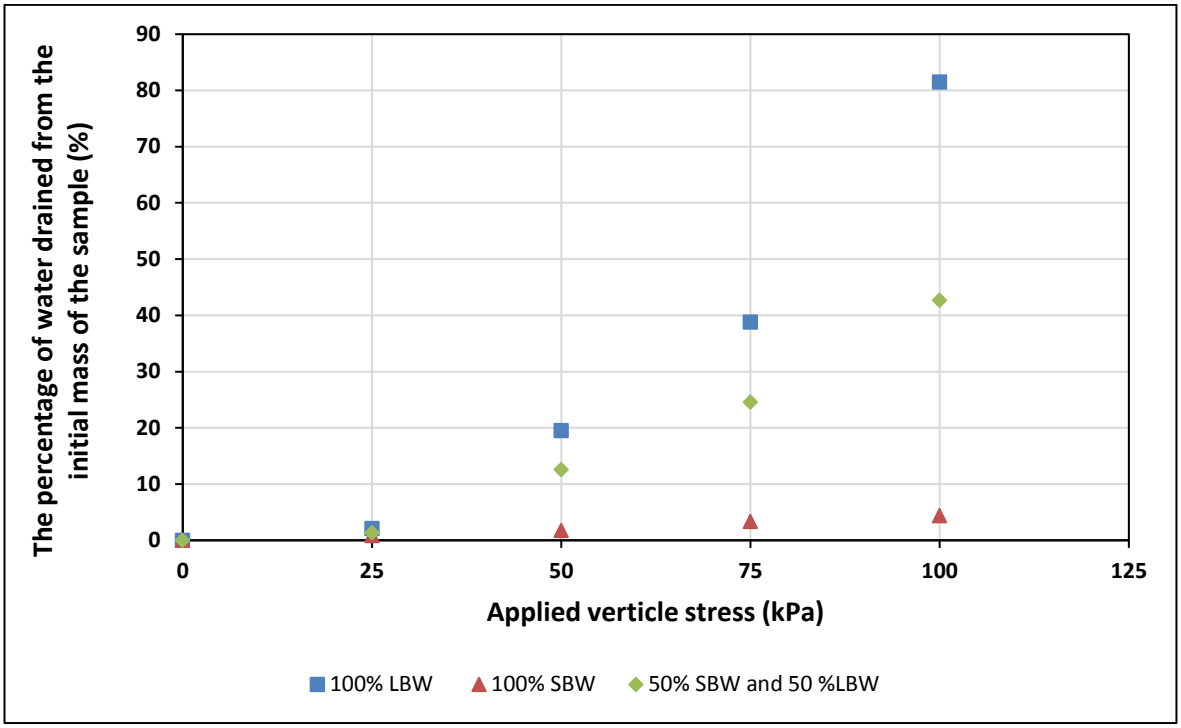

Figure 4-9: The relationship between water bound strength of food material and vertical stress.

However, if a compression cell is not available, food material can be classified using moisture content and material structure. As seen in Table 4-2, the moisture content of LBW food waste (e.g., oranges, lemons, cucumbers, tomatoes, and apples) was higher in comparison to SBW food material (e.g., chicken, rice, pasta, and bread). Moreover, cooking the rice and pasta led to these materials absorbing water. From the experimental results, the release of water under pressure suggest that the water was absorbed by the cell wall of the food material (Figure 2-8) although further work would be needed to confirm this. In addition, the results showed that the moisture content is not the only factor to be considered when classifying the bound water of food materials. For instance, although the moisture content of cooked chicken, rice, and pasta was high, but they classified as SBW waste due to their structure which made migrating water difficult (Figures 4-3 and 4-7). The correlation between moisture content and bound water (LBW and SBW) of food material needs further investigation.

Table 4-2: Moisture content of different types of food waste.

Type of food materials	Moisture content% (based on wet weight basis)
Orange	87.25
Lemon	88.21

Cucumber	97.13
Tomato	95.83
Apple	86.83
Cooked chicken	69.67
Cooked rice	72.86
Cooked pasta	56.91
Bread	34.06

4.3 Physical properties of different waste composition run under saturated condition

The physical properties of different waste types [case 1 (73%), case 2 (58%), case 3 (43%), and case 4 (28%) are described in the following sections. The physical properties include moisture content, saturated moisture content, dry density, and bulk density. The waste compositions of all different waste types are described in detail in Table 3-2. The tests were conducted to assess the impact of organic content on the physical properties of high organic content in MSW. The results of these parameters have been analysed, discussed and compared with previous studies. The test samples were conducted twice to make sure that the results were accurate and reliable.

4.3.1 Particle size distribution (PSD)

The methods and procedures for obtaining particle size distribution (PSD) are described in detail in Chapter 3 (Section 3.6.1). The percentage, total mass and type of the retained waste in each sieve are shown in Table 4-3. The PSD curves of the waste of this study and other studies (Reddy et al. (2009) and Siddiqui (2011)) are shown in Figure 4-10. As Figure 4-10 illustrates, there is a clear difference between the PSD curves of the different types of waste. These differences may be attributed to many factors, such as the waste type, the waste pre-treatment and the degree of waste degradation. Also, the PSD for the sample does not contain any material less than 4 mm as this is smallest size that could be prepared. This may have an impact on how the waste behaves

during compression. As expected, the PSD curve of waste in this study is greater than the PSD curve of MBT waste. Siddiqui (2011) studied the PSD of MBT waste which was pre-treated by eliminating the larger particles and crushable materials from the raw waste. Reddy et al., (2009) showed the PSDs of fresh waste (78% organic matter) and landfilled waste (61% organic matter). The differences in the PSDs can be attributed to the greater amount of finer material presented in the landfilled waste, which may be referred to as the degradation of waste.

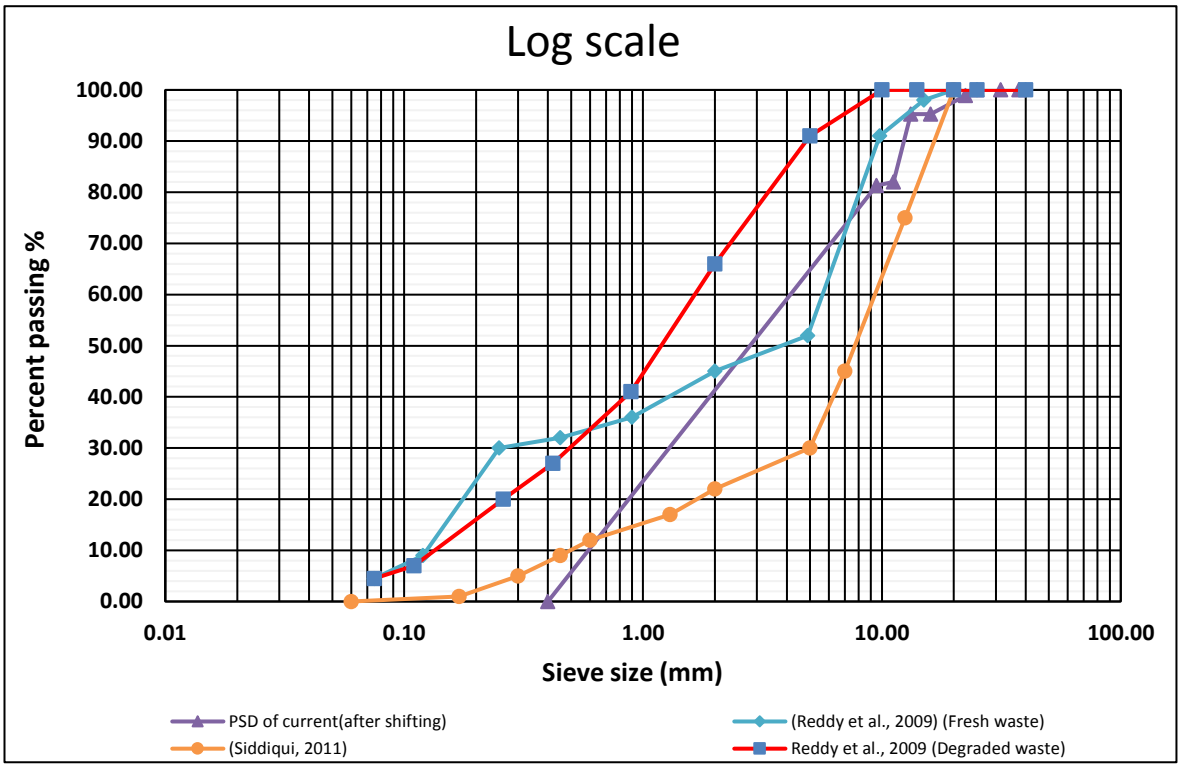

Figure 4-10: PSD comparisons between this study and other studies

Table 4-3: MSW components of the retained waste in each sieve expressed as total weight percentage

	Sieve size (mm)										
Components (%) by mass	**375**	**315**	**250**	**224**	**160**	**132**	**112**	**95**	**4**	**Σ Percent from the total mass (%)**	**Mass of the sample from the total mass (g)**
Plastic				0.76	1.27		0.56	0.69	0.56	2.77	554.86
Carton				0.33			0.16		0.56	1.05	209.00
Paper					1.06					1.06	212.70
Metals					2.409		12.50		5.067	19.00	3995.20
Glass									1.87	1.87	374.60
Organic materials									72.88	72.90	14576.14
Textile									0.39	0.39	77.50

4.3.2 Water content

The water content of the different high organic materials was obtained through two different methods: dry weight and wet weight. Water content was calculated after heating the sample at 70 ˚C until the sample had dried and the change in sample mass was kept constant. The moisture content of different high organic waste types are presented in Table 4-4. The moisture content (on % wet weight basis) decreased from 60%, 49%, 41% and 25%, as the organic fraction of MSW diminished from 73%, 58%, 43% and 29%, respectively. The high moisture content observed in high organic content waste is mainly attributed to the high fraction of organic material present in MSW.

Table 4-4: Moisture content of different high organic content waste types

Samples (food waste content %)	Moisture content (%)	
	Dry weight basis	Wet weight basis
Case 1 (73)	150	60
Case 2 (58)	96	49
Case 3 (43)	71	41
Case 4 (29)	34	25

The water content of the materials in this study was comparable to the results obtained from related studies (Ahmadifar et al., 2015; Gao et al., 2015; Machado et al., 2010; Pandey and Tiwari, 2015; Feng et al., 2016). The differences in the moisture content observed in this study and other studies can be attributed to waste composition, as the organic content is considerably higher than that used in other studies (Table 4-5). It can be clearly seen that the higher the organic content of MSW, the greater the water content obtained (Gao et al., 2015; Reddy et al., 2011; Zhao et al., 2016).

Table 4-5: Water content and composition of different waste MSW composition

Reference	Organic	Paper/ cardboard	Textile/ leather	Plastic	Glass	Metals	Other	Water content (wet basis)	Water content (dry basis)
Case 1, (73%)	72.9	2.1	0.4	2.8	1.9	20.0	-	60	150
Case 2, (58%)	58.30	3.24	0.60	4.26	2.88	30.72	-	49	96
Case 3, (43%)	43.73	4.38	0.81	5.75	3.88	41.46	-	41	71
Case 4, (29%)	29.15	5.51	1.02	7.24	4.89	52.20	-	25	34
Ahmadifar et al. (2015)	78.9	4.8	3.4	9.6	1.7	1.6	-	60 - 65%	NA
Pandey and Tiwari (2015)	39.25	20.50	7.50	17.25	2.75	< 1	11.75	47 - 51%	90 -145%
Machado et al. (2010)	42.9	19.7	4.5	18.7	-	1.5	12.7	50%	NA
Feng et al. (2016)	22.3	23.6	-	18.8	6.2		30.1	32.9	NA

4.3.3 Bulk density (ρ_{wet})

The bulk density of different high organic content waste types was determined under differentially applied loads: 0 kPa to 300 kPa with 25 kPa increments. Initially, the sample was placed in the reactor in its present condition (wet sample). The main reason for not drying the sample prior to placing it in Rowe cell was to ensure that the structure of the organic matter (food waste) was not affected by drying. This also simulated waste in the landfill site, as waste that is sent to the landfill is wet waste. Bulk density was determined using Equation 3.7 (see Section 3.6.5). As it is shown in Figure 4-11, organic content has a critical impact on bulk density, where high organic content waste has higher bulk density compared with low organic content waste. The bulk density of all the cases increases as the vertical stress increases. A high percentage increase in bulk density was observed in this study (152.50%), while the lowest value was 53.36%. This may be attributed to the high amount of water released during compression, leading to an increase in settlement, which resulted in increasing bulk density.

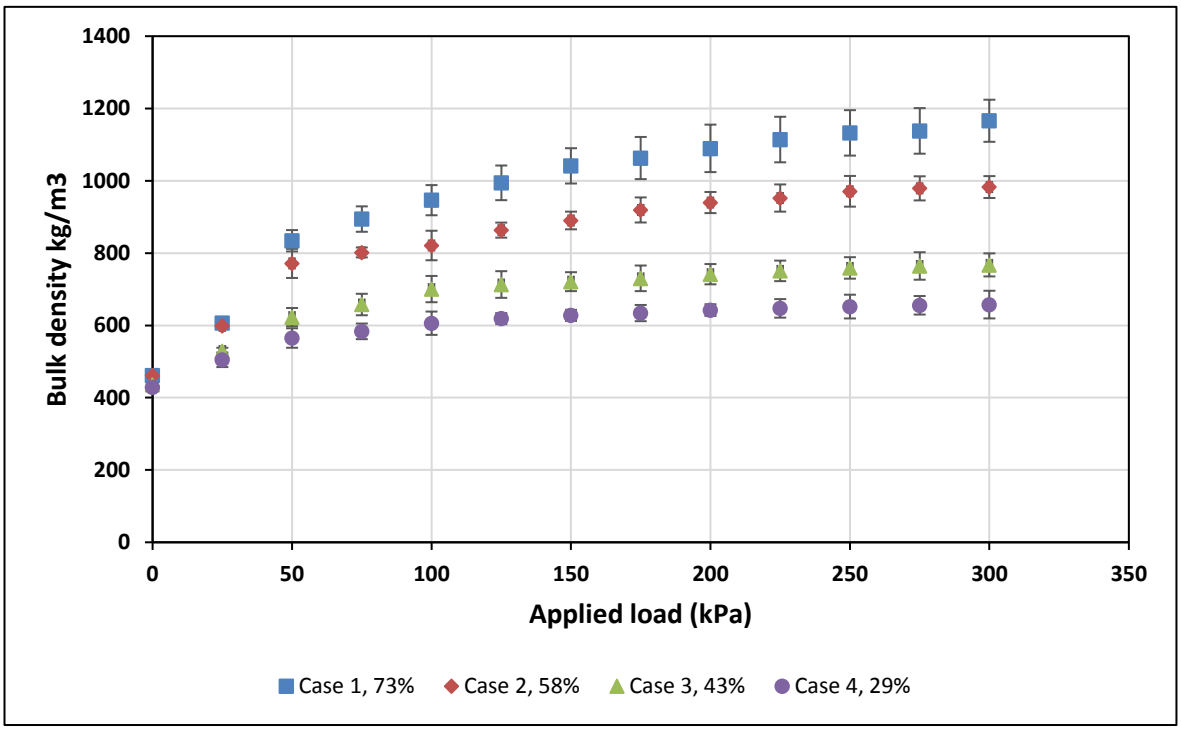

Figure 4-11: Variation of waste bulk density (kg/m3) with vertical stress (kPa)

The bulk density of different organic content waste types in this study is comparable with those reported elsewhere (Figure 4-12) with the exception of aged waste (Beaven, 2000). The difference

between the different studies may be linked to waste composition and water content of the different samples, and the vertically applied stress. The final bulk density of aged domestic waste, reported by Beaven (2000), was higher than the final bulk density found in this study in all cases, which may be related to the high bulk density of the aged waste at the initial stage (P = 0 kPa).

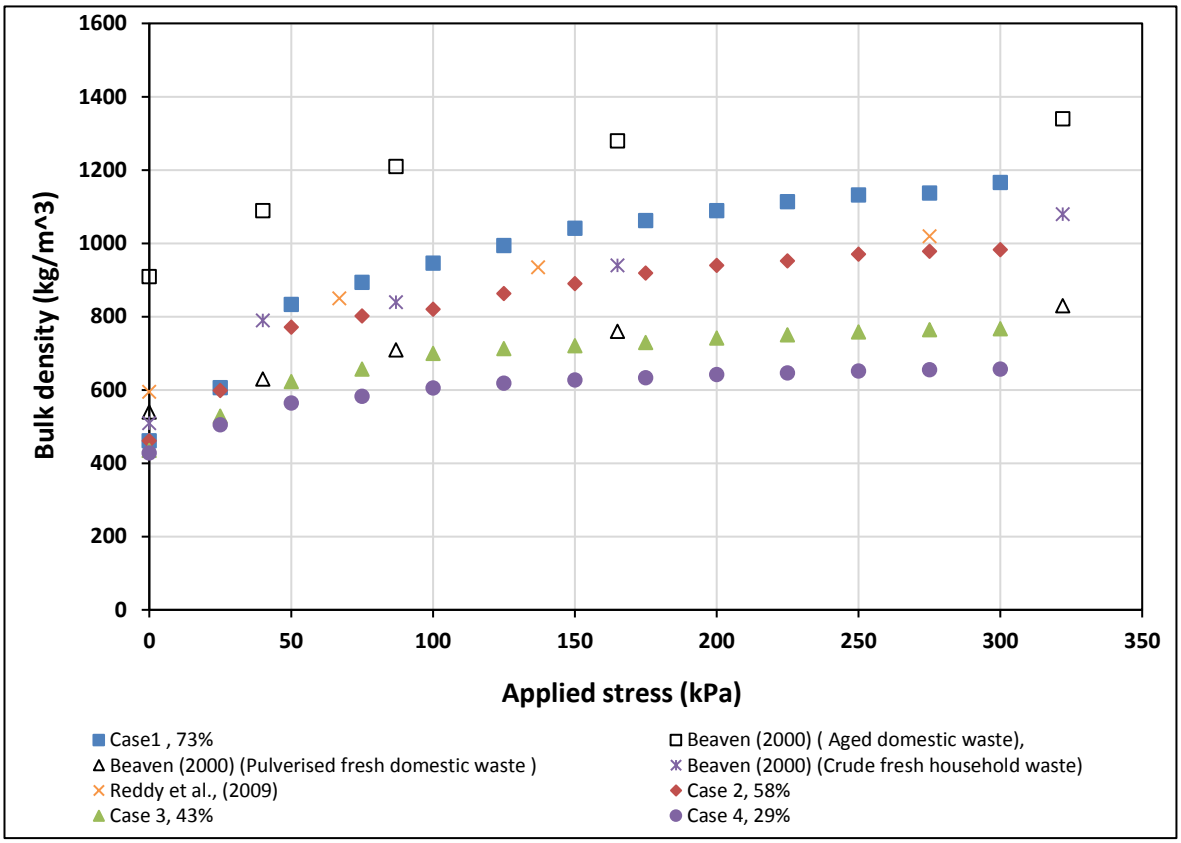

Figure 4-12: Variations of waste bulk density (kg/m3) with vertical stress (kPa) and other related studies.

4.3.4 Dry density (ρ_{dry})

The dry density of different waste types, having different fractions of organic material was determined using Equation 3.8 (see Chapter 3, Section 3.6.6). As can be seen in Figure 4-13, the initial dry density (P = 0 kPa) was 184.82, 236.00, 251.21 and 318.24 kg/m^3 for cases 1 to 4 while at the end stage (P = 300 kPa) dry density of the samples was 467.07, 502.30, 442.64 and 488.07 kg/m^3. The high percentage increase in dry density was obtained in Case 1 (73% organic content) with a value of 152.71%, while the lowest value was found in Case 4 (29% organic contnent) with a value of 53.36% (Table 4-6). The reduction in the dry density of the other two cases (i.e. Case 2 (58% organic content) and Case 3 (43%)) was 112.84% and 76.20%, respectively. The differences of initial

and final dry density across all the cases can be ascribed to the variations of moisture content and bulk density, as dry density varies according to moisture content and bulk density. Thus, higher moisture content and bulk density in high organic content waste lead to a greater increase in dry density with increasing load.

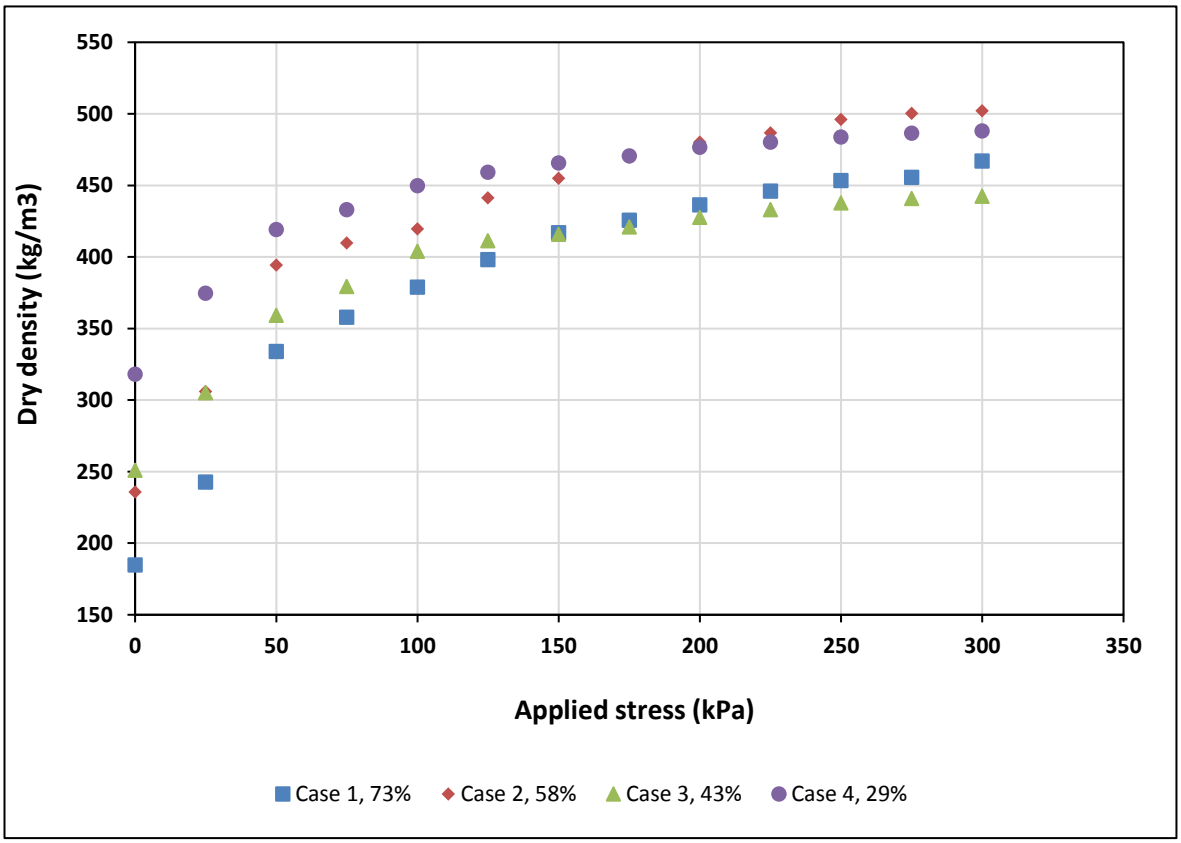

Figure 4-13: Variation of waste dry density (kg/m3) with vertical stress (kPa)

Table 4-6 shows the percentage increase in dry density in this study and that of other studies in order to understand the impact of high organic content waste on dry density. The difference may be attributed to waste composition, water content and the vertically applied stress. Another factor that may impact on dry density is shredding MSW. Shredding MSW increases the void space and allows MSW to compact easily. For instance, the second highest increase (103.84%) was found in the pulverised fresh domestic waste. It is important to note that the moisture content of the sample in Case 1 (73% organic content) was 60% (based on wet weight); therefore, dry density was influenced by high water content.

Table 4-6: Correlations between the vertical stress and increase in dry density in this study and other related studies

Samples (%)	**Moisture content (%)**	**Applied stress (kPa)**	**% increase in dry density from the initial to the end stage**
Case 1 (73)	60 (wet weight)	0-300	152.71
Case 2 (58)	49 (wet weight)	0-300	112.84
Case 2 (43)	41 (wet weight)	0-300	76.20
Case 2 (29)	25 (wet weight)	0-300	53.36
Beaven (2000) (Aged domestic waste)	41.6 (wet weight)	0-322	62.30
Beaven (2000) (Pulverised fresh domestic waste)	28.8 (wet weight)	0-322	103.84
Beaven (2000) (Crude fresh household waste)	34 (wet weight)	0-322	82.35
Reddy et al., (2009a) (Fresh MSW in Orchard Hills landfill)	45 (dry weight)	0-275	71.43
Siddiqui (2011)	36.1 (dry weight)	0-150	49.54

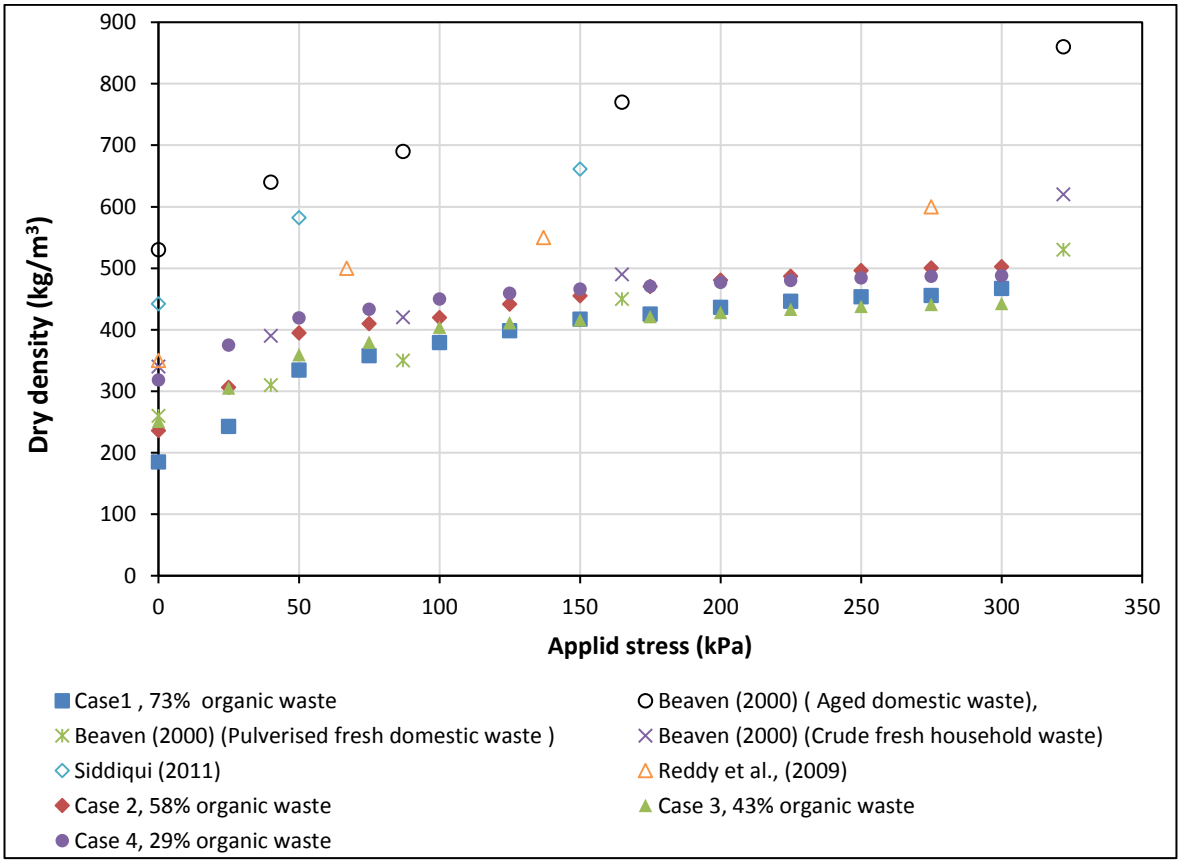

Figure 4-14: Variations of waste dry density (kg/m3) with vertical stress (kPa)

4.3.5 Saturated moisture content

The procedure of obtaining the saturated moisture content was described in Section 3.6.4. The saturated moisture content was obtained under differentially applied loads, 0 kPa and 300 kPa with 25 kPa increments. The initial saturated moisture content (%) at P = 0 kPa was 467%, 349%, 287% and 205%, for waste samples with organic content of 73%, 58%, 43% and 29%, respectively; at the end stage (P = 300 kPa) saturated moisture content was 108.60%, 116.60%, 130.20% and 107.70%. This reduction is expected because as the vertical stress increases, voids within the waste are reduced; the bulk density increases as the moisture is squeezed out. The saturated moisture content was plotted against bulk density, showing a positive relationship between the two (Figure 4 - 15). The general trend of the results for the saturated moisture content was similar to the results reported by Tiwari (2014), where the saturated moisture content ranged from 263.30% to 55.90%, as dry density increased from 280 kg/m3 to 714 kg/m3. The variations in saturated moisture content between this study and the other related studies can be attributed to waste composition, percentage of organic matter and the particle size of MSW. In addition, the high percentage of

saturated moisture content in Case 1 (73%) can be due to the high moisture content of MSW (150% based on dry weight basis), as the amount of water released from high organic content waste was considerably higher than that released from low organic content waste (Figure 4-16). As illustrated in Figure 4 -15, a high reduction in saturated moisture content found in Case 1 (73%) with a value of 66.71% when the vertical stress was applied from 0 kPa to 100 kPa. This high reduction was caused by the large volume of water released, as the vertical stress increased from 0 kPa to 100 kPa (Figure 4 -16). This principle is also applicable to the other waste cases.

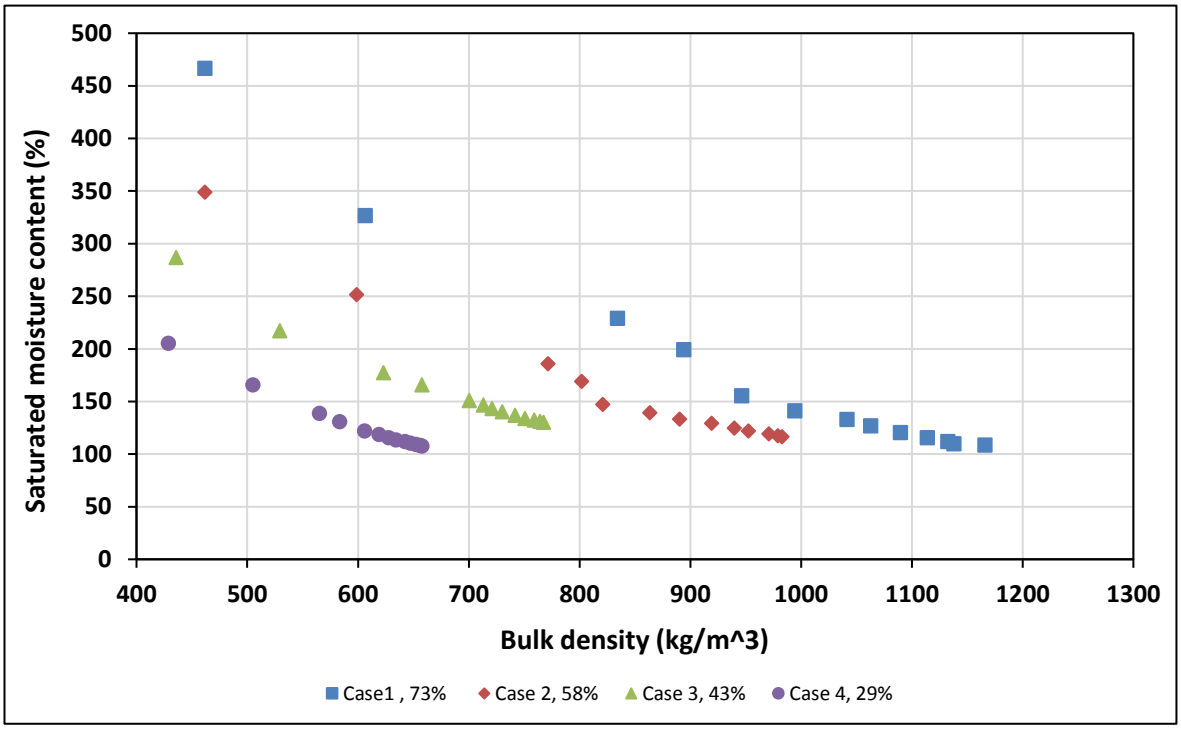

Figure 4-15: Correlations between the saturated moisture content and bulk density

4.3.6 Water (leachate) produced

The water or leachate released from different high organic content waste types was identified under different vertical stresses from 0 kPa to 300 kPa at 25 kPa increments. The effect of organic material can be clearly seen in Figure 4-16, where greater leachate is released due to the compression with higher organic content waste types. The results obtained were expected for high organic content waste types because of their high moisture content, which generates a considerable amount of water.

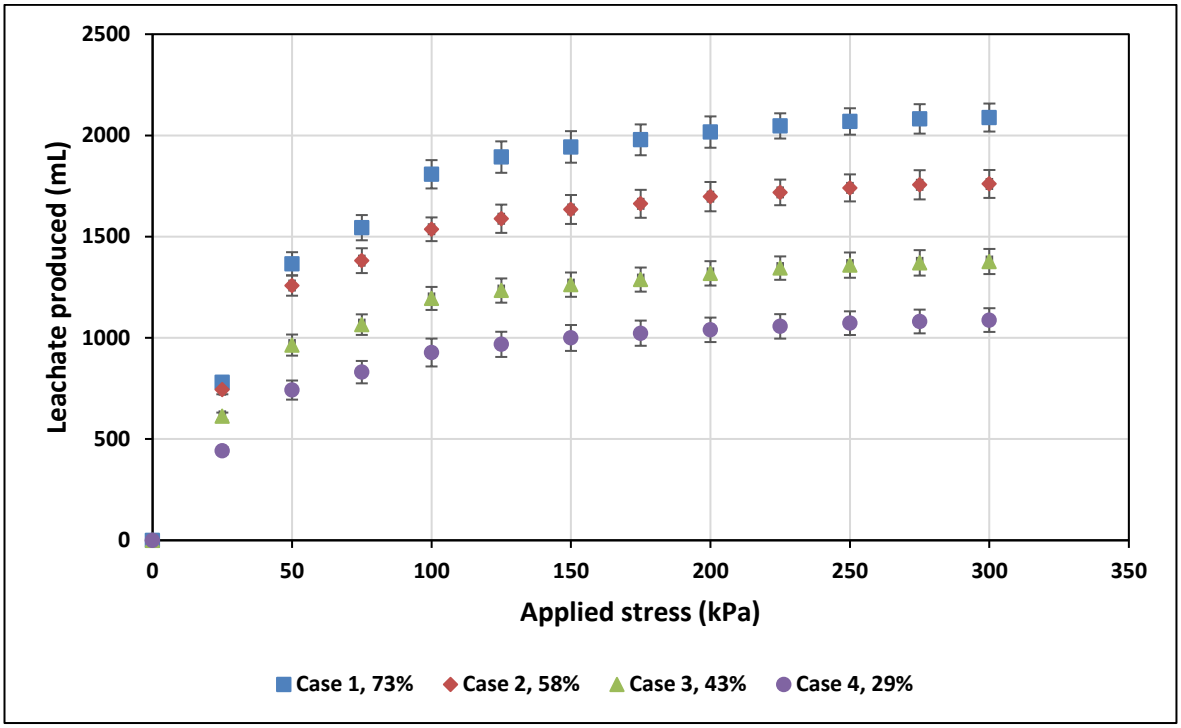

Figure 4-16: Leachate produced from different high organic content waste types

4.3.7 Specific gravity

Specific gravity (particle density) was calculated in accordance with a standard gas jar method (BS 1377-2, 1990). The experiment of specific gravity was conducted twice and the average was taken. The specific gravity reported increased from 1.53, 1.60, 1.69 and 1.90, as the ratio of organic content decreased from 73%, 58%, 43% and 29%, respectively. MSW has lower specific gravity when the fraction of organic content is high (Feng, 2013; Reddy et al., 2011, 2009b; Yesiller et al., 2014). The results of the specific gravity of different organic content waste types were consistent with the results reported by Feng (2013), Reddy et al. (2011), Ojuri (2012) and Reddy et al. (2009b). Feng (2013) stated that the specific gravity of 69.3% of organic content kitchen waste was 1.70 in Chongqing, China. In addition, Reddy et al. (2011) reported that the specific gravity of fresh synthetic MSW, containing 57.5% organic content, was 1.09. The variations in the results between this study and the other related studies may be attributed to waste composition and particle size (fraction of organic content). Particle size of MSW can be considered an important factor that influence the specific gravity. Yesiller et al., (2014) stated that the specific gravity of MSW increased with decreasing waste particle size. Based on the results of these studies and others, the effect of high organic content on the specific gravity of MSW can be clearly seen.

4.3.8 Mass balance

Mass balance was obtained in order to make sure that the results and the water collected were accurate. Table 4-7 shows the weight of water and test samples at the initial and end stages. The change in the weight of the test samples can be related to water loss due to compression. The differences between the weight of the samples at the initial and end stages were 605 g, 479 g, 356 g and 236 g, as the organic fraction of MSW decreased from 73%, 58%, 43% and 29%, respectively. On the other hand, the slight difference in the water added to and released from the test sample may be attributed to waste adsorption, as waste was left for about 24 hours prior to starting the test. Hence, some of the waste such as paper, carton, textile and organic matter absorbed the water.

Table 4-7: Mass balance of different high organic content waste types before and after the test

Samples (organic content %)	Volume of water added at the initial stage (mL)	Weight of sample at the initial stage (g)	Amount of water drained during the test (mL)	Weight of sample at the end stage (g)	Weight of sample after drying at 70 ^{0}C	Weight of water drained after the test (g)	Mass balance error (%)
Case 1 (73)	1840	1500	2088	895	600	275	2.46
Case 2 (58)	1910	1500	1760	1021	767	460	4.96
Case 3 (43)	2020	1500	1377	1144	879	735	7.49
Case 4 (29)	2120	1500	1088	1264	1113	1050	6.02

4.4 Settlement and hydraulic properties of different high organic content waste under saturated conditions

Test were carried out to investigate the impact of organic content on the hydraulic properties of high organic content MSW. The hydraulic properties include total porosity, void ratio, settlement and saturated hydraulic conductivity. The results of these parameters are discussed and compared with the previous studies.

4.4.1 Settlement

The settlement of different high organic content waste types was conducted under differentially applied stresses (i.e. 25 kPa to 300 kPa). At the beginning of the test, the sample was subjected to 25 kPa, and it was kept at this pressure until the consolidation of the test sample occurred (no further settlement happened). This procedure was repeated in 25 kPa increments until the vertical load was 300 kPa. The changes in settlement with the applied loads of different high organic content waste types are presented in Figure 4-17. The general trend of all the cases indicates that settlement increases as the vertical stress increases alongside the vertically applied loads. The overall settlement (%) at the end stage was 60%, 53%, 42% and 35%, as the organic ratio decreased from 73%, 58%, 43% and 29%, respectively. Based on the results of settlement of all the cases, it can be clearly seen that the effect of organic content has a critical impact on the settlement behaviour of MSW.

The highest overall settlement of 51.15% from the initial height was observed in Case 1 (73%), when the vertical stress increased from 0 kPa to 100 kPa. The high settlement observed at 100 kPa may be attributed to waste type, which is considered a compressible material due to its high organic content and the water released during compression. The further reduction in settlement from 125 kPa to 300 kPa, compared with settlement from 0 kPa to 100 kPa, may be attributed to the large amount of water initially released from the sample (Figure 4-16). The slight reduction in settlement, when the vertical stress increased from 125 kPa to 300 kPa, can be related to the small changes in bulk density (i.e. 997.70 to 1169.98 kg/m^3, respectively). Moreover, as the vertical stress increased from 125 kPa to 300 kPa, this brought the particles of the sample closer to each other. Therefore, the resistance of the sample against the vertical load was seen to be higher. This explains the low percentage of settlement reduction across all the cases, when the vertical stress rose from 125 kPa to 300 kPa.

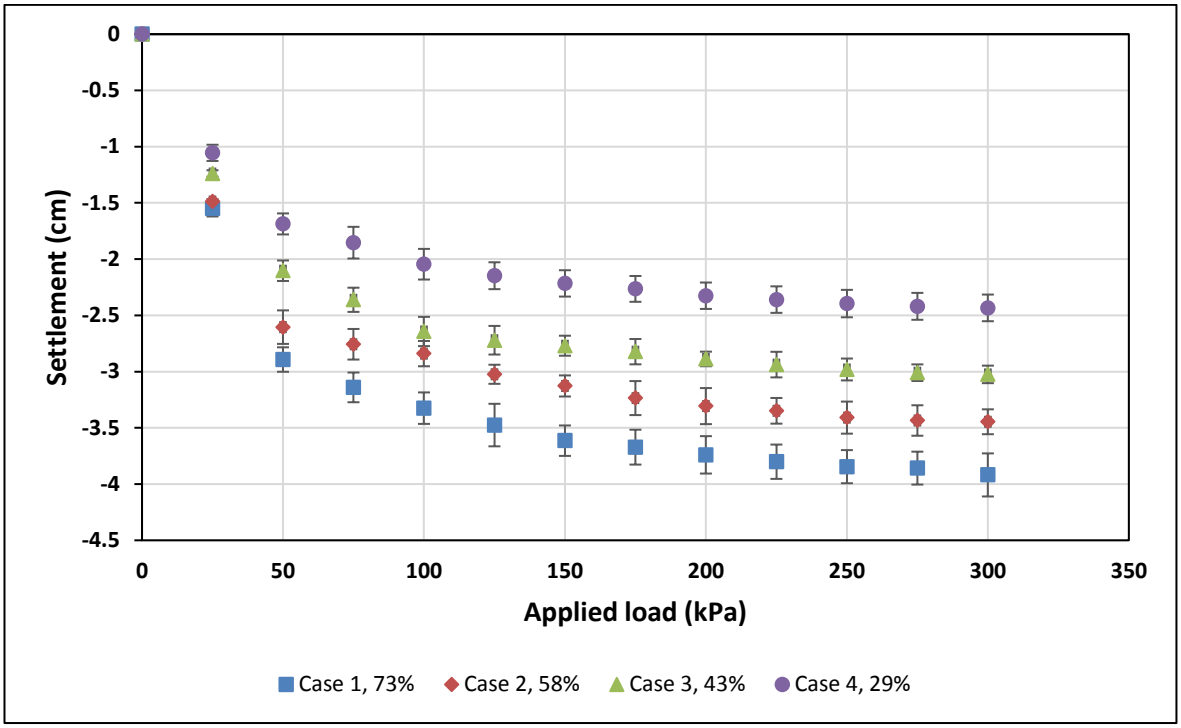

Figure 4-17: Correlations between settlement and vertical stress of different organic content waste types

Several authors have identified the total settlement of different types of waste using different types of reactors (e.g. Benson et al., 2007; Ivanova, 2007; Siddiqui et al., 2012; Zeiss, 1995). The total settlement from these studies ranged from 26% to 5%. The differences observed between this study and the other earlier studies may be attributed to the composition of the waste tested and the stress applied. The settlement results in this study may be reasonable, because the test sample is more susceptible to compression due to the high ratio of organic content. This agrees with the results reported by Elagroudy (2013) who probed the settlement of three different waste compositions: LP (100% paper), LT (100% textile) and LM (40% paper, 40% textile and 20% food waste). The results showed that the final settlement of LP, LT and LM were 18.5%, 8.3% and 20.9%, respectively.

4.4.1.1 Primary compression (C_c)

The primary compression for waste samples showed a decreasing trend from 0.620, 0.544, 0.426 and 0.325 for Case 1 (73%), Case 2 (58%), Case 3 (48%) and Case 4 (29%) (Figure 4-18). C_c increased in tandem with an increase in the organic content because of the larger initial void ratio (see section 4.4.3), which matches the settlement results presented in Figure 4-17. The results obtained from

this study were closely comparable with the results found by Machado et al., (2002) who determined that the range of the C_c of MSW contains about 55% organic matter under different applied loads. They found that the C_c ranged from 0.52 to 0.92 as the applied loads varied between 60 and 640 kPa.

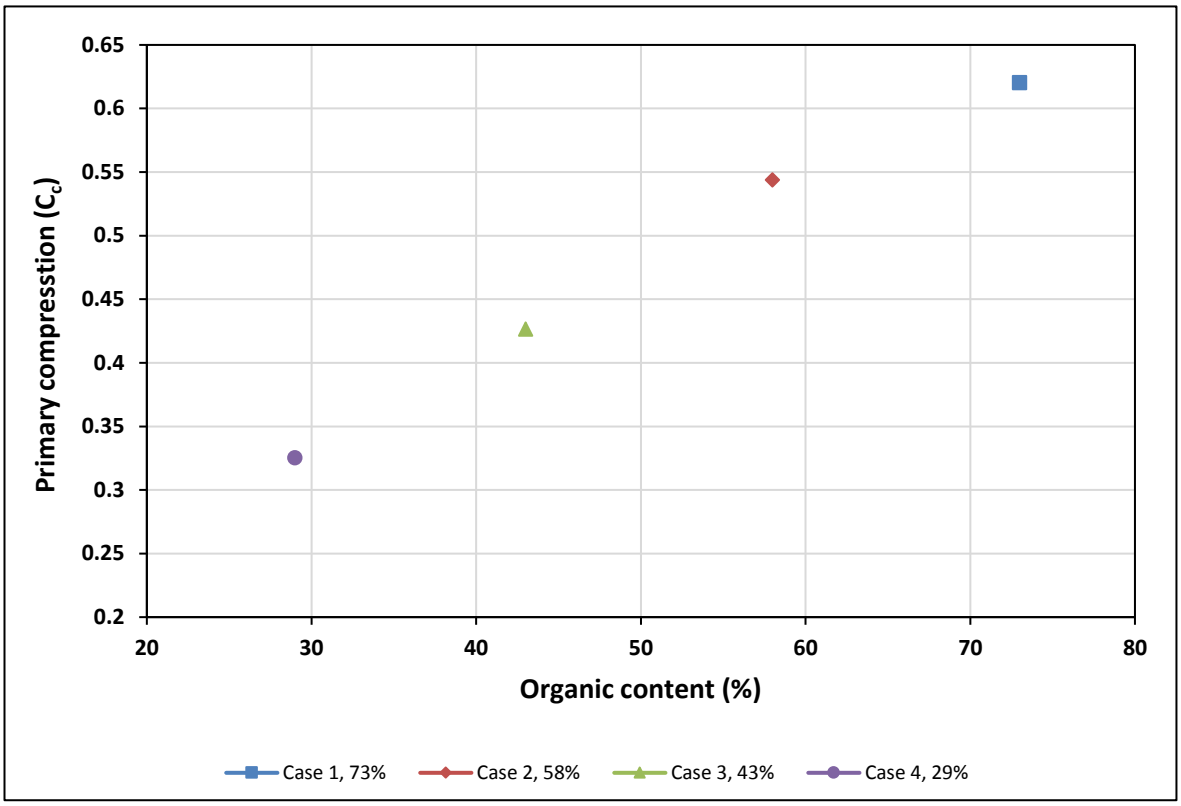

Figure 4-18: Correlation between primary compression and different high organic content waste types.

4.4.1.2 Coefficient of consolidation (c_v)

The coefficient of consolidation (c_v) is a parameter used to describe the rate of consolidation under a change in applied pressure (Indraratna et al., 2015). The coefficient of consolidation (c_v) was determined using hydraulic conductivity of waste. The following equation (4.1) describes the definition of the coefficient of consolidation(c_v).

$$c_v = \frac{k\, E_0}{\gamma_w} \qquad \textbf{(4.1)}$$

where $E_0 = \frac{\Delta\sigma_v}{\Delta\varepsilon_v}$ and $\Delta\varepsilon_v = \frac{\Delta h}{h}$, where Δh is the change in sample height due to an increase in vertical stress of $\Delta\sigma'_v$, k = hydraulic conductivity of waste and γ_w = unit weight of water.

The coefficients of consolidation of different high organic content waste types are presented in Tables 4-8, 4-9, 4-10. As the tables demonstrate, the consolidation coefficients decrease in tandem with an increase in the ratio of the organic content. For instance, when the vertical stress increases from 0 kPa to 50 kPa, the consolidation coefficient (m^2/s) of Cases 1, 2, 3 and 4 increases from 4.44 × 10^{-9}, 6.84 × 10^{-9}, 1.95 × 10^{-8} and 3.54 × 10^{-8} (m^2/s). Similarly, the same increase in the consolidation coefficient has been noted when the vertical stress increases to 150 kPa and 300 kPa. Similarly, the coefficient of consolidation of all the cases in this study were considerably smaller than the results reported by Siddiqui (2011). Siddiqui (2011) results showed that the coefficients of consolidation of MBT waste for the differentially applied loads of 50 kPa and 150 kPa were 6.4 × 10^{-7} m^2/s and 4.3 x 10^{-7} m^2/s, respectively. The differences in the coefficients of consolidation in this study and other studies (e.g. Siddiqui, 2011) may be attributed to the differences in hydraulic conductivity and waste composition.

Table 4-8: Consolidation analysis (50 kPa loading) using hydraulic conductivity of waste

Parameters	Case 1 (73%)	Case 2 (58%)	Case 3 (43%)	Case 4 (29%)
Δσ'v (kPa)	50	50	50	50
k (m/s)	7.12 × 10^{-8}	9.15 × 10^{-8}	1.68 × 10^{-7}	2.25 × 10^{-7}
h (mm)	36.10	38.95	48.97	53.13
Δh (mm)	28.92	26.04	21.03	16.87
E_0 (kPa)	62.35	74.85	116.43	157.49
$c_v = \frac{k E_0}{\gamma_w}$ (m^2/s)	4.44 × 10^{-9}	6.84 × 10^{-9}	1.95 × 10^{-8}	3.54 × 10^{-8}

Table 4-9: Consolidation analysis (150 kPa loading) using hydraulic conductivity of waste

Parameters	Case 1 (73%)	Case 2 (58%)	Case 3 (43%)	Case 4 (29%)
Δσ'v (kPa)	100	100	100	100
k (m/s)	1.82×10^{-8}	2.70×10^{-8}	7.62×10^{-8}	1.04×10^{-7}
h (mm)	28.86	33.72	42.30	47.84
Δh (mm)	36.14	31.28	27.70	22.16
E_0 (kPa)	79.85	107.83	116.28	215.91
$c_v = \frac{k E_0}{\gamma_w}$ (m²/s)	1.45×10^{-9}	2.91×10^{-9}	1.16×10^{-8}	2.25×10^{-8}

Table 4-10: Consolidation analysis (300 kPa loading) using hydraulic conductivity of waste

Parameters	Case 1 (73%)	Case 2 (58%)	Case 3 (43%)	Case 4 (29%)
Δσ'v (kPa)	150	150	150	150
k (m/s)	3.28×10^{-9}	9.10×10^{-9}	2.14×10^{-8}	3.40×10^{-8}
h (mm)	25.81	30.54	39.75	45.66
Δh (mm)	39.19	34.46	30.25	24.34
E_0 (kPa)	98.81	132.94	197.12	281.47
$c_v = \frac{k E_0}{\gamma_w}$ (m²/s)	3.24×10^{-10}	1.21×10^{-9}	4.21×10^{-9}	9.56×10^{-9}

4.4.2 Total porosity (n)

The total porosity of different high organic content waste types was measured based on void ratio under differentially applied loads (i.e. 0 kPa to 300 kPa with increments of 25 kPa). The procedures for obtaining total porosity was described in Sections 3.7.3. The relationship between total porosity

and vertical stress for each loading stage presented in Figure 4-19. The initial total porosity (0 kPa) decreased from 71.65%, 70.16%, 69.41% and 68.12%, as organic content of the test samples declined from 73%, 58%, 43% and 29%, respectively. The high initial porosity in this study is consistent with the findings of Zhao et al. (2012), in that high organic content waste has high initial total porosity. The total porosity at the end stage (P = 300 kPa) dropped to 24.65%, 36.50%, 42.75% and 50.22%, as the organic content waste decreased from 73%, 58%, 43% and 29%, respectively. The highest reduction in total porosity of case 1 (73%) might be related to the higher settlement observed (Figure 4-17), which reduces the water flow within waste. Powrie and Beaven (1999) reported that total porosity decreased from 55.5% to 45.5%, as vertical stress increased from 34 kPa to 463 kPa. Zhao et al.'s results (2012) also confirm this; they reported that the total porosity of MSW, containing 40% food waste, decreased from 68.0 ± 0.7% to 27.7 ± 0.6%, when the bulk density increased from 0.75 ± 0.01 to 0.91 ± 0.02 kg/m^3, respectively. (Zeng et al., 2017). Figure 4-20 shows the correlations between total porosity and bulk density (kg/m^3). The highest reduction in total porosity found in case 1 (73%) is clearly related to the high reduction in bulk density which is related to increase in the total settlement (Figure 4-17).

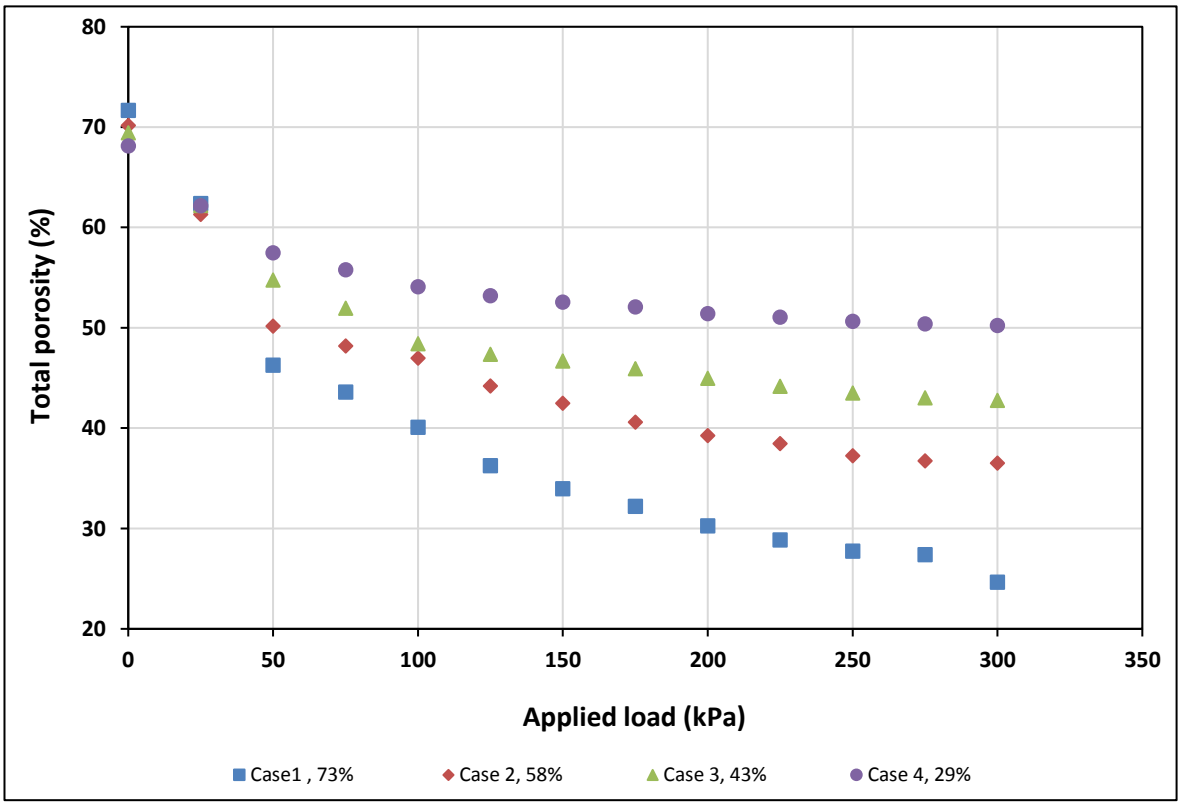

Figure 4-19: Variations of total porosity and vertical stress of different high organic content waste types

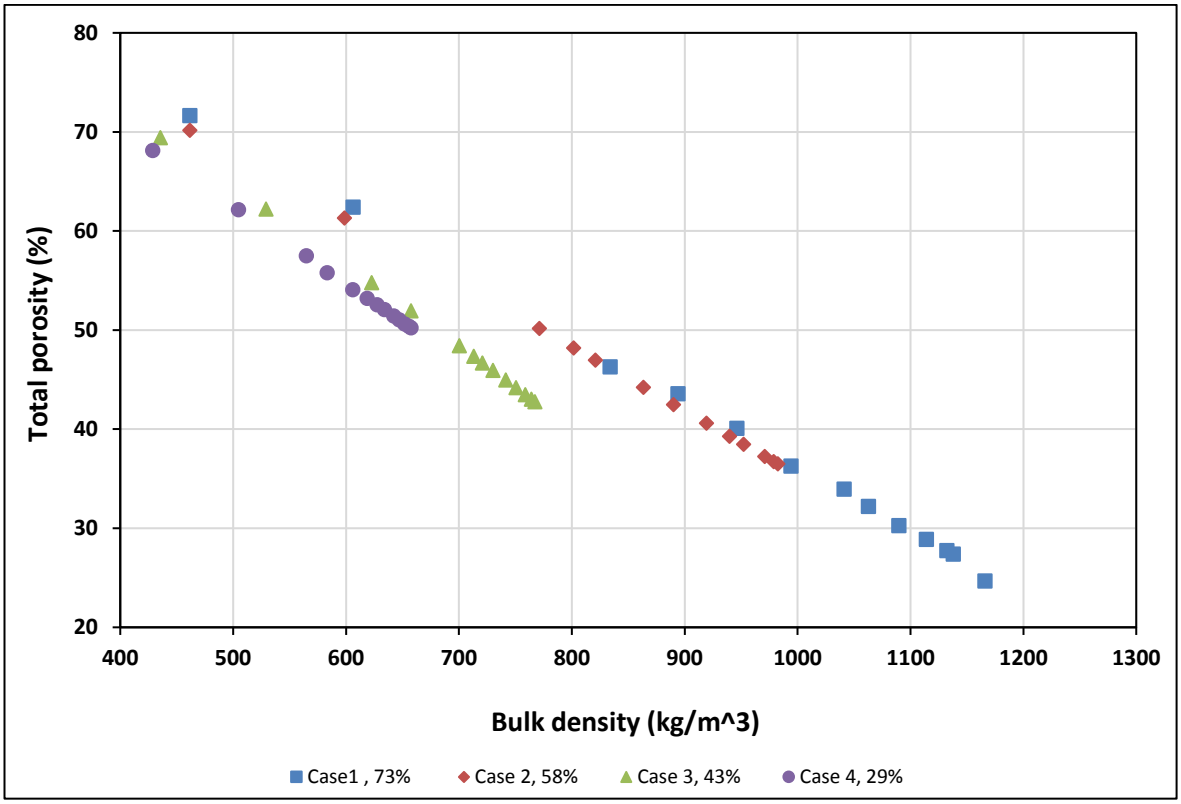

Figure 4-20: Variations of total porosity and bulk density of different high organic content waste types

4.4.3 Void ratio (e)

The void ratio (e) of different high organic content waste types was obtained using the equation (3.13 and 3.14; section 3.7.4). Figure 4-21 describes the relationship between void ratio and vertical stress for each loading stage. The initial void ratio at 0 kPa decreased from 2.53, 2.35, 2.26 and 2.13, as the organic content waste types decreased from 73%, 58%, 43% and 29%, respectively. The variations in the initial void ratio of all the cases may be related to high initial total porosity. In addition, the trend in all the cases shows that high reduction in void ratio was observed in the waste which had highest organic content and gradually decreased in tandem with a decrease in the ratio of organic content. The void ratio at the end stage (300 kPa) was 0.33, 0.57, 0.74 and 1.01, as the organic content decreased from 73%, 58%, 43% and 29%, respectively. This difference in void ratio in the last stage may be attributed to the high compressibility of the test samples, where void ratio is considered to be a key factor for assessing the compressibility of waste. The results of this study were consistent with those reported by Zhao et al. (2012) who studied the influence of synthetic MSW on void ratio with different high organic food waste types (53.40%, 46.73% and 40.05%) under

different vertical loads, ranging from 0 kPa to 400 kPa. The high initial void ratio was 4.266, found in 53.40% of food waste, while the void ratio was 3.269 and 3.671 for 46.73% and 40.05%, respectively (Figure 4-22). The variations in the initial void ratio results in this study and the results obtained by Zhao et al. (2012) can be due to the composition of the organic content, as in this study the organic matter is based on LBW and SBW.

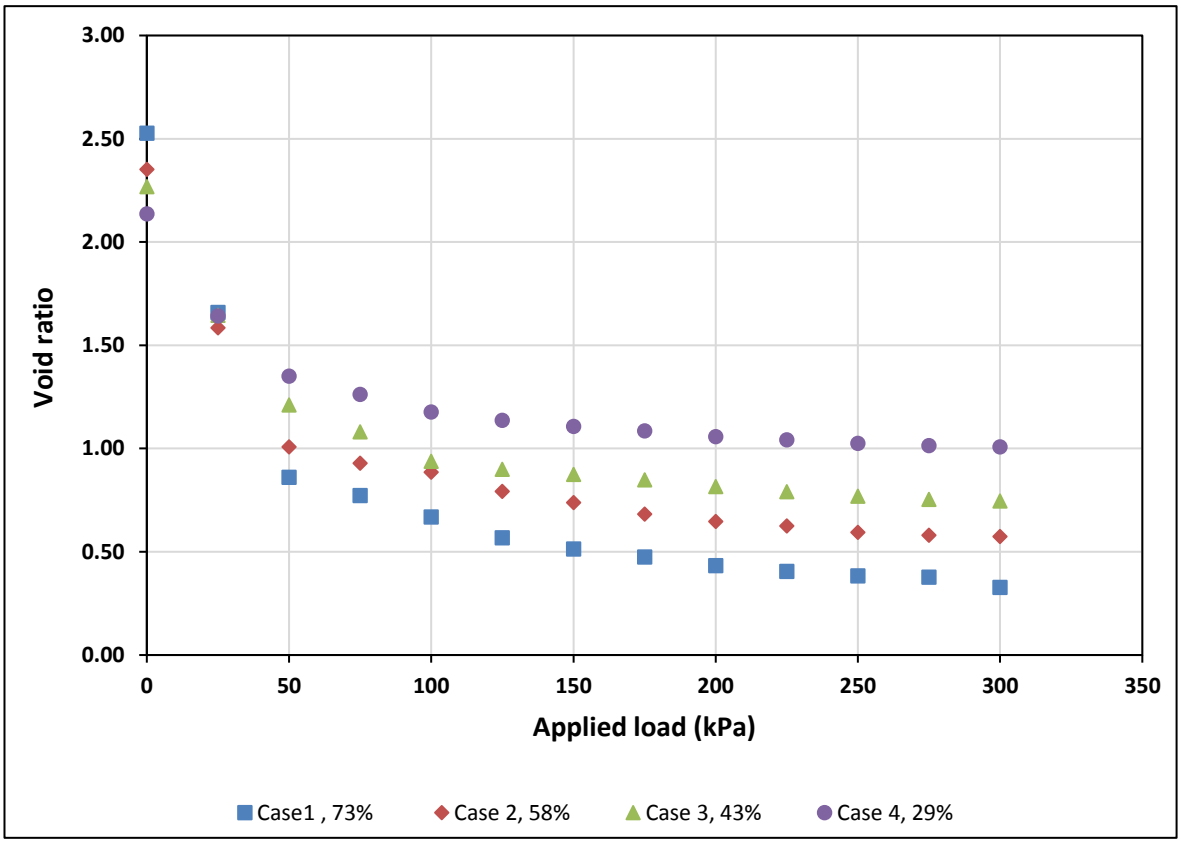

Figure 4-21: Relationship between void ratio and vertical stress of different high organic content waste types.

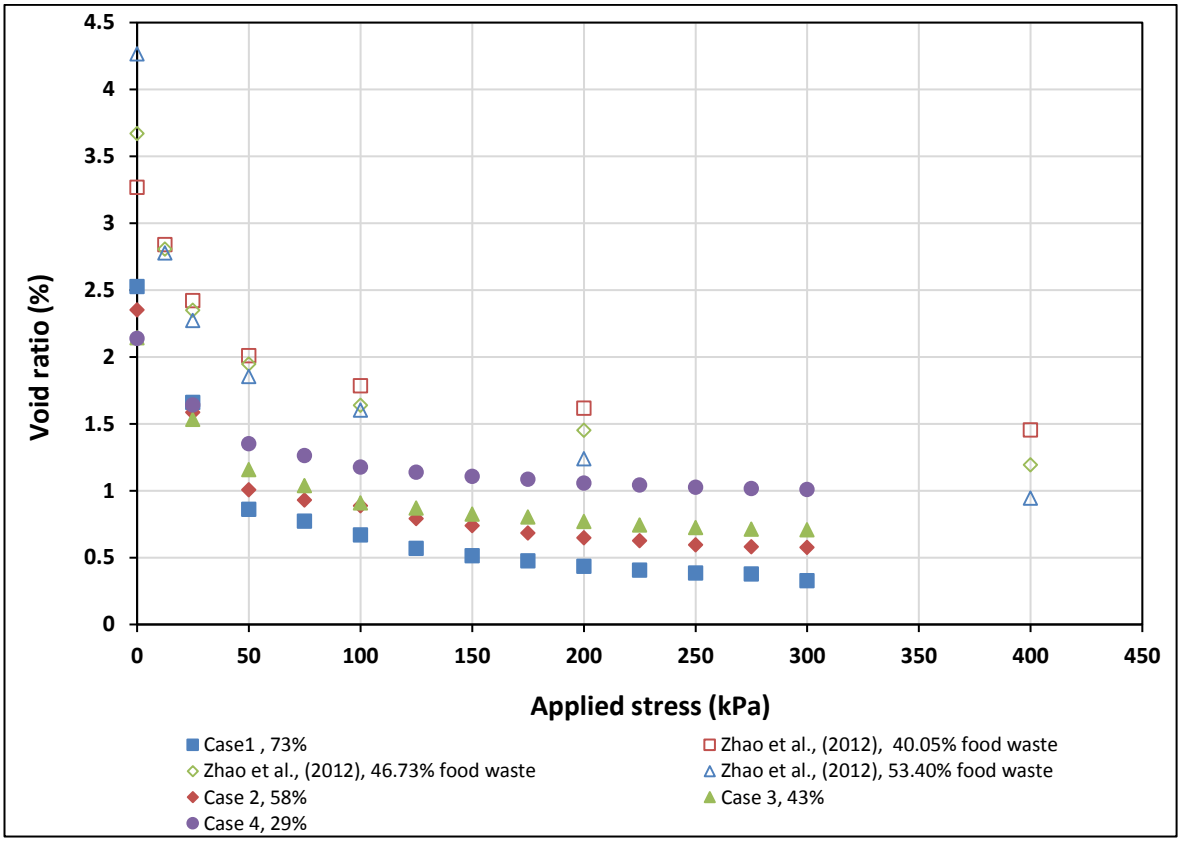

Figure 4-22: Relationship between void ratio and vertical stress of this study and other related studies

4.4.4 Saturated hydraulic conductivity (k_s)

The saturated hydraulic conductivity of fresh MSW with high organic content values of 73%, 58%, 43% and 29% were carried out for differentially applied stresses (i.e. 50 kPa, 150 kPa and 300 kPa). The hydraulic conductivity test was conducted twice, and the average was reported. As it can be clearly seen in Figure 4-23, the saturated hydraulic conductivity was clearly affected by bulk density, where it increased in tandem with an increase in the vertical stress (see section 4.3.3). The greatest reduction in hydraulic conductivity was observed in Case 1 (73% of organic matter) organic matter, where the hydraulic conductivity (m/s) decreased from 7.12×10^{-8} m/s to 3.28×10^{-9}, as the vertical stress increased from 50 kPa (ρ_{wet} ~ 836.95 kg/m^3) to 300 kPa (ρ_{wet} ~ 1169.98 kg/m^3), respectively. A less reduction in the hydraulic conductivity was found in Case 4 (28% of organic matter) with a value of 2.25×10^{-7} m/s to 3.40×10^{-8} m/s, as the vertical stress increased from 50 kPa (ρ_{wet} ~ 566.95 kg/m^3 to 300 kPa (ρ_{wet} ~ 659.78 kg/m^3) respectively. The higher organic content material has lower hydraulic conductivity, mainly because of the material structure where it is considered to be more

compressible compared with low organic content waste types. In addition, the reduction in saturated hydraulic conductivity may be attributed to high reduction in pore size in the high organic content waste types, which is likely to result in a reduction of water flowing out through the waste (see section 4.4.2). Therefore, reduction in organic matter leads to a higher pore size, which results in a higher value of hydraulic conductivity. The hydraulic conductivity of all the cases in this study is compared with the other studies in Figure 4-24 and 4-25. The hydraulic conductivity of all cases in this study was clearly lower than the hydraulic conductivity of the previous studies. The variations on the hydraulic conductivity between this study and other related studies can be contributed to the difference in waste compositions and particles size of MSW. Another possible explanation for the variations in the saturated hydraulic conductivity between the results of this study and the findings from other studies is the particle size of MSW, as the saturated hydraulic conductivity grows if the particle size increases. On the other hand, the correlations between hydraulic conductivity and void ratio evidently point to the fact that high organic content waste has low permeability.

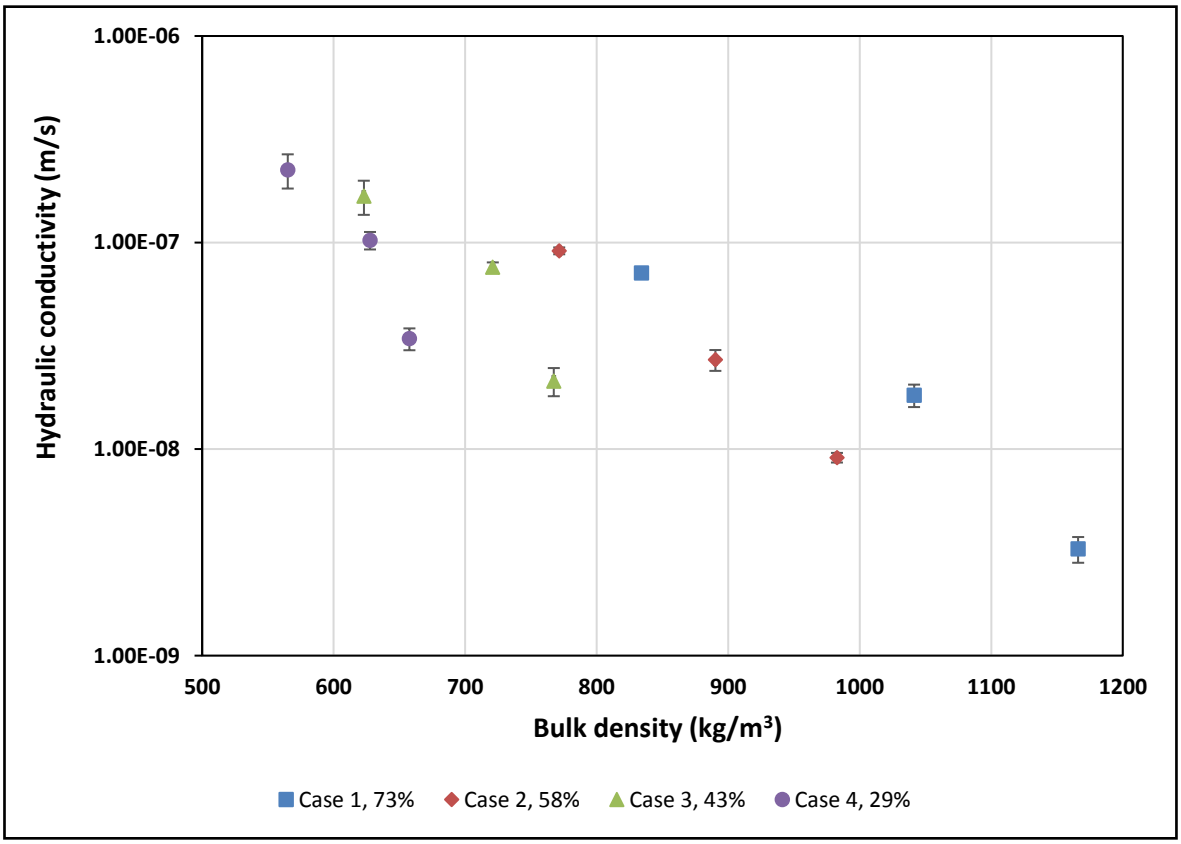

Figure 4-23: Correlations between hydraulic conductivity and bulk density of different high organic content waste types.

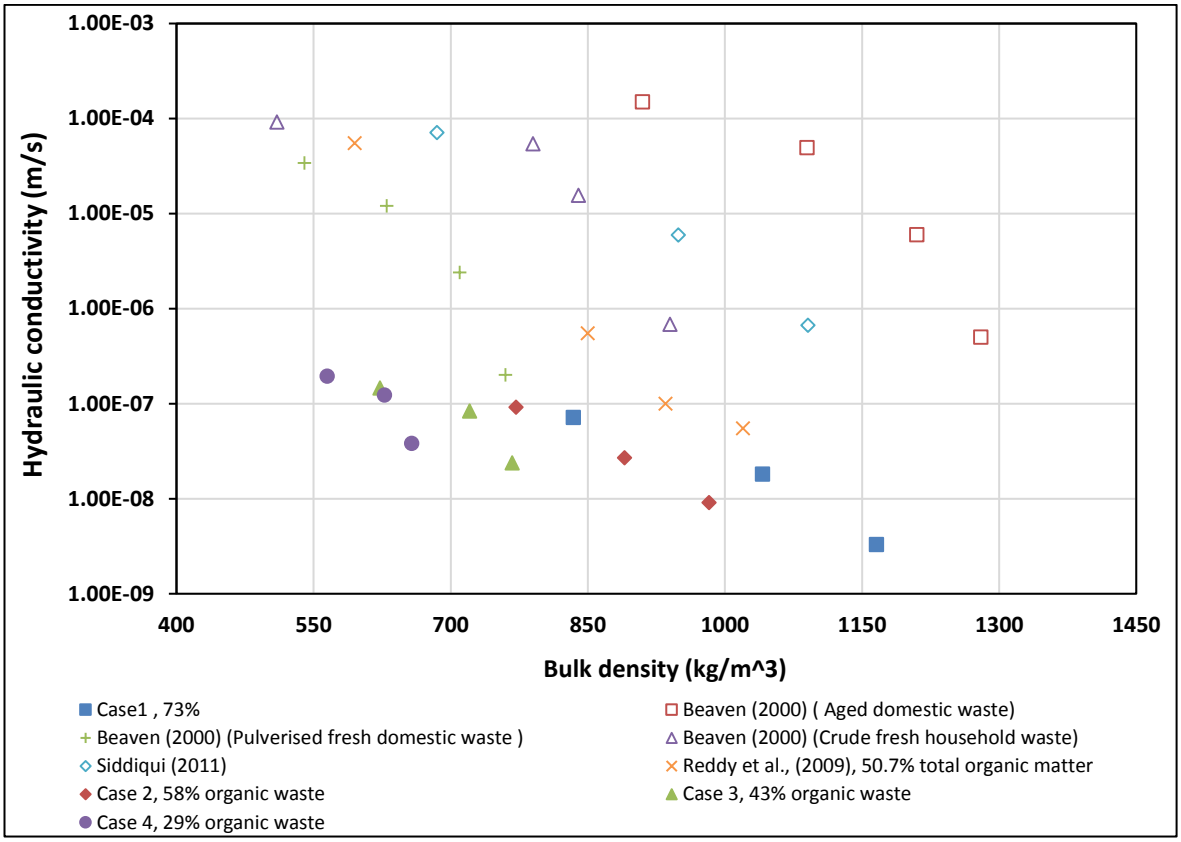

Figure 4-24: Correlations between hydraulic conductivity and bulk density of this study and other related studies

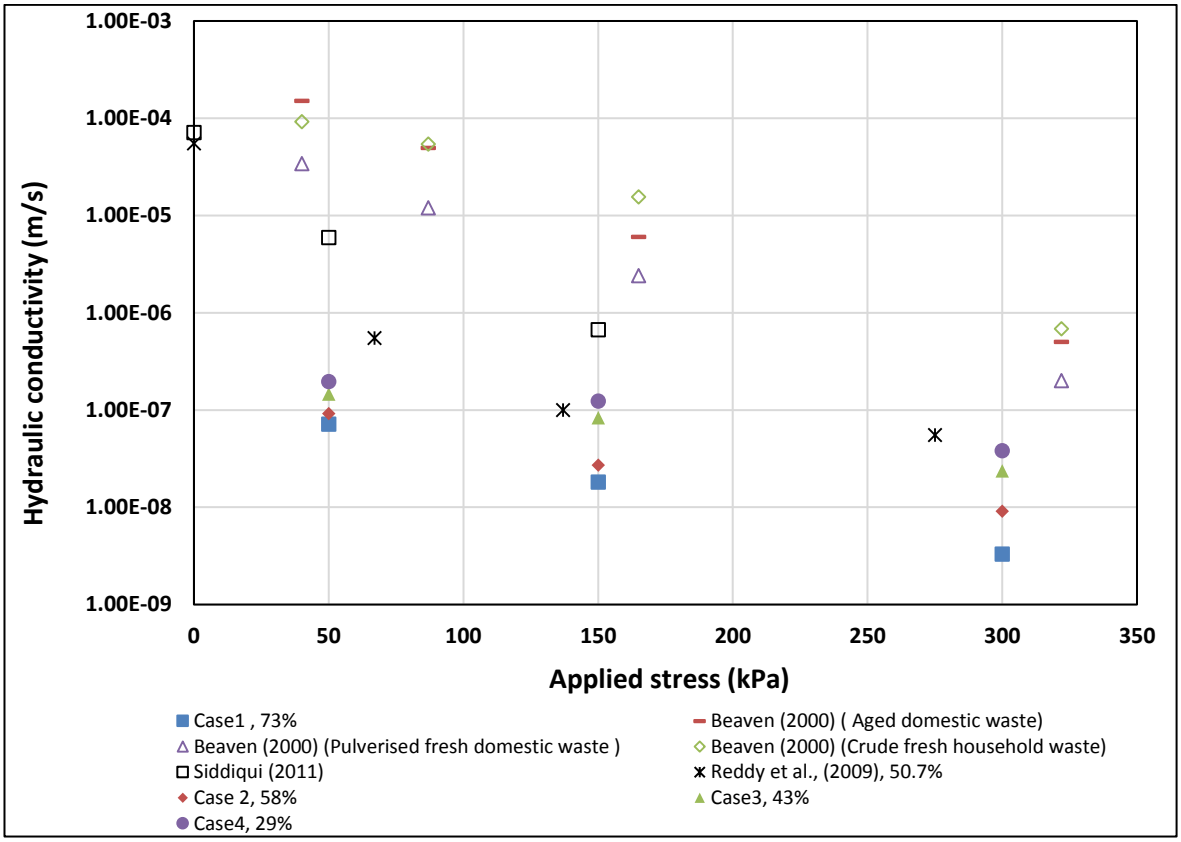

Figure 4-25: Variations of hydraulic conductivity and vertical stress of the current and previous studies.

The variations in the saturated hydraulic conductivity with dry density are presented in Figure 4-26. The literature review revealed that several studies have examined the hydraulic conductivity of waste as a function of density (Table 3-3). The general trend of a decreasing saturated hydraulic conductivity and an increasing dry density in this study follows the same trend as those reported by Beaven (2000), Siddiqui (2011) and Reddy et al. (2009) (Figure 4-26). The high dry density found in this research leads to a decreasing pore size of MSW and, therefore, reduces the flow of the water path within the waste, which causes a reduction in the saturated hydraulic conductivity.

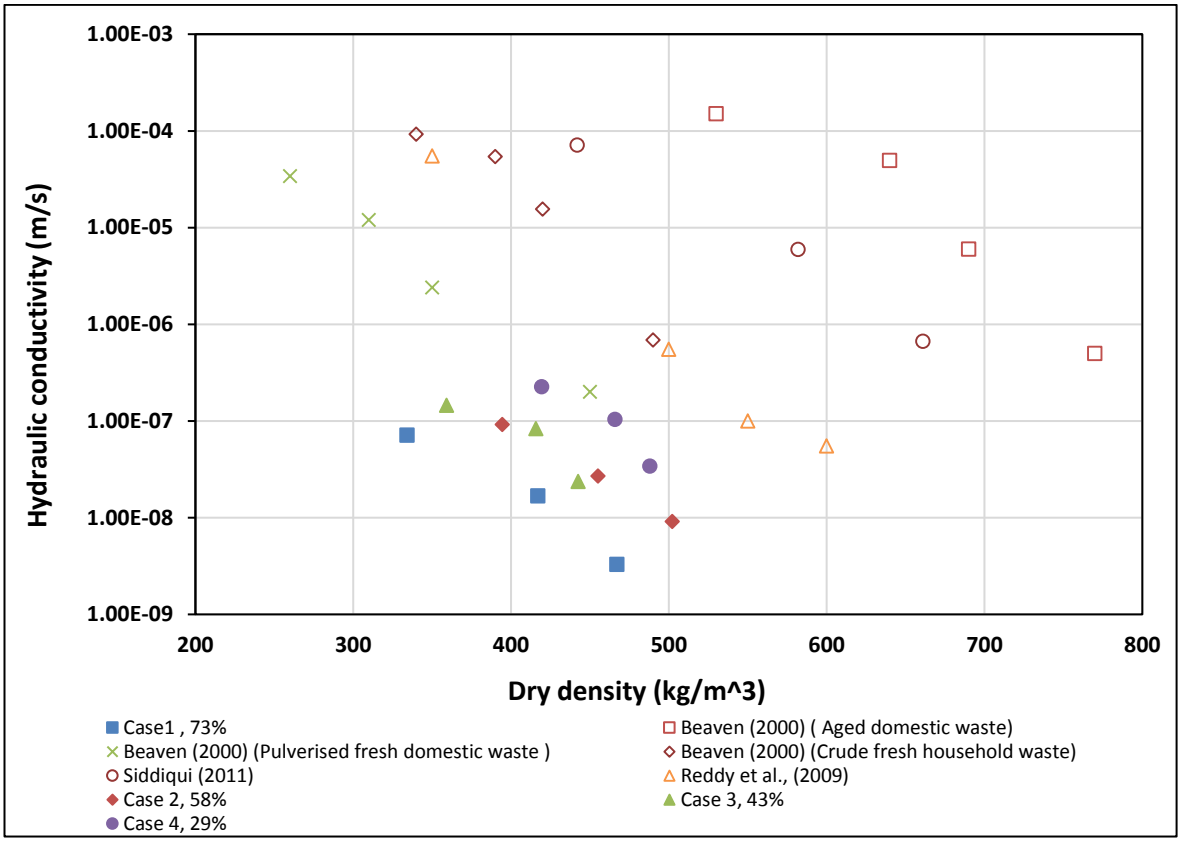

Figure 4-26: Correlation between hydraulic conductivity and dry density of different high organic content waste types.

4.5 Biogas (CH_4 and CO_2)

The methods and results of determining biogas produced (CH_4 and CO_2) of different high organic content wastes under anaerobic condition were determined and analysis (see appendix A). The main objective of not placing the method and results in chapter 3 and 4 because it was not related to the main goal of this research

Chapter 5 Reconciliation of Rowe cell data sets

5.1 Introduction

The reconciliation of Rowe cell data sets was carried out to assess the mass balance of the initial and final states of the Rowe cell tests results for each sample and to derive variables which will be used in the conceptual model in chapter 6. Some of the results of the mass balance for both 100% food tests and mixed wastes tests were also discussed in Chapter 4 (see section 4.2.4 and 4.3.8). Most of the parameter values were obtained from test measurements whereas others were derived from equations described below.

5.2 Test procedure using Rowe cell

All of the samples had a mass of 1500 g (see Table 3-2) which is the sum of the mass of both the non-food and food solids, including the mass of the bound or trapped liquid within the food. The sum does not include any free or added liquid in the pore space formed by the solid particles. The pore space in the sample placed in the Rowe cell can be classified into two different types: one type is found within the cellular structure of each food particle, while the other comprises the fully connected zone formed by the interstices between the solid particles. To distinguish between the two types, the former is called the cellular pore space and the latter the sample pore space. The sample was placed in the Rowe Cell without any additional water; however, by the time the sample had been assembled in the Rowe cell, some liquid may have left the bound state and become part of the free pore liquid. This liquid fraction could not be measured in the Rowe cell tests. It was assumed that the pore space was equal to the water added, which does not include any water derived from food waste already in the pore space; this liquid is likely to be a small fraction of the pore space at the start of the test.

In the 100% food waste test, no additional liquid was added to the sample pore space. Whereas in the mixed waste (food + incompressible materials) tests, the sample pore space was fully saturated prior to loading.

The procedures and methods used for all test samples using Rowe cell were discussed in Chapter 3 (section 3.4). At the end of the test, the wet mass of the sample was measured (M_{wet}^{f}). The sample was then oven-dried, and the dry mass recorded (M_{dry}) . The difference between these masses was

assumed to be the mass of the liquid retained in the sample, apart from any additional liquid that was drained after the cell was unloaded and while the sample was being removed for weighing. Any unrecorded mass detected (m_e) as a result of mass balance in Tables (4.1) and (4.6) for both 100% food and mixed wastes test respectively was applied to the water released after the cell was unloaded in order to correct the overall mass balance of the test.

5.3 Reconciliation of the Rowe cell tests

The essential variables used to reconcile the initial and final states of the Rowe cell test results for each sample in terms of water produced from the organic material (food material) during the compression were determined. These variables include the mass of non-food solids (m_S), the initial mass of trapped liquid within the cellular material (m_T^0), the mass of cellular material (m_C), the volume of non-food solid particles (v_S), the volume of cellular materials (v_C), the volume trapped liquids within the cellular material (v_T), the material particle density (ρ_s) and cellular material density (ρ_C). Thus, the volume of the sample in the Rowe cell can be defined as:

$$V = H\,A = v_S + v_C + v_T + v_F + v_G \qquad \textbf{(5.1)}$$

where A is the cross-section area of the Rowe cell, H is the depth of the sample in the cell, v_F = volume of free liquid occupying the pore space (that is, the volume of water added to saturated the sample) , and v_G = volume of gas occupying the pore space..

5.3.1 Determining the essential masses of the saturated and unsaturated conditions

The mass of non-food solids (m_S), liquid trapped by the cellular material (m_T), ; liquid remaining in the sample at the end of the test (m_F^f), and the cellular material (m_C) of the samples in both the saturated and unsaturated tests was determined. The saturated condition refers to tests in which food waste is mixed with other incompressible material, whereas experiments under the unsaturated condition were conducted for 100% food material (see section 3.9 and 3.10, Chapter 3). The following equations show the determination of each required mass in the reconciliation process:

$$M_{wet}^0 = m_s + m_c + m_T \qquad \textbf{(5.2)}$$

where M_{wet}^{0} is the initial mass of the waste sample

The values of m_s and m_c will remain at their initial values throughout the test, and is equivalent to the dry mass (M_{dry}) of the sample which is measured by a drying test:

$$m_s + m_c = M_{dry} \quad \textbf{(5.3)}$$

The value of the fraction by mass of the food waste w_f is known from the characteristics of the waste. This means that,

$$m_c + m_T^0 = w_f M_{wet}^0 \quad \textbf{(5.4)}$$

So, equation (5.2) can be rearrange to give equation (5.5) at the start of the test

$$M_{wet}^0 = m_s + m_c + m_T^0 = M_{dry} + m_T^0 \quad \textbf{(5.5)}$$

The mass of the 'solid' components in the sample can therefore be calculated as follows,

$$m_s = \left(1 - w_f\right) M_{wet}^0 \quad \textbf{(5.6)}$$

$$m_T^0 = M_{wet} - M_{dry} \quad \textbf{(5.7)}$$

$$m_c = M_{dry} - \left(1 - w_f\right) M_{wet}^0 \quad \textbf{(5.8)}$$

The mass of liquid remaining in the sample at the end of the test (m_F^f) can be expressed as:

$$m_F^f = M_{wet}^f - M_{dry} + m_{res} \quad \textbf{(5.9)}$$

where M_{wet}^f is the mass of wet sample after the test, M_{dry} is the mass of dry sample, and m_{res} is the mass of liquid remaining in the cell after the sample was unloaded (including any unrecorded mass detected (m_u) as a result of mass balance).

5.3.2 Determining the required volumes of the saturated and unsaturated conditions

The initial volume of the sample in the Rowe cell is equal to the sum of v_p (volume of the particles) plus the volume of voids v_v. The volume of the particles v_p is equal to the sum of the volume of cellular material (v_C), the volume of non-food solid particles (v_S) (which are considered not to

contain liquid) and the volume of trapped liquid (v_T) included within the cellular material. Thus, $v_S + v_C + v_T$ in equation 5.1 can be expressed as:

$$v_P = v_S + v_C + v_T \quad \textbf{(5.10)}$$

The liquids trapped in the cellular material will be treated as part of the solid phase while trapped (even though they are liquids). They become part of the liquid phase when they are released due to compression and join the undrained (or free) liquid in the pore space.

The determination of the essential volume of non-food solids (v_S); the initial trapped volume (v_T); the cellular volume (v_C); the initial pore-water volume (v_F^0) and the final pore-water volume (v_F^f) involves the following equations for each parameter:

$$v_S = \frac{m_S}{\rho_{SP}} \quad \textbf{(5.11)}$$

$$v_T^0 = \frac{m_T^0}{\rho_L} \quad \textbf{(5.12)}$$

$$v_C = \frac{m_C}{\rho_C} \quad \textbf{(5.13)}$$

ρ_L = the density of liquid.

ρ_C = the density of cellular material.

ρ_{SP} = the density of non-food solid particles.

v_F^0 = the volume of water added to the test samples in the initial stage.

v_F^f = the volume of water released from the test samples in the end stage.

5.3.3 Estimation of the volume fraction of the total cellular structure

The fraction of trapped liquid in relation to the total cellular material plus the initial trapped liquid is delineated as α_T. The α_T varied from 0-1 depending on the material. Since the results allowed v_T and v_C, to be determined, α_T can be expressed as:

$$\alpha_T = \frac{v_T}{v_C + v_T} \quad \textbf{(5.14)}$$

5.3.4 Determining the density of cellular and non-food solid particles material

The values of particle density were measured using the gas jar method (BS 1377-2, 1990). The density of the cellular material can be found from the volume weighted summation of the density of its components, for example:

$$\rho_C = \frac{\left(v_i\rho_i + v_j\rho_j\right)}{v_i + v_j} = \frac{\left(m_i + m_j\right)}{\frac{m_i}{\rho_i} + \frac{m_j}{\rho_j}} = \frac{1}{\frac{m_i}{\rho_i} + \frac{m_j}{\rho_j}} \quad \textbf{(5.15)}$$

where m_i and m_j are the mass fractions of food waste or solid.

The same equations (5.15) can be used to calculate the density of non-food solid particles when a mixture density is known, together with the other components' density, therefore the density of non-food solid particle is defined as:

$$\rho_{SP} = \frac{m_i}{\frac{1}{\rho_s} - \frac{m_j}{\rho_C}} \quad \textbf{(5.16)}$$

In this regard, the particle density of different fractions of food waste types were measured for solids, and food mixture were measured for the whole sample. Thus, the non-food solid particle density in the mixture was determined by extracting using equation (5.16). The results for solid particle density (g/cm^3) were 3.26, 2.45, 2.23, and 2.37 for cases (1), (2), (3), and (4) respectively. In theory the solid particle density, which in itself is the result of a mixture of particles with quite a wide range of densities, should be constant and independent of the food fraction. However, as always with waste materials, some variation is to be expected from one sample to another. Therefore, in the reconciliation process, the solid particle density of mixed waste used was assumed to be 2.58 g/cm^3 which represents the average of the values that were measured from the experimental work.

5.4 Mass balance

It is assumed that mass in the solid phase and liquid phase is conserved independently. That is, no significant mass transfers occur from one phase to another due to, for example, dissolution, degradation or evaporation. During all stages in the test, the total mass of solids and liquids in the testing system remained constant. Ignoring the mass of gas, this may be expressed as:

$$m_s + m_c + m_T + m_F + m_D = m_s^0 + m_c^0 + m_T^0 + m_F^0 + m_D^0 \quad \textbf{(5.17)}$$

where m_F is the mass of pore water volume and m_D is the mass of drained liquid.

Equation (5.17) can then be split as follows:

$$m_s + m_c = m_s^0 + m_c^0 \quad \textbf{(5.18)}$$

$$m_T + m_F + m_D = m_T^0 + m_F^0 + m_D^0 \quad \textbf{(5. 19)}$$

In the liquid mass balance, equation (5.19), the value of each term is equivalent to its volume, since we can assume that the liquid density throughout the system is ρ_L= 1 g/cm^3. Thus:

$$V_T + V_F + V_D = V_T^0 + V_F^0 + V_D^0 \quad \textbf{(5.20)}$$

where V_F is the volume of pore water volume and V_D is the volume of drained liquid.

This equation holds for both the end state of the test and for incremental changes in liquid volumes throughout the test can be expressed as:

$$V_T^f + V_F^f + V_D^f = V_T^0 + V_F^0 + V_D^0 \quad \textbf{(5.21)}$$

5.5 Results of 100% food waste running under unsaturated condition

The results obtained from the reconciliation processes are classified into: input and calculated variables. The data for the input and calculated variables are described and discussed in the following section.

5.5.1 Input variables of 100 % food wastes

The results obtained from the Rowe cell of the 100% food waste with 100% food materials were used as input variables for determining the essential variables used in the reconciliation processes spreadsheets. The calculation focused on the change measured in the initial and final stages of the Rowe cell tests (0–300 kPa). The waste composition of each case is presented in Chapter 3 (Table 3.2). Table 5.1 shows the input variables used for the reconciliation processes.

Table 5-1: Input variables used in the reconciliation processes

Test / Input variables	Case (5)	Case (6)	Case (7)	Case (8)
Mass of sample (M_{wet}^{0}), g (see Table 4.1)	1500	1500	1500	1500
Initial depth of sample, (H_0), cm	5.00	5.00	5.00	5.00
Initial volume, cm^3 (See e.q. 5.1)	2553.50	2553.50	2553.50	2553.50
Settlement at end of test (S_f), cm (see Fig 4.4)	3.60	3.00	3.30	3.50
Depth of sample at end of test ($H_0 - S_f$), mm	13.60	20.30	17.10	15.20
Final volume (V_f), cm^3 (V_f = ($H_0 - S_f$) $\times A$)	697	1037	875	778
Total liquid production (v_D), cm^3 (See Table 4.1)	1312	175	734	825
Mass fraction of mass of food solids	1	1	1	1

Mass of sample after test (M_{wet}^{f}), g, See Table 4.1	175.00	1300.00	752.00	650.00
Mass of dried sample (M_{dry})	120.00	660.00	375.00	336.00
Initial porewater volume v_F^0 (volume of water added to saturate sample), (cm^3)	0.00	0.00	0.00	0.00
Porewater volume released when sample removed (volume of water drained at the end of test)	0.00	0.00	0.00	0.00

5.5.2 Results of calculated masses of 100% food wastes in the reconciliation process

The results of calculating masses in the reconciliation processes varied depending on the waste composition, moisture content, and water released from each sample at each compression increment during compression. For instance, the masses of liquid remaining in the sample at the end of the test m_F^f were 68, 664, 391, 339g for case 5, 6, 7, and 8 respectively. The low value of m_F^f in Case (5) can be attributed to the high volume of liquid that flowed out from the sample during compression.

The mass of non-food solids (m_S) was zero for all four cases, as all four cases contained 100% food waste. In addition, the initial mass of trapped liquid (m_T^0) for all four (Case 5, 6, 7, and 8) were 1380, 840, 1125 and 1164 g, respectively. In contrast, the mass of cellular material (m_c) for all four cases was 120, 660, 375 and 336 g, respectively. The variations in m_c are associated with the weight of the test samples after drying at 70 ^{0}C, with the sample in case (5) losing most weight during sample drying. The cellular material in case (6) was higher than that for the other cases. The results of the essential masses obtained are presented in Table (5.2).

Table 5-2: Summary results of important masses of 100% food wastes using the reconciliation processes

Test / Waste or liquid mass	Case 5	Case 6	Case 7	Case 8
Unrecorded mass (net mass balance) (See table 4.4)	13.30	24.75	14.50	25.50
Mass of liquid remaining in the sample at the end of the test (m_F^f) includes unrecorded mass, (g), (See e.q. 5.9)	68.00	665.00	391.00	339.00
Mass of non-food solids (m_S) , g, (See e.q. 5.6)	0.00	0.00	0.00	0.00
Initial mass of trapped liquid (m_T^0) g, (See e.q. 5.7)	1380.00	840.00	1125.00	1164.00
Mass of cellular material (m_C), g, (See e.q. 5.8)	120.00	660.00	375.00	336.00

5.5.3 Results of calculated waste densities of 100% food wastes types

The cellular density was determined using equation 5.15. The validity of equation (5.15) was investigated by calculating the particle density of cases (7) and (8) based on the particle density of case (5) and (6). Thereafter, the cellular density calculated from equation (5.15) was compared with the cellular density obtained from the experimental work using the gas jar method. Table (5.3) shows the difference in the cellular density determined using two different approaches. There was a slightly difference between the two approaches with an error of 1.54% and 1.57% for case (7) and (8) respectively.

Table 5-3: Comparison on cellular density using different approaches

Particle density, (ρ_C)	**m_i (mass fraction of LBW)**	**m_j (mass fraction of SBW)**	**Results from experimental work**	**Results obtained from equation (5.15)**
Case (5), 100% LBW	1.00	0.00	1.17	NA
Case (6), 100% SBW	0.00	1.00	1.41	NA
Case (7), 50% LBW and 50% SBW	0.50	0.50	1.30	1.28
Case (8), 55%LBW, and 45%SBW	0.55	0.45	1.25	1.27

Table 5-4: Densities of cellular material and liquid used for 100% food waste

Test / **Parameters**	**Case (5)**	**Case (6)**	**Case (7)**	**Case (8)**
Density of liquid (ρ_L), (g/cm^3)	1.00	1.00	1.00	1.00
Cellular density (ρ_C), (g/cm^3) (See Table 5.3)	1.17	1.41	1.30	1.25

5.5.3.1 Results of calculated essential volumes of 100% food wastes in the reconciliation process

The volume of solid particles (v_S); the initial trapped volume (v_T^0); the cellular volume (v_C), and the initial liquid fraction trapped in the cellular material (α_T) of different high organic content waste

types were determined. The v_S was assumed to be zero for all four cases. The v_T^0 were 1380, 840, 1125 and 1164 cm^3 for case (5), case (6), case (7) and case (8), respectively. The variation in the v_T^0 of all four cases was expected, as the high initial trapped volume found on the waste had a high value of moisture content. The cellular volume was 102.56, 468.09, 292.97, and 264.57 cm^3 for cases 5, 6, 7, and 8 respectively. Table (5.5) shows the results for the essential volumes used in the reconciliation process.

Table 5-5: Summary results of important volumes using the reconciliation processes

Test / **Food or liquid volume**	**Case 5**	**Case 6**	**Case 7**	**Case 8**
Non-food solids volume (v_S), cm^3 (see e.q. 5.11)	0.00	0.00	0.00	0.00
Initial trapped volume (v_T^0), cm^3 (See e.q. 5.12)	1380.00	840.00	1125.00	1164.00
Cellular volume (v_C), cm^3 (See e.q. 5.13)	102.56	468.09	292.97	264.57
Initial liquid fraction trapped in cellular material (α_T), (See e.g. 5.14)	0.931	0.642	0.793	0.815

5.5.3.2 Mass and volume balance

The mass and volume balance were determined using the equations provided in section 5.4. Table 5-6 demonstrates the volume and mass balance of waste running under unsaturated conditions.

Table 5-6: Summary of mass and volume balance of 100 % food waste using in the reconciliation processes.

Test / Waste mass or volume	Case (5)	Case (6)	Case (7)	Case (8)
Initial wet mass (M_{wet}^{0}), g	1500	1500	1500	1500
Mass of solids (m_c), (g)	120.00	660.00	375.00	336.00
Unrecorded mass (m_e), (g)	13.30	24.75	14.50	25.50
Initial liquid volume (($M_{wet}^{0} - m_s$) × ρ_L), (cm^3)	1380.00	840.00	1125.00	1164.00
Total liquid production (v_D), (cm^3)	1311.7	175.25	733.50	824.50
Mass of sample after test (M_{wet}^{f}), (g)	175.00	1300.00	752.00	650.00
Final liquid volume (($M_{wet}^{f} - m_c$) + $m_e + m_D$) × ρ_L), (cm^3)	1380.00	840.00	1125.00	1164.00

5.6 Results of mixed wastes running under the saturated condition

The procedures, methods, and equations used to determine the variables in terms of masses and volumes of samples run under unsaturated conditions were followed for the samples run under saturated conditions. In addition, there were some differences in the input and calculated variables used in the reconciliation processes, and these are related to the waste composition and to the objectives of the experimental work. The input variables were selected from the results determined from the experimental work. The following sections discuss the results of the input and calculated variables. The waste compositions of Cases 1, 2, 3, and 4 are presented in Chapter 3, section 3.3 (Table 3-2).

5.6.1 Input used for waste run under saturated condition

The results obtained from the Rowe cell of the mixed wastes with different material types were used as input variables. Table 5-7 shows the input variables used in the reconciliation process. The calculation focused on the change measured at the initial and final stages of the Rowe cell tests (0–300 kPa).

Table 5-7: Input variables gained from the experimental work used in reconciliation process

Test / Input Variables	Case 1	Case 2	Case 3	Case 4
Mass of sample (M_{wet}), (g), (See Table 4.1)	1500	1500	1500	1500
Initial depth of sample, (H_0), cm	6.50	6.50	7.00	7.00
Initial volume, cm^3 (See e.g. 5.1)	3249.66	3249.66	3499.63	3499.63
Settlement at end of test (S_f), cm (See Fig 4.17)	3.92	3.43	3.02	2.43
Depth of sample at end of test ($H_0 - S_f$), cm	2.58	3.07	3.98	4.57
Final volume (V_f), cm^3 (V_f = ($H_0 - S_f$) $\times A$)	1290	1535	1990	2285
Total liquid production (v_D), cm^3 (See Fig 4.16)	2088	1760	1377	1088
Mass fraction of mass of food solids	0.73	0.58	0.44	0.29
Mass of sample after test (M_{wet}^f), g, (See Table 4.7)	895.00	1021.00	1144.00	1264.00

Mass of dried sample (M_{dry}), g,	600.00	767.00	879.00	1121.00
Initial porewater volume v_F^0 (volume of water added to saturate sample), cm^3 (See Table 4.7)	1840.00	1910.00	2020.00	2120.00
Porewater volume released when sample removed (volume of water drained at the end of test), cm^3 (See Table (4.7))	275.00	460.00	735.00	1050.00

5.6.2 Results of calculated masses of mixed wastes under saturated condition

In this section the required masses determined in the reconciliation processes of Case 1, 2, 3, and 4 were calculated based on the results obtained from the Rowe cell, which are used as input variables. The results calculated from the masses are presented in Table (5.8). The mass of non-food solids (m_s) for case 1, case 2, case 3 and case 4 was 405, 630, 840 and 1065 g, respectively. Conceptually, the higher fraction of organic content in the total mass of waste resulted in less mass in the m_s. The trapped liquid in the initial mass (m_T^0) was higher in case 1, with a value of 900 g, whereas the lowest result was found for case 4, with a value of 378.86 g. The disparities in the m_T^0 can be attributed to differences in waste composition and water content in all four cases. The same results for m_T^0 were found for the m_C where the large value of 195 g of cellular mass was observed in case 1, and the cellular mass decreased as the fraction of food material decreased.

Table 5-8: Summary results of important masses of mixed wastes

Test / Mass of solids and liquids	Case (1)	Case (2)	Case (3)	Case (4)
Mass of non-food solids (m_S) , g (See e.q. 5.6)	405.00	630.00	840.00	1065.00
Initial mass of trapped liquid (m_T^0) g, (See e.q. 5.7)	900.00	733.50	621.30	378.86
Mass of cellular material (m_C), g (See e.q. 5.8)	195.00	136.50	38.70	56.14

5.6.3 Results of calculated essential volumes of mixed wastes in the reconciliation process

The volume in terms of non-food solids (v_S), the initial trapped volume (v_T^0) and the cellular volume (v_C) were determined using the equation mentioned in section 5.3.2. The cellular density was 1.30 g/cm^3 which represents the average of the results for cellular density for all four cases. The volume of each element was determined by knowing the mass and density of each parameter. The waste composition and water content play an important role regarding the masses and volumes determined in the reconciliation process. Therefore, the explanation and discussion of the results regarding the essential volumes of 100% food waste samples are the same as for the mixed waste. For instance, the results of v_S and v_C for case (1) were 156.98 and 150 cm^3 which are considerably lower compared with other cases. In contrast, the value of v_T^0 for case (1) was 900 cm^3 which is considerably higher than other cases. The variation in the volumes can be referred to the different waste competition where the higher fraction of food waste in MSW resulted in a high moisture content.

Table 5-9: Summary results of important volumes of mixed wastes

Test / Waste or liquid volume	Case (1)	Case (2)	Case (3)	Case (4)
Non-food solids volume (v_S), cm^3 (See e.q.5.11)	156.98	244.19	325.58	412.79
Initial trapped liquid volume (v_T^0), cm^3 (See e.q. 5.12)	900.00	733.50	621.30	378.86
Cellular volume (v_C), cm^3, (See e.q 5.13)	150.00	105.00	29.77	43.18
Initial liquid fraction trapped in cellular material (α_T), (See e.q. 5.13)	0.857	0.875	0.954	0.898

5.6.4 Mass and volume balance

The mass balance were determined using the equations provided in section 5.4. Table 5-10 demonstrates the volume and mass balance of waste running under unsaturated conditions.

Table 5-10: Mass balance of mixed waste in the reconciliation processes

Test / Mass	Case 1	Case 2	Case 3	Case 4
Mass of solids (m_s), (g)	405.00	630.00	840.00	1065.00
Unrecorded mass (m_e), (g)	82.00	169.40	264.10	217.55

Weight of water drained after the test (m_u), (g)	275.00	460.00	735.00	1050.00
Initial liquid volume, (($M^0_{wet} + m^0_F - m_s$) × ρ_L) (cm^3)	2935.00	2780.00	2680.00	2555.00
Final liquid volume, (($M^f_{wet} - m_s + v_D + m_u + m_e$) × ρ_L), (cm^3)	2935.00	2780.00	2680.00	2555.00

5.6.4.1 Summary of the results

The content of this chapter was mainly focused on the reconciliation processes which were used to check and correct the mass balance between the beginning and end of the Rowe cell tests. In this regards, the variables such as the mass and volume of initial trapped liquids, non-food solids, and cellular material of the Rowe cell tests for different waste types run under saturated and unsaturated conditions were determined. The results show that the high moisture content found in the high organic content wastes have a critical impact on these masses and volumes. For instance, the higher moisture content results lower volume and masses of non-food material and cellular material, whereas the value of initial trapped liquid was higher. As mentioned above, the reconciliation processes were just used to balance the masses and volumes of the results obtained from the Rowe cell, therefore; the changes of these variables alongside with increasing the vertical stress is needed. The variables produced above are used in Chapter 6 in the development of the conceptual model.

Chapter 6 A conceptual model of the release of bound water in relation to applied stress

The LDAT model can be used to predict and determine landfill processes in terms of leachate produced, settlement, and the gases produced. The leachate produced in LDAT results from the reaction processes through the solid matrix where it is coupled with settlement and the degradation of solid. At present, the LDAT model is not sufficient to fully simulate the results obtained from the Rowe cell, as the majority of water released (LBW and SBW) from the test samples in the current study are due to the trapped liquid released under vertical applied stress. The conceptual model described here defines the essential variables that could be used thereafter with LDAT to further develop the model's prediction of water released from food waste.

The values reported were obtained from the quantities measured directly in the physical tests. However, in the case of the load phase analysis, the change in the quantity of the free liquid contained in the pore space of the sample at any point in time was estimated. To start with, it was assumed that the sample water released ratio changes linearly between the initial and final values. The changes in these variables due to an increase in the applied stress was analysed.

6.1 Concepts of the processes evidenced by the test

The overall concept of the processes that are taking place during a compression test is as follows.

1. The test involves raising the effective stress σ' in incremental steps.

2. In response to an increase in stress, the waste material in the sample compresses, reducing the void ratio (e) and the porosity (n), therefore, the dry density, ρ_d, increases. These three parameters are related, and either one of them will serve as a measure of the compressed state, or level of compaction of the material.

4. The conventional geotechnical approach is to link effective stress to one of these state parameters through a logarithmic or power law relationship. This relationship can then be used to transfer the properties of the experimental sample to field scale, or be used as part of a numerical model algorithm. In soil mechanics the void ratio is typically used, but here Powrie and Beaven

(1999) will be followed. Such that the dry density is used to obtain an analytical form of the effective stress compression relationship.

3. Above a threshold value of σ' the cellular material will begin to release some of the trapped liquid that is bound up within the cellular structure of the food waste. This sets up liquid filled voids in the material, which are then collapsed by the compressive stresses back to values compatible with the effective stress compression relationship.

4. The key assumption in this model of the behaviour of a compression cell containing food waste particles that release trapped water, is that at the end of a compression increment the waste compression state returns to the state that it would be at, even if the trapped liquid remains bound up within the cellular structure. Implicit in this assumption is that the compression state parameters are calculated based on the further assumption that the bound liquid is treated as part of the solid phase until it is released.

5. Two things happen following a compression increment :(1) The element of trapped liquid that is not retained in the cell as free liquid drains out of the cell, and (2) an additional element of the free liquid contained in the cell may also be expelled as the result of a reduction in pore space. Therefore, by measuring the volume of water that is drained from the cell (v_D), it is possible to gain some insight into what is happening inside the cell.

Figure 6.1 shows the phases of food and non-food particles during compression in the Rowe Cell. The initial state comprises the volume of solid particles (v_s), the cellular material (v_c), the pore water volume (v_F^0) and the trapped liquid volume within the food cellular material (v_T^0). As vertical stress increases, v_s and v_c remain constant, whereas a fraction of the trapped liquid within the food cellular material and a fraction of the pore water are released as leachate is expelled from the cell.

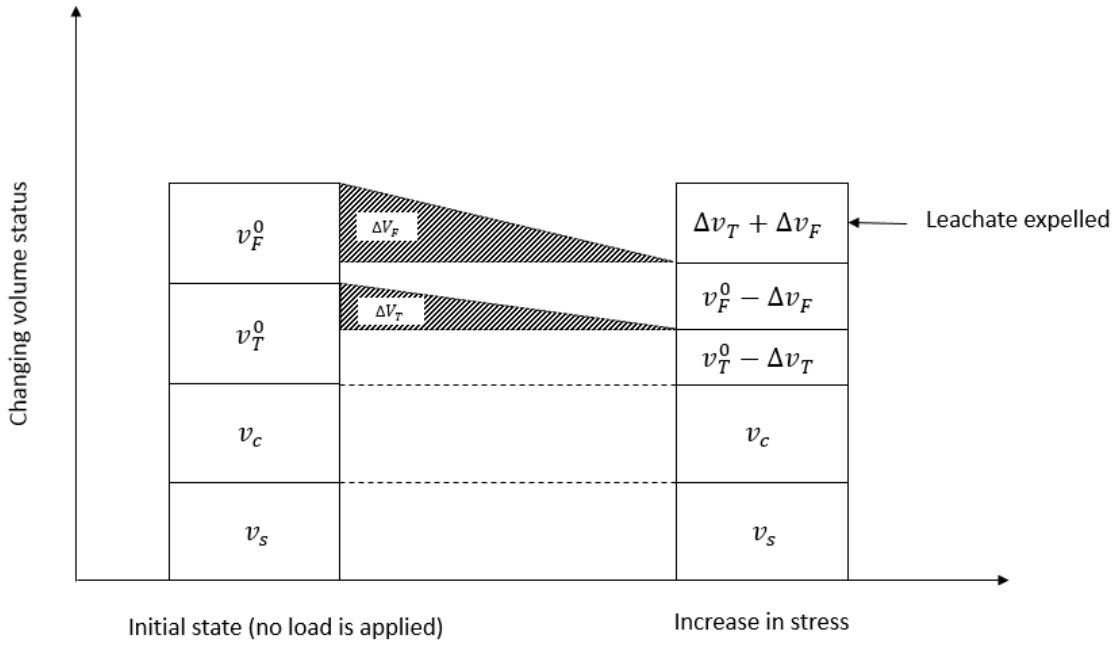

Figure 6-1: The phases of food and non-food waste particles: A) at the initial stage, and B) during compression in the Rowe cell.

6.2 Determining the input variables used in the conceptual model

The input variables of all the mixed wastes assume saturated conditions in the conceptual model were selected from the results obtained from the reconciliation processes (See section 5.6.1). The following sections define the test variables and the equations used in the conceptual model's spreadsheet calculations. The methods and procedures used in the experimental work using Rowe cell of all test samples are presented in section (5.2).

6.3 Determining the calculated volumes used on the conceptual model

The impact of applied loads from 0 kPa to 300 kPa with increments of 25 kPa on the calculated variables have been investigated for all mixed wastes run under saturated conditions. The calculated variables include the cellular volume (v_c), solid volume trapped liquid volume (v_T), and volume of free liquid occupying the pore space (v_F). The following sections explain the equations used to determine these volumes used in the conceptual model.

6.3.1 Determining the cellular and solid volume

The non-food solid volume (v_S) and cellular volume (v_C) were assumed to be constant at any stage during the compression in the conceptual model. Therefore, equations 5.9 and 5.11 applied in the reconciliation processes were used to determine the v_c and v_S in the conceptual model.

6.3.2 Determining the change in the volume of trapped liquid and free liquid occupying the pore space

The initial volume of trapped liquid (v_T^0) was determined using equation (5.10) provided in section 5.3.2. The change in the trapped liquid volume (v_T^{i}) as the vertical of stress increased in the conceptual model is expressed as:

$$v_T^{\mathrm{i}} = v_T^{\mathrm{P}} - \Delta v_F - v_D \quad \textbf{(6.1)}$$

Where v_T^{P} is the volume of trapped liquid from the previous incremental stress and v_D is the volume of leachate produced, measured from the experimental test, and Δv_F is the change in quantity of free pore space

On the other hand, the initial free liquid pore space v_F^0 was assumed to be the volume of water injected into the test samples at the initial stage (pressure = zero). The change in free liquid pore space as the vertical stress increased (v_F^{i}) has been defined as:

$$v_F^{\mathrm{i}} = v_F^{\mathrm{P}} + \Delta v_F \quad \textbf{(6.2)}$$

where v_F^{P} is the volume of free liquid occupying the pore space resulting from the previous stage of vertical stress.

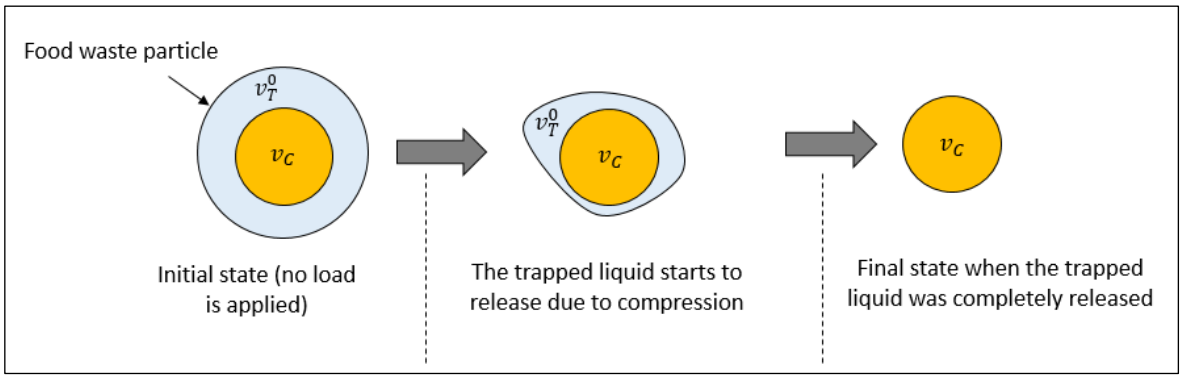

Figure 6-2: The phases of food waste particle at initial stage and during compression until trapped liquid was completely released.

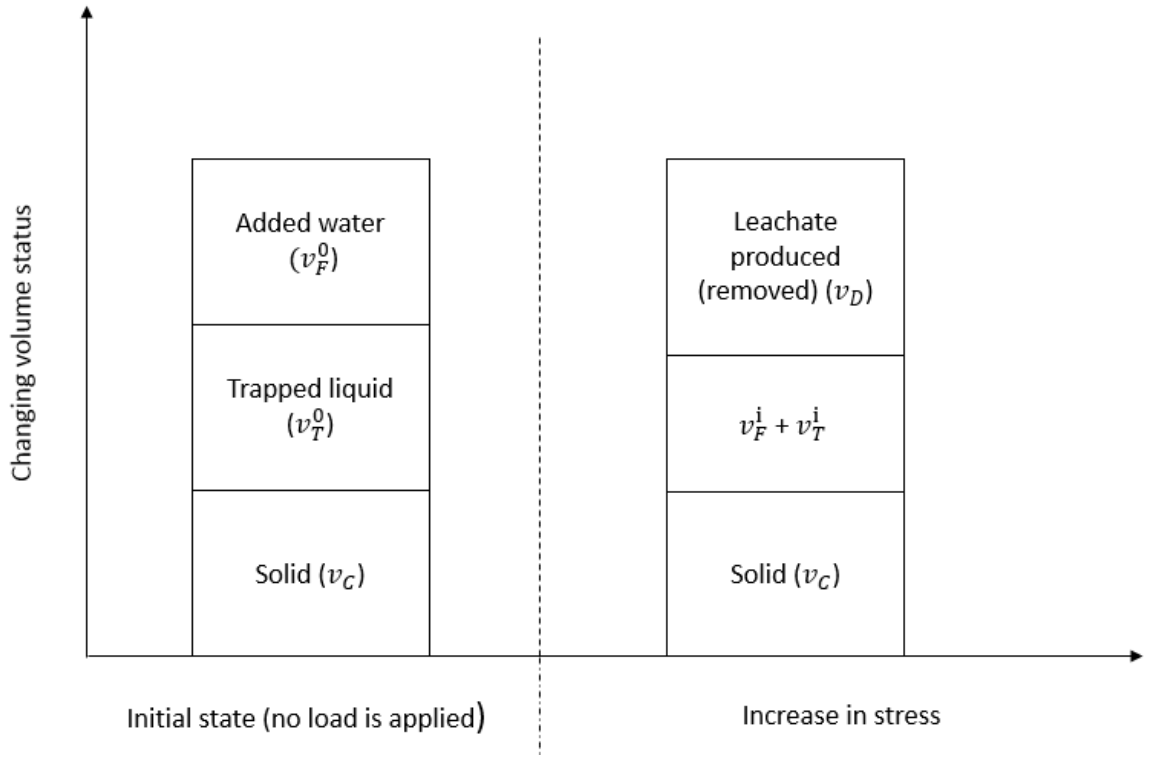

Figure 6-3: The change of volumes at initial stage and during compression

6.3.3 Determining the change in water release ratio at initial and final stage

The change in water released ratio is defined as a ratio of combined two elements of liquid: bound water and added water to the cell volume. The volume of non-food material (v_S) and the volume of cellular material (v_c) remained constant during the initial and final stages. The initial water release ratio (ϕ_i) can be expressed as (6.3):

$$\phi_i = \frac{V_0 - \left(v_T^0 + v_S + v_C\right)}{V_0} \quad \textbf{(6.3)}$$

The final water release ratio (ϕ_f) can be calculated by subtracting v_S and v_c from the final volume (V_f). The v_T was assumed to be zero since there no water trapped remaining at the final stage. Thus, final water release ratio (ϕ_f) can be expressed as:

$$\phi_f = \frac{V_f - \left(v_S + v_C\right)}{V_f} \quad \textbf{(6.4)}$$

6.3.4 Determining the change in quantity of free pore fluid Δv_F

The conceptual model spreadsheets apply equation (6.5) automatically by assuming that the sample water released ratio changes linearly between the initial and final values that have been derived on the conceptual model spreadsheets. In the load phase analysis spreadsheet calculations, the change in the quantity of free pore fluid, Δv_F, was calculated using an estimate of the change in water released ratio $\Delta\phi$, using the relationship:

$$\Delta v_F = V_1 \Delta\phi - \Delta v_D - \Delta V\left(1 - \phi_0\right) \quad \textbf{(6.5)}$$

The subscripts 0 and 1 in equation (6.5) designate the values at the beginning and end of a load increment.

Equation (6.5) was derived from:

$$\phi_0 = \frac{V_0 - \left(v_S + v_C + v_T^0\right)}{V_0} \quad \textbf{(6.6)}$$

$$\phi_1 = \frac{V_1 - \left(v_S + v_C + v_T^1\right)}{V_1} \quad \textbf{(6.7)}$$

This equation holds for both the end state of the test and for incremental changes in liquid volumes throughout the test. That is:

$$v_T^f + v_F^f + v_D^f = v_T^0 + v_F^0 + v_D^0 \quad \textbf{(6.8)}$$

And,

$$\Delta v_T + \Delta v_F + \Delta v_D \quad \textbf{(6.9)}$$

Eliminating $v_S + v_C$, gives

$$-\left(v_T^1 - v_T^0\right) = V_1\phi_1 - V_0\phi_0 - \left(V_1 - V_0\right) \quad \textbf{(6.10)}$$

This equation can be rearranged using equation (6.9) to give equation (6.5).

6.3.5 Determining the calculated masses used in the conceptual model

The mass of cellular (m_C), non-food solid particles (m_S), trapped liquid (m_T) and pore water occupying pore space (m_F) were determined using the density of each component. The following equations show the determination of each required mass used for each case:

$$m_C = v_C \times \rho_C \quad \textbf{(6.11)}$$

$$m_S = v_S \times \rho_S \quad \textbf{(6.12)}$$

$$m_T = v_T \times \rho_L \quad \textbf{(6.13)}$$

$$m_F = v_F \times \rho_L \quad \textbf{(6.14)}$$

6.3.6 Total mass of water (m_{tw})

The total mass of water in the conceptual model at each incremental stress was determined using equation (6.15). In the initial stage, the total water mass was equal to the initial mass of trapped liquid (m_T) plus the mass of pore water occupying the pore space (m_F). The objective of determining the total mass was to ensure that the mass of water in the initial stage was equal to mass of water in the final stage.

$$m_{tw} = m_T + m_F + m_D \quad \textbf{(6.15)}$$

6.3.7 Results of the initial and final water released ratio

The initial and final water released ratio of different mixed wastes run under saturated conditions were determined using equations 6.3 and 6.4 respectively. Table (6.1) shows the results of the initial

and final water released ratio of different mixed waste types. As it can be seen in Table 6-1, the initial water released ratio was 62.86, 66.68, 72.09, and 76.15 % for Cases 1, 2, 3, and 4 respectively. The final water release ratio of all four cases were slightly higher compared with initial water released ratio, and this can be attributed to the volume reduction due to increase in vertical stress. As seen in table (6.1), the calculated water released gradient increased with increasing fraction of organic content. Thus, the high water released gradient observed in Case 1 was resulted from the high reduction in volume compare with other cases (Figure 6-4).

Table 6-1: Initial and final water released ratio of mixed wastes determined in the reconciliation processes

Test / Ratios	Case 1	Case 2	Case 3	Case 4
Initial water released ratio (%), See Eq. (6.3)	62.90	66.70	72.10	76.10
Final water released ratio (%), See Eq. (6.4)	76.20	77.25	82.10	80.00
Water released gradient	0.011	0.009	0.008	0.003

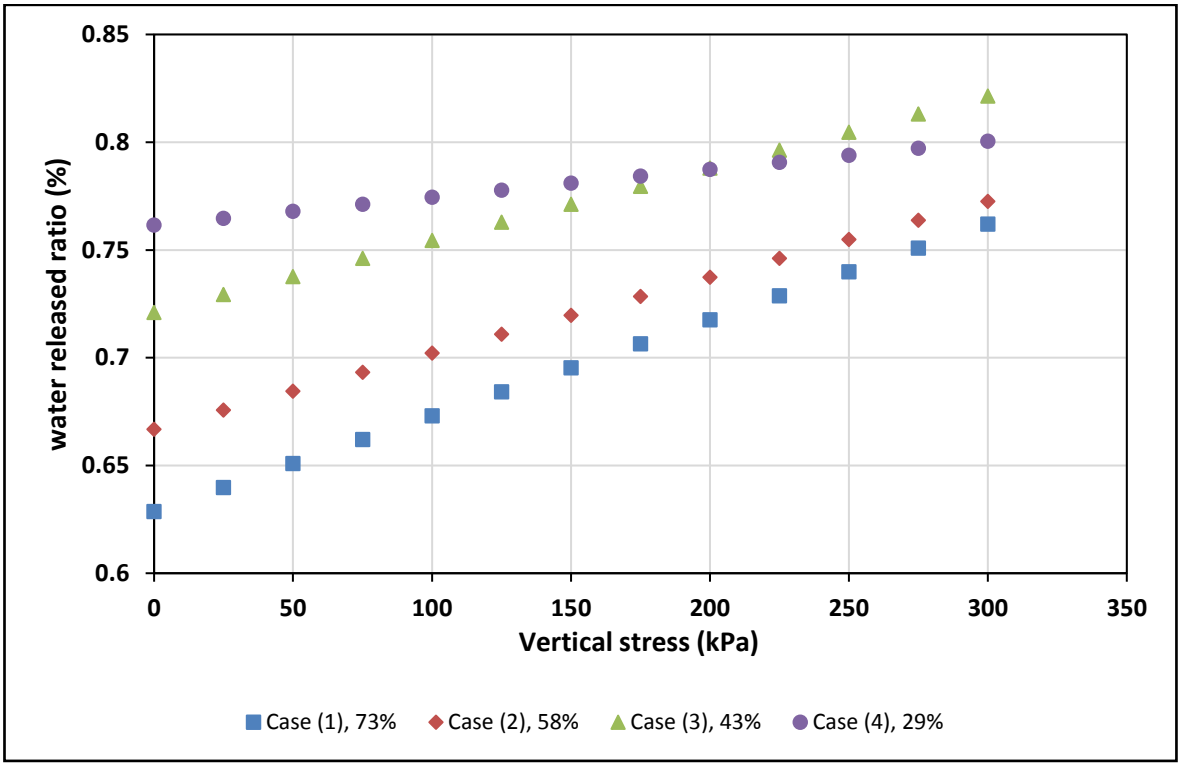

Figure 6-4: The relation between water released ration and vertical stress of different types of organic content wastes.

6.4 Results of mixed wastes running under the saturated condition

The results obtained from the conceptual model have been classified into: input and calculated variables. The input variables represent the results achieved from the results of the experimental work and reconciliation processes. While the calculated variables were obtained based on the equations mentioned in section 6.3. The following sections show the conceptual model's results for each mixed waste case.

6.4.1 Input variables of mixed wastes used on the conceptual model

The input variables of each case used in the conceptual model are presented in Tables 6.2, 6.3, 6.4 and 6.5. The results of these input variables were discussed in detail in Chapter 4.

Table 6-2: Input variables used in the conceptual model for Case (1)

Effective stress	Settlement (See Fig 4.17)	Cell depth (*H*)	Cell volume (*V*)	del V	Cumulative leachate (See Fig 4.16)	Leachate production
kN/m^2	cm	cm	cm^3	cm^3	cm^3	cm^3
0.00	0.00	6.50	3249.66		0.00	0.00
25.00	-1.55	4.95	2474.74	-774.92	780.00	780.00
50.00	-2.89	3.61	1803.44	-671.30	1366.00	586.00
75.00	-3.14	3.36	1679.70	-123.74	1544.00	178.00
100.00	-3.33	3.17	1587.31	-92.39	1808.00	264.00
125.00	-3.48	3.02	1512.19	-75.12	1893.00	85.00
150.00	-3.61	2.89	1442.77	-69.42	1943.00	50.00
175.00	-3.67	2.83	1414.00	-28.77	1978.00	35.00
200.00	-3.74	2.76	1379.73	-34.27	2017.00	39.00
225.00	-3.80	2.70	1349.21	-30.52	2047.00	30.00
250.00	-3.85	2.65	1327.21	-22.00	2069.00	22.00
275.00	-3.86	2.64	1320.78	-6.43	2082.00	13.00
300.00	-3.92	2.58	1290.54	-30.25	2088.00	6.00

Table 6-3: Input variables used in the conceptual model for Case (2)

Effective stress	Settlement (See Fig 4.17)	Cell depth (*H*)	Cell volume (*V*)	del V	Cumulative leachate (See Fig 4.16)	Leachate production
kN/m^2	cm	cm	cm^3	cm^3	cm^3	cm^3
0.00	0.00	6.50	3249.66		0.00	0.00
25.00	-1.49	5.01	2505.74	-743.92	737.00	737.00
50.00	-2.60	3.90	1947.45	-558.29	1235.00	498.00
75.00	-2.76	3.74	1871.38	-76.07	1361.00	126.00
100.00	-2.84	3.66	1829.73	-41.65	1528.00	167.00
125.00	-3.02	3.48	1737.97	-91.77	1587.00	59.00
150.00	-3.13	3.37	1686.02	-51.94	1634.00	47.00
175.00	-3.24	3.26	1632.10	-53.92	1663.00	29.00
200.00	-3.31	3.19	1596.48	-35.62	1698.00	35.00
225.00	-3.35	3.15	1575.53	-20.95	1719.00	21.00
250.00	-3.41	3.09	1545.26	-30.27	1739.00	20.00

275.00	-3.43	3.07	1532.41	-12.85	1754.00	15.00
300.00	-3.45	3.05	1526.84	-5.57	1760.00	6.00

Table 6-4: Input variables used in the conceptual model for Case (3)

Effective stress	Settlement (See Fig 4.17)	Cell depth (*H*)	Cell volume (*V*)	del V	Cumulative leachate (See Fig 4.16)	Leachate production
kN/m^2	cm	cm	cm^3	cm^3	cm^3	cm^3
0.00	0.00	7.00	3499.63		0.00	0.00
25.00	-1.24	5.76	2879.70	-619.93	612.00	612.00
50.00	-2.10	4.90	2449.74	-429.95	964.00	352.00
75.00	-2.36	4.64	2319.76	-129.99	1065.00	101.00
100.00	-2.64	4.36	2179.77	-139.99	1195.00	130.00
125.00	-2.72	4.28	2139.78	-40.00	1234.00	39.00
150.00	-2.77	4.23	2114.78	-25.00	1263.00	29.00
175.00	-2.82	4.18	2089.78	-25.00	1288.00	25.00
200.00	-2.89	4.11	2054.78	-35.00	1319.00	31.00
225.00	-2.94	4.06	2029.79	-25.00	1345.00	26.00
250.00	-2.98	4.02	2009.79	-20.00	1359.00	14.00
275.00	-3.01	3.99	1994.79	-15.00	1370.00	11.00
300.00	-3.02	3.98	1989.79	-5.00	1377.00	7.00

Table 6-5: Input variables used in the conceptual model for Case (4)

Effective stress	Settlement (See Fig 4.17)	Cell depth (*H*)	Cell volume (*V*)	del V	Cumulative leachate (See Fig 4.16)	Leachate production
kN/m^2	cm	cm	cm^3	cm^3	cm^3	cm^3
0.00	0.00	7.00	3499.63		0.00	0.00
25.00	-1.05	5.95	2974.69	-524.94	443.00	443.00
50.00	-1.69	5.31	2654.72	-319.97	742.00	299.00
75.00	-1.85	5.15	2574.73	-79.99	831.00	89.00
100.00	-2.05	4.95	2474.74	-99.99	928.00	97.00
125.00	-2.15	4.85	2424.75	-49.99	968.00	40.00
150.00	-2.22	4.78	2389.75	-35.00	1000.00	32.00
175.00	-2.26	4.74	2369.75	-20.00	1023.00	23.00

200.00	-2.33	4.67	2334.75	-35.00	1040.00	17.00
225.00	-2.36	4.64	2319.76	-15.00	1057.00	17.00
250.00	-2.40	4.60	2299.76	-20.00	1073.00	16.00
275.00	-2.42	4.58	2289.76	-10.00	1081.00	8.00
300.00	-2.43	4.57	2284.76	-5.00	1088.00	7.00

6.4.2 Results of calculated volumes and masses of mixed waste in the conceptual model

The volume results determined by the conceptual model using an Excel spreadsheet are presented in Table 6.6. As can be seen in Table 6.6, the volume of cellular material (v_C) and non-food solid volume (v_S) for all cases of mixed waste remained constant during the compression process.

However, there was a change in the volume of trapped liquid (v_T) as the vertical increase of all cases were investigated in the conceptual model. The volume of trapped liquid in the initial stage (vertical stress = zero) of the conceptual model was equal to the volume of the initial trapped liquid (v_T^0) determined in the recalculation processes. It can clearly be seen that the volume of trapped liquid for all cases started to release as the vertical stress increased. In the final stage where the vertical stress was 300 kPa, the volume of trapped liquid was 0.16, 0.46, 0, and 0 cm^3 for cases 1, 2, 3 and 4 respectively. It can be noted that the majority of trapped liquid was released in the conceptual model during the final stage of vertical stress.

The initial pore water volumes (v_F^0) in the conceptual model were assumed to be equivalent to the volumes of water injected in the test samples (See Table 4-7). The pore water volume for all cases decreased as the vertical stress increased (Table 6-6). The variations in the reduction in the pore water volume between all four cases can be referred to the different waste composition in each case where the reduction in pore water volume in the high organic content waste was considerably more compared with the low organic content waste.

Table 6-6: A summary of the results of calculated volumes using the conceptual model

Effective stress	Volume of cellular material (v_C) (See E.q. 5.13)				Non-food solid volume (v_S) (See E.q. 5.11)				Volume of trapped liquid$\left(v_T^{\mathrm{i}}\right)$ (See E.q. 6.1)				Pore water volume $\left(v_F^{\mathrm{i}}\right)$ (See E.q. 6.2)			
Case	1	2	3	4	1	2	3	4	1	2	3	4	1	2	3	4
0	150.00	105.00	29.77	43.18	156.98	244.19	325.58	412.79	900.00	733.50	621.30	378.86	1840.0	1910.0	2020.0	2120.0
25	150.00	105.00	29.77	43.18	156.98	244.19	325.58	412.79	584.67	463.90	424.18	243.97	1375.33	1442.92	1605.12	1811.89
50	150.00	105.00	29.77	43.18	156.98	244.19	325.58	412.79	322.75	265.83	287.28	160.06	1051.25	1143.15	1390.02	1596.80
75	150.00	105.00	29.77	43.18	156.98	244.19	325.58	412.79	260.86	225.56	233.75	133.14	935.14	1057.63	1342.55	1534.72
100	150.00	105.00	29.77	43.18	156.98	244.19	325.58	412.79	211.98	196.89	179.95	102.22	720.02	919.52	1266.35	1468.64
125	150.00	105.00	29.77	43.18	156.98	244.19	325.58	412.79	170.61	154.42	152.21	83.07	676.39	903.16	1255.09	1447.79
150	150.00	105.00	29.77	43.18	156.98	244.19	325.58	412.79	132.64	124.73	128.57	67.53	664.36	886.03	1249.73	1431.33
175	150.00	105.00	29.77	43.18	156.98	244.19	325.58	412.79	108.15	95.41	105.35	55.45	653.85	886.52	1247.95	1420.41
200	150.00	105.00	29.77	43.18	156.98	244.19	325.58	412.79	82.75	71.84	80.43	40.31	640.25	875.25	1241.87	1418.55
225	150.00	105.00	29.77	43.18	156.98	244.19	325.58	412.79	59.13	52.64	58.13	29.59	633.87	873.62	1238.17	1412.27
250	150.00	105.00	29.77	43.18	156.98	244.19	325.58	412.79	38.40	31.51	37.23	17.93	632.60	874.92	1245.07	1407.93
275	150.00	105.00	29.77	43.18	156.98	244.19	325.58	412.79	22.04	15.04	17.60	8.44	635.96	876.56	1253.70	1409.42
300	150.00	105.00	29.77	43.18	156.98	244.19	325.58	412.79	0.16	0.46	0.00	0.00	651.84	885.32	1264.30	1410.86

6.4.3 Results of calculated masses of mixed waste in the conceptual model

The calculated masses such as m_C, m_S, m_T, and m_F reached in the conceptual model determined using the equations provided in section 6.3.5 were investigated. The masses of m_C and m_S of all mixed wastes in the conceptual model were constant during the compression, as well as their sum $m_S + m_C$ which is the dry mass (M_{dry}) of the sample and is measured through a drying test at the end of the test. The mass of m_T and m_F were equivalent to its volume, since it was assumed that the liquid density throughout the conceptual model was 1 g/cm^3. On other hand, the cellular density (ρ_C) and non-food solid density (ρ_{SP}) were assumed to be 1.30 g/cm^3 and 2.58 g/cm^3 for all cases. The equations used to determine the densities of each mass for different waste types are mentioned in Chapter 5 section 5.3.4 respectively.

Table 6-7: A summary of the results of calculated masses using the conceptual model

Effective stress	Mass of cellular material (m_C) (See E.q. 6.11)				Non-food solid volume (m_S) (See E.q. 6.12)				mass of trapped liquid(m_T) (See E.q. 6.13)				Pore water volume (m_F) (See E.q. 6.14)				Total mass (See section 6.3.6)			
Case	1	2	3	4	1	2	3	4	1	2	3	4	1	2	3	4	1	2	3	4
0	195	136.5	38.7	56.14	405	630	840	1065	900.00	733.50	621.30	378.86	1840.00	1910.00	2020.00	2120.0	2740.00	2643.50	2641.30	2498.86
25	195	136.5	38.7	56.14	405	630	840	1065	584.67	463.90	424.18	243.97	1375.33	1442.60	1605.12	1811.89	2740.00	2643.50	2641.30	2498.86
50	195	136.5	38.7	56.14	405	630	840	1065	322.75	265.83	287.28	160.06	1051.25	1142.67	1390.02	1596.80	2740.00	2643.50	2641.30	2498.86
75	195	136.5	38.7	56.14	405	630	840	1065	260.86	225.56	233.75	133.14	935.14	1056.94	1342.55	1534.72	2740.00	2643.50	2641.30	2498.86
100	195	136.5	38.7	56.14	405	630	840	1065	211.98	196.89	179.95	102.22	720.02	918.61	1266.35	1468.64	2740.00	2643.50	2641.30	2498.86
125	195	136.5	38.7	56.14	405	630	840	1065	170.61	154.42	152.21	83.07	676.39	902.08	1255.09	1447.79	2740.00	2643.50	2641.30	2498.86
150	195	136.5	38.7	56.14	405	630	840	1065	132.64	124.73	128.57	67.53	664.36	884.77	1249.73	1431.33	2740.00	2643.50	2641.30	2498.86
175	195	136.5	38.7	56.14	405	630	840	1065	108.15	95.41	105.35	55.45	653.85	885.09	1247.95	1420.41	2740.00	2643.50	2641.30	2498.86
200	195	136.5	38.7	56.14	405	630	840	1065	82.75	71.84	80.43	40.31	640.25	873.66	1241.87	1418.55	2740.00	2643.50	2641.30	2498.86
225	195	136.5	38.7	56.14	405	630	840	1065	59.13	52.64	58.13	29.59	633.87	871.86	1238.17	1412.27	2740.00	2643.50	2641.30	2498.86
250	195	136.5	38.7	56.14	405	630	840	1065	38.40	31.51	37.23	17.93	632.60	872.99	1245.07	1407.93	2740.00	2643.50	2641.30	2498.86
275	195	136.5	38.7	56.14	405	630	840	1065	22.04	15.04	17.60	8.44	635.96	874.46	1253.70	1409.42	2740.00	2643.50	2641.30	2498.86
300	195	136.5	38.7	56.14	405	630	840	1065	0.16	0.46	0.00	0.00	651.84	883.04	1264.30	1410.86	2740.00	2643.50	2641.30	2498.86

6.5 Theoretical relationship between Rowe cell settlement and drainage volumes

The volume of Rowe cell was defined in equation (5.1), and the initial volume can be expressed as

$$V_0 = H_0 A = v_S^0 + v_C^0 + v_T^0 + v_F^0 + v_G^0 \quad \textbf{(6.16)}$$

With the 0 index denoting initial conditions.

Define percentage settlement as

$$s = \frac{H_0 - H}{H_0}\,100 = \frac{100}{H_0\,A}\,(-\Delta v_S - \Delta v_C - \Delta v_T - \Delta v_F - \Delta v_G) \quad \textbf{(6.17)}$$

Where $\Delta v_S = v_S - v_S^0$ etc. In the case of the solid phase $-\Delta v_S$ and $-\Delta v_C$ represent compression of the solids particles. In the case of the liquid phase $-\Delta v_T$ and $-\Delta v_F$ represent reductions in pore volume occupied by the liquids. In the case of the gas phase $-\Delta v_G$ represent the reduction in pore volume occupied by any gas present.

Note that the total change in the liquid volumes represents a transfer of liquid from the cell to the Rowe cell drain so that,

$$-\Delta v_F - \Delta v_T = \Delta v_D \quad \textbf{(6.18)}$$

We can define the percentage changes in compression, drainage and pore gas volume as:

$$c = \frac{100}{H_0\,A}\,(-\Delta v_S - \Delta v_C) \quad \textbf{(6.19)}$$

$$d = \frac{100}{H_0\,A}\,\Delta v_D \quad \textbf{(6.20)}$$

$$g = \frac{100}{H_0\,A}\,\Delta v_G \quad \textbf{(6.21)}$$

Thus the theoretical relationship between settlement percentages, and percentage changes in the various phase volumes is:

$$s = c + d + g \quad \textbf{(6.22)}$$

If the sample in the cell is perfectly saturated throughout a test, then there will be no change in the gas volume so $g = 0$.

If it is assumed that the solid phase particles are incompressible, then $c = 0$

Under these circumstances $(s = d)$ and a plot of percentage settlement against the applied load on the sample should be identical to the percentage drainage volume plot. (Percentages defined as above. That is relative to initial conditions.)

The pore water volume in the conceptual model can be linked to the settlement results found in the experimental work. Figures 6.5, 6.6, 6.7 and 6.8 illustrate the correlation between the percentage reduction of the pore water determined from the conceptual model and the settlement determined from the experimental observations of each case. A high reduction in the pore water volume (%) was found at vertical stress between 0 to 100 kPa with a value of 60.86%, 51.85%, 37.86, and 30.72 for Cases 1, 2, 3 and 4 respectively. The same trend in terms of the reduction of pore water volume was observed with settlement resulting from the experimental work. The plots diverge between the settlement and pore water volume (%) can be attributed to the solid particle compression, presence of pore gas, and differences in water released ratio.

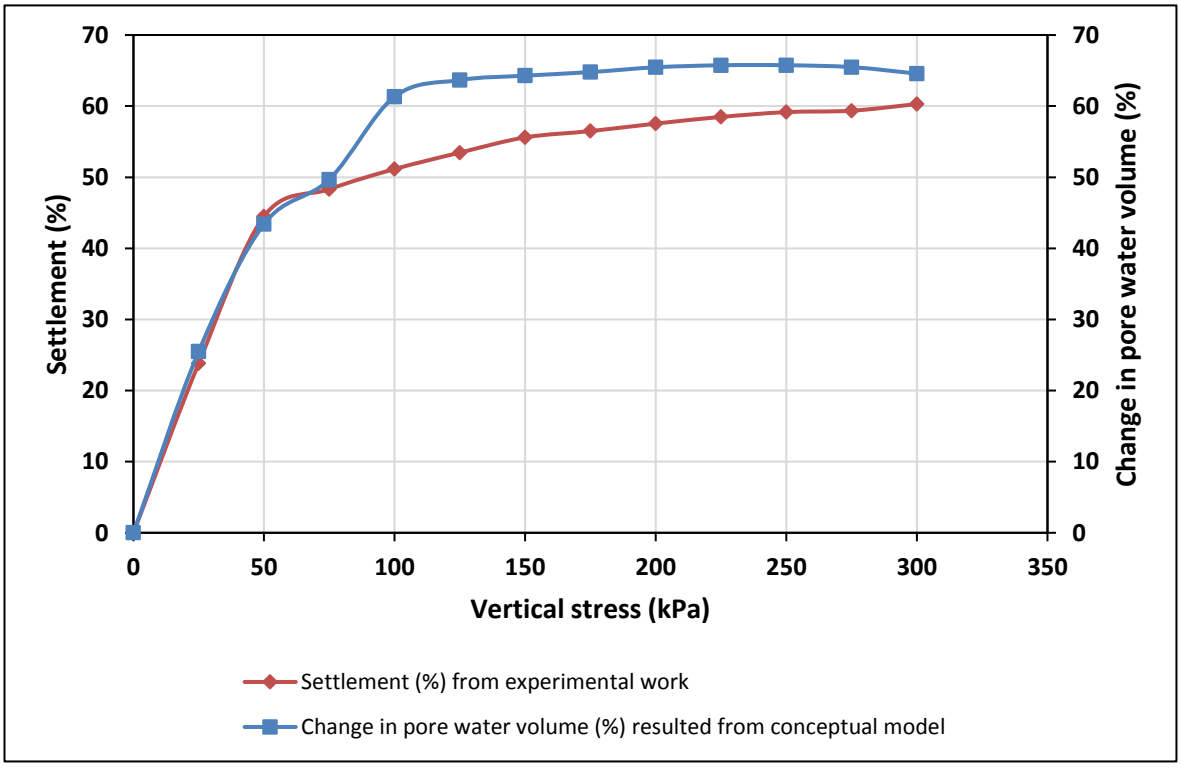

Figure 6-5: Correlation between settlement and pore water volume with vertical stress of Case (1)

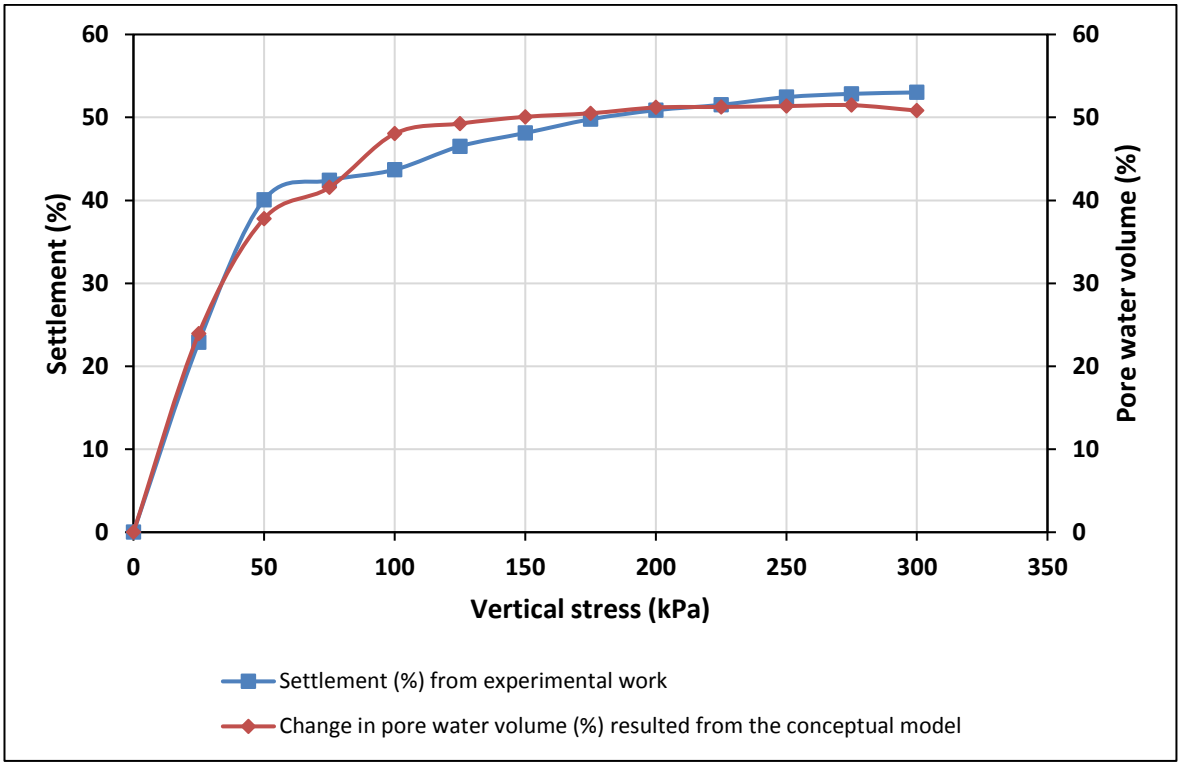

Figure 6-6: Correlation between settlement and pore water volume with vertical stress of Case (2)

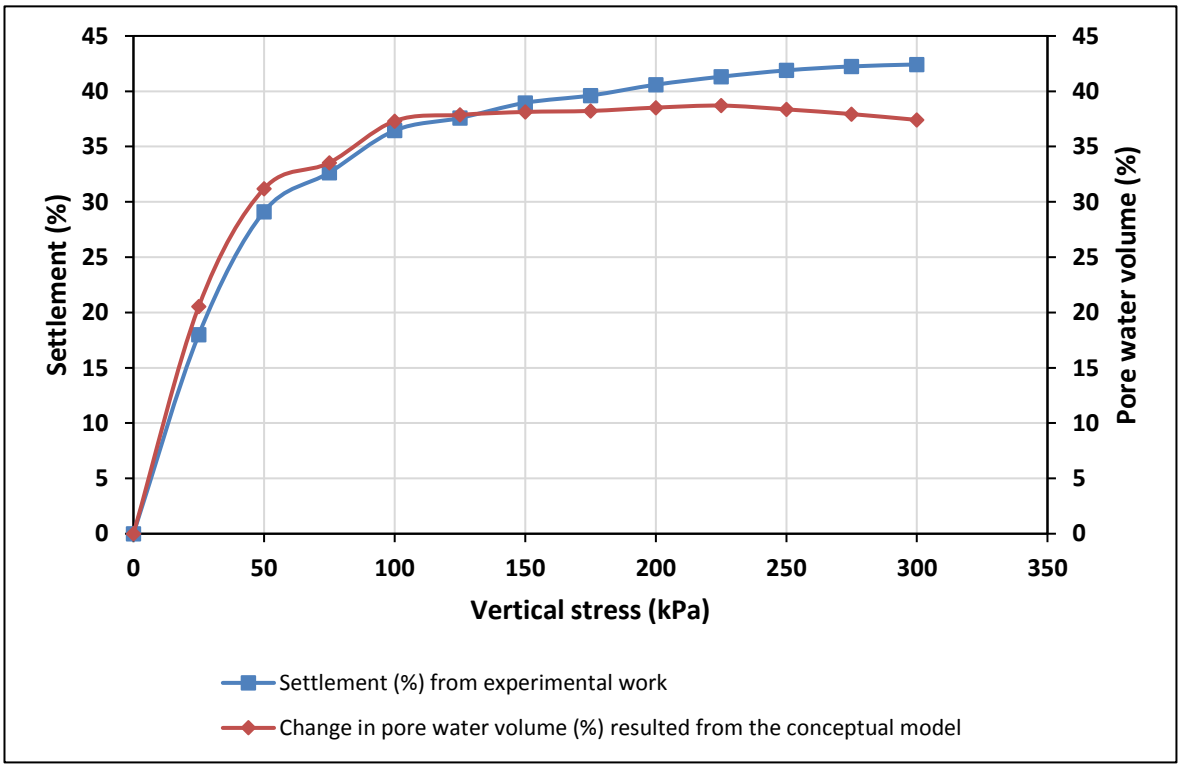

Figure 6-7: Correlation between settlement and pore water volume with vertical stress for Case 3

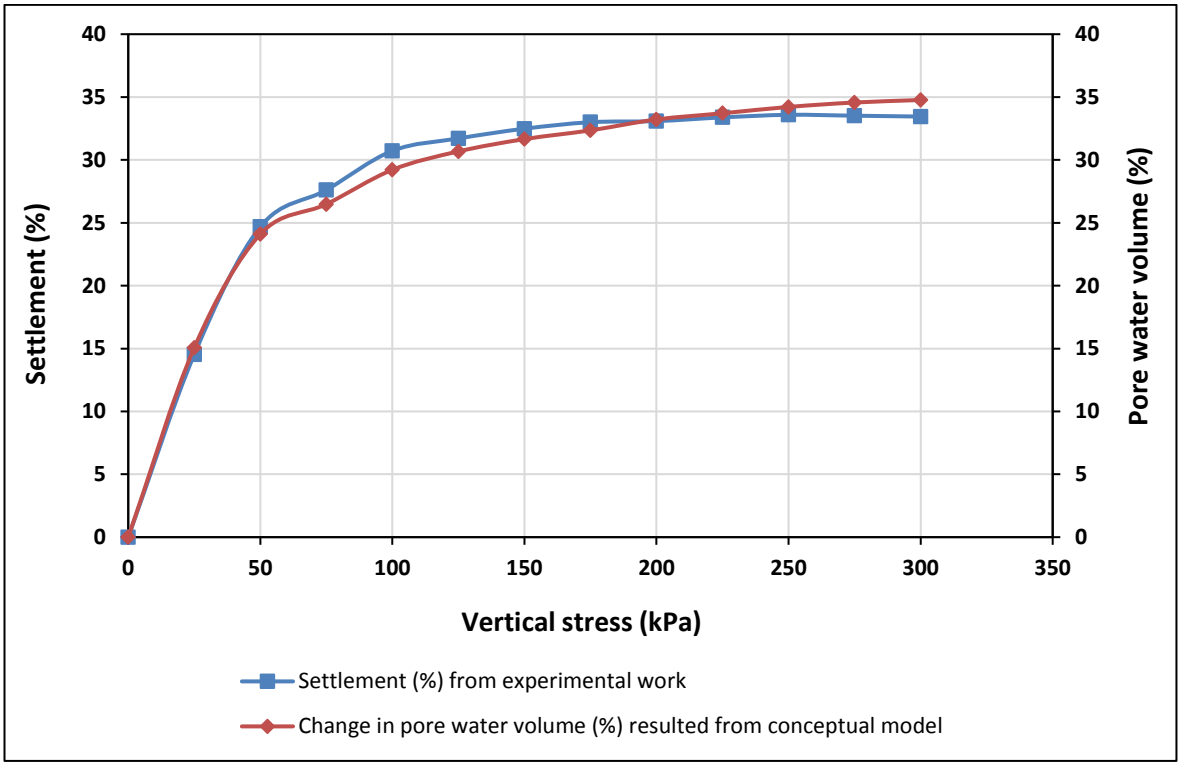

Figure 6-8: Correlation between settlement and pore water volume with vertical stress for Case 4

6.6 The application of the results to a numerical model of landfill processes

In this section a method for applying the results to a numerical model of landfill processes is proposed. The method is explained in the context of the specific architecture of the Landfill Degradation and Transport Model LDAT. The core architecture of LDAT consists of a group of landfill process sub-models that simulate the processes of degradation, gas solubility, diffusion, dissolution, chemical equilibrium, liquid and gas flow, settlement and heat generation and transfer. Each process sub-model calculates the change caused by the process in one or more of the primary parameters that define the state of the waste at any particular time.

The results obtained from the tests on food waste focus on estimating the release of bound liquids in response to changes in effective stress, which is the difference between direct stress and a combination of the liquid and gas pore pressures, which are three of the primary parameters defining the state of the waste in LDAT. The impact of changes on effective stress in the key parameters related to settlement - void ratio, porosity and dry density - has also been recorded. These results will therefore be relevant to the settlement sub-model of LDAT.

Currently, the settlement sub-model ensures that the relationship between the effective stress in the waste, and the dry density of the waste, follows the power law relationship developed by Powrie and Beaven (1999). The parameters of this power law can be selected to suit different wastes. Therefore, the extent to which the settlement characteristics observed in this study vary from those found by Powrie and Beaven (1999) may be accommodated directly by presenting them in the same power law format. Alternatively, they could be presented as a numerical look-up function, which could be read by LDAT following some simple modifications to the code in the settlement sub-model.

Modelling the release of bound liquids in response to changes in effective stress can be achieved by using an appropriate relationship between the current bound liquid volume, v_T, (or the non-dimensional bound liquid fraction, $\alpha_T = \frac{v_T}{v_C + v_T}$ and effective stress, σ' as shown schematically in Figure 6.9. Note that v_C is the cellular material volume of the food particles and $v_C + v_T$ is the total volume.

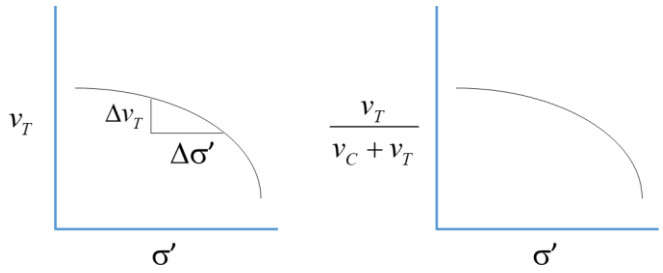

Figure 6-9: Relationship between the bound liquid volume and effective stress

This information can be integrated into the settlement sub-model either as an analytical function, or as a numerical look-up function. This has already been achieved in the dissolution sub-model of LDAT for a function relating to the release of bound liquid in response to the dissolution of food waste. The data defining the function shown schematically in Figure 6.9 has been extracted from the results of the Rowe cell tests using the conceptual model spreadsheet. For example, Figure 6.10 shows the data extracted for 28% of the mixed waste sample Rowe cell tests. In this example α_T is plotted against σ' where,

$$\alpha_T = \frac{v_T}{v_C + v_T} = \alpha_T^0 \left(\frac{\sigma_T' - \sigma'}{\sigma_T'} \right)^n \quad \textbf{(6.22)}$$

where α_T^0 is the value of α_T when $\sigma' = 0$, and σ_T' is the value of σ' when all of the bound liquid has been released, and n is the power law index.

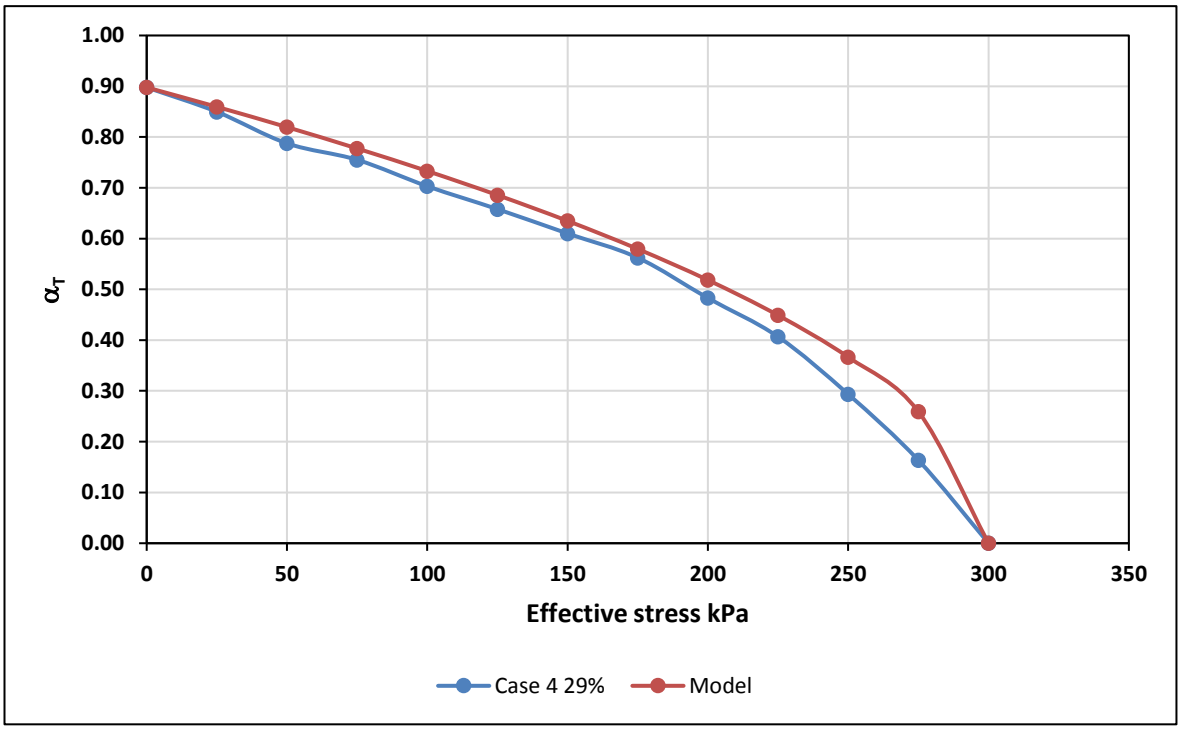

Figure 6-10: The model data is plotted for σ'_T= 300 kPa and the test data is for the Case (4) sample.

6.7 Summary

This chapter focused on the changing of test variables such V_C, V_S, and V_T as the vertical stress increases. The results obtained from the conceptual model spreadsheet of samples run under saturated conditions were discussed and analysed. We assumed that in the case of food waste when an increment of effective stress $\Delta\sigma'$ was applied, the volume of particles changes by an amount Δv_P as the results of the trapped liquid released. A good correlation was found between settlements determined from the experimental work and pore water volume V_F calculated from the conceptual model spreadsheet where the high reduction on settlement lead to increase to water released as the vertical stress increases. On the other hand, a numerical function of the volume fraction of trapped liquid (α_T) which can be read by LDAT model was proposed. The α_T

obtained from the conceptual model spreadsheet and LDAT model was compared. The trend of the results of α_T for both conceptual and LDAT model spreadsheet closely matched as the α_T decrease when the vertical stress increased.

Chapter 7 Conclusion and Future work

7.1 Conclusion

The waste composition on less developed countries such as Riyadh landfill has a critical influence in terms of physical properties, hydraulic properties, settlement, and compressibility of MSW. Therefore, understanding the influence of these waste compositions is considered essential for the landfill designer and operator to build a safe and effective landfill. In this study, comprehensive laboratory scale tests were conducted to investigate the impact of organic content on the geotechnical properties of MSW. To accomplish this, four samples with different high organic content wastes: case 1, (73%), case 2, (58%), case 3, (43%), and case 4, (28%) were tested using one-dimensional consolidation using a Rowe cell. The Rowe cell was set up to evaluate the physical properties, hydraulic properties, settlement characteristics, and leachate produced of these different waste compositions. The work presented has improved the fundamental knowledge of the behaviour change on the geotechnical properties of different types of organic content wastes, and potential benefits by comparing the results with other related previous studies.

The organic fraction of the waste was a key component on this study. The results obtained showed that the moisture content, dry density, bulk density, and saturated moisture content were higher for case 1 and reduced as the organic fraction decreased to case 2, case 3, and case 4, respectively. The specific gravity was found to be higher in the low organic content sample case 4 and decreased as the organic fraction increased. The results of hydraulic properties such as hydraulic conductivity, total porosity, and void ratio were clearly affected by organic content. There was a greater reduction in hydraulic conductivity, total porosity, and void ratio observed in case 1 and this started to increase as the organic fraction decreased. This can be explained by the high compressibility of high organic content waste in which the total porosity and void ratio are low, leading to a reduction in the hydraulic conductivity. In addition, the settlement results demonstrated high settlement in the waste having high organic content since the material was easy to compress when subjected to a vertical stress. The results showed that the total reduction on settlement from the initial height were 60.23%, 53.10%, 42.42%, and 35.96% as the organic content decreased from 73%, 58%, 43%, and 29% respectively.

The leachate produced from MSW in arid countries is mainly due to the organic fraction of MSW, thus, higher organic content leads to greater production of leachate. This research investigates the link between waste composition and leachate production in terms of organic content. The organic content was classified into two different categories: loose bound water (LBW), and strong bound water (SBW). Four samples with different fractions of LBW and SBW: 100%, 100% SBW, 50% LBW and 50% SBW, and 55% SBW and 45% SBW were tested under different vertical stresses. The results showed that LBW waste plays an important role; the settlement and water released were higher as the percentage of LBW increased in the waste. In addition, the mass reduction from different types of LBW and SBW wastes due biodegradation was investigated. The results indicated that a high reduction on mass was found in LBW wastes compared to SBW wastes. The variation on the reduction of mass between LBW and SBW wastes can be attributed to the water content and material structure where the water content was considerably higher on LBW wastes compared with SBW wastes. In addition, the material structure of LBW waste was easy to breakdown due to biodegradation processes compared to SBW wastes.

A conceptual model was developed in this study to improve the LDAT model. The model presented was used to determine test variables which the LDAT model does not consider in terms of bound water released from the food waste. These variables include mass and volume, which can predict the water released form food material due to compression. With these variables, the LDAT model can be used to simulate the landfill processes in terms of gas emitted, leachate produced, physical properties, hydrological properties alongside with biodegradation processes for high organic content wastes. Due to time constraints in this research, the equations developed in the conceptual model were not introduced into the LDAT model.

Despite a wide body of research on the geotechnical properties of MSW landfills, the impact of high organic content wastes, which can represent a significant portion of the wastes processed at landfills, have not been critically investigated. Thus, this research has contributed to the knowledge regarding the effect of high organic content waste on the geotechnical properties of MSW. The results obtained from experimental work, and conceptual model coupled with LDAT model would be useful to the landfill designers, and operators to design a safe and effective landfill. For example, the volume of leachate produced from high organic content waste is considerably large, thus; the landfill designer should be able to predict these important parameters to account for designing leachate collection system. Thus, this work can help in the design of existing and proposed landfills, especially in those countries where MSW has a high organic content, as the settlement, physical

and hydraulic properties are critical parameters that affect the performance and efficiency of the landfill.

7.2 Future work

This research demonstrated the effect of high-organic-content waste on the geotechnical properties of MSW. Despite this study's achievements, due to the time constraints and instrumental issues with the Rowe cell, experimental work was limited. The results of the study also pointed towards further investigation. The following points describe the suggestions for future work:

1. Further investigation could be carried out into different high organic content wastes using large scale consolidating anaerobic reactors (CARs), where the particle size is considerably larger compared with the Rowe cell, to test scale effects in high organic content wastes.
2. Additional work is needed to introduce the proposed conceptual model into a numerical model, such as LDAT, and to develop the links between physical waste properties and leachate production in high-organic-content MSW.
3. In addition to producing large volumes of waste, high organic content waste produces high strength leachates. Further investigation is needed to study the leachate composition of different high organic content wastes.
4. Further investigation is needed to define the relationship between moisture content and LBW/SBW wastes.

Appendix A Biogas (CH_4 and CO_2)

There has been an increase in demand for energy alongside growing concerns about the unsustainability of non-renewable energy. In this case, the high demand for fossil fuels can significantly contribute to environmental pollution (Deepanraj et al., 2017). Thus, the organic matter that produces gas (CH_4, CO_2) has been considered an sustainable solution to energy production. In this regard, anaerobic digestion can be used to break down the organic materials and convert them into biogas (CH_4, CO_2) where methane is then used for electricity (Nadu and Nadu, 2017; Agrahari and Tiwari, 2013).

The biogas produced from MSW might vary, depending on waste composition and fraction of degradable materials. For instance, Agrahari and Tiwari (2013) studied the total gas production of various amounts of kitchen waste, using a portable floating type biogas plant with a capacity of 0.018 m^3 under a real climate condition. They found that the total biogas produced (m^3) was 0.22, 0.26, 0.13 and 0.12, as the amount of kitchen waste (kg) increased from 6 to 8, 10 and 12 kg, respectively. This agrees with the findings of Cesaro et al. (2016) who studied energy recovery from organic content, produced from MBT plant. Three reactors (i.e. R1, R2 and R3) with different organic content (i.e. 100%, 67% and 10%, respectively) were performed, using anaerobic digester with a capacity of 0.125 m^3. The researchers found that the cumulative amounts of gas produced for R1, R2 and R3 were about 37, 25 and 21 NL/kg VS, respectively. Elsewhere, Sutthasil et al. (2014) compared the methane rate of MSW from a landfill site in Thailand, using semi-aerobic and anaerobic lysimeters (0.9 in diameter and 2.7 m in height); the waste composition contained 19.1% food waste, 19.1% paper, 16.4% plastic, 17.7% textile, 5.7% wood, 19.4% glass and 2.7% foam. The researchers found that the methane rate ($g/m^2/day$) in an aerobic lysimeter was much higher than the methane rate in the semi-aerobic lysimeter (i.e. 62.6 and 2.8 $g/m^2/day$, respectively); the authors did not report the cumulative amount of biogas produced.

A.1 Small scale Biochemical Methane Potential (BMP) reactors

The BMP test determines the biogas or methane yield of different high organic wastes under anaerobic degradation (Gibson & Smyth, 2007; Bilgili et al., 2009). BMP is a small-scale solution that can be used to evaluate the efficiency of anaerobic methods by measuring the amount of organic carbon that is anaerobically converted to CH_4 and biogas (Moody et al., 2009). The supplemental nutrients and bacteria can be useful for enhancing microbial methanogenic conditions (mesophilic

at 30°C). However, several factors can affect the performance of a BMP test, such as the particle size of the substrate, the temperature and the substrate/inoculum ratio (Esposito, 2012).

BMP reactors are made from Nalgene bottles, and each reactor has a capacity of 375 mL. In this study, four BMP test reactors were used, and each test was conducted in duplicate to measure the variability of the test results. The volume of gas produced were measured by the gas collection system connected to each bottle. The amount of waste added to each of the reactors is presented in Table A-1. The characteristics and compositions of the representative sample used for each reactor in this study were the same as those of the MSW described in Table 3-3. The nutrients and inoculum (sludge) were used in order to enhance the mesophilic methanogenic conditions. In addition, all the reactors were placed in a water bath at 30°C. Before the reactors were filled with the waste, the waste samples were shredded to a maximum particle size of 10 mm. The displacement method was used to measure gas production from each bottle by collecting the gas produced in an inverted glass bottle burette containing acidified water (pH = 2) to prevent the dissolution of CO_2 (Siddiqui et al., 2011). A schematic of the BMP apparatus used in this study is shown in Figure A-1.

Table A-1: The amount of substrate added to each reactors

% Organic content	**73.00**		**58.00**		**43.00**		**29.00**	
VS substrate (%)	70.15	70.52	57.70	57.32	44.99	44.61	30.98	31.90
Mass on inoculum added (g)	200.00	200.00	200.00	200.00	200.00	200.00	200.00	200.00
VS inoculum %	2.66	2.66	2.66	2.66	2.66	2.66	2.66	2.66
Total VS inoculum g	5.32	5.32	5.32	5.32	5.32	5.32	5.32	5.32
Weight of substrate to be added (g)	3.79	3.77	4.61	4.64	5.91	5.96	8.59	8.34

Substrate Ratio	2.66	2.66	2.66	2.66	2.66	2.66	2.66	2.66
Average VS substrate (%)	70.33		57.51		44.80		31.44	
Average weight of substrate added (g)	3.78		4.63		5.94		8.46	

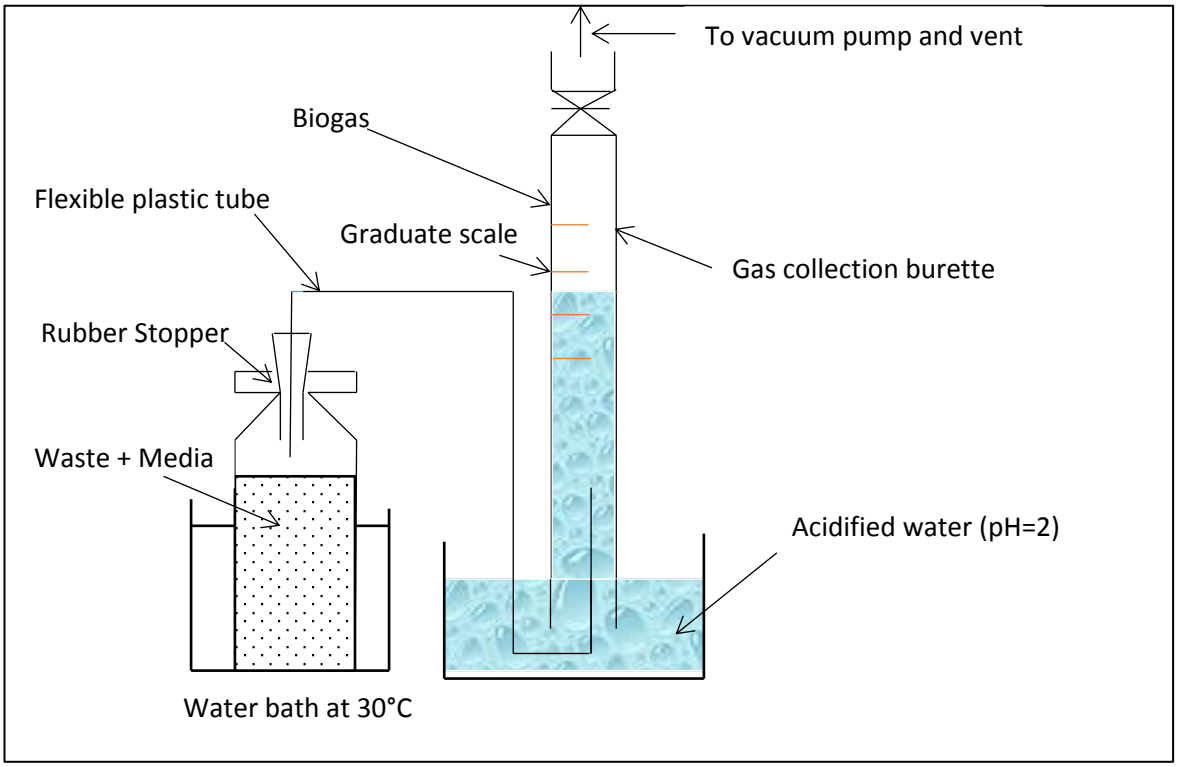

Figure A-1: Schematic of the BMP test reactors.

A.2 Biogas analysis

The biogas (CH_4 and CO_2) produced from the reactors was collected using a gas sampling bag. It was analysed immediately using gas chromatography (GC) (Varian GC-3800 Gas Chromatograph), which has two columns: a HaySep C column and a molecular sieve 13×60-80 mesh. The operating temperature was 50°C. Argon was used as the transporting gas

A.3 Gas generation from different types of high organic content waste

The gas produced from the landfill is directly linked to the type and waste composition (Campuzano and González-Martínez, 2016). This may be attributed to the microbial activity inside the landfill, which converts the degradable material into biogas (CH_4 and CO_2) according to the anaerobic stages. The effect of high organic content waste types on the gas produced (CH_4 and CO_2) is shown in Figures A-2 and A-3. The total gas produced was 495.30, 352.10, 178.80 and 97.21 L/kg DM over a period of 40 days, as the organic material decreased from 73%, 58%, 44% and 29%, respectively. This is reasonable, mainly because, as the high organic content waste increases, the amount of gas produced increases too. As it is shown in Figure A-2, the large amount of CH_4 produced was 327.60 (L/kg DM), which was found in the waste that had 73% of organic material and decreased to 234.21, 114.92 and 63.54 L/kg DM, as the fraction of organic content was reduced to 58%, 44% and 29%, respectively.

Erses et al. (2008) measured the cumulative methane, produced from shredded synthetic waste (19.5 kg), representing the waste composition of Istanbul using anaerobic digester. The waste contains 45% organic material (food + garden), 14.5% paper, 9.5% plastic, 5.6% textile, 3.8% glass, 2.2% metal, 4.4% ceramic and 15% other materials according to weight. The authors found that the cumulative methane produced was 158 L/kg DM, which is slightly higher than the methane obtained in this study when the fraction of organic content is 44%. The slight difference may be due to the different composition of organic waste used in this study, where the organic material chosen is LBW and SBW waste. In addition, Bilgili et al. (2009) obtained the methane-production potential of MSW from Odayeri Sanitary Landfill, Istanbul, Turkey, containing 44% organic material, 8% paper, 6% glass, 6% metals, 5% plastic, 5% textile and 26% miscellaneous. The potential methane produced from the test sample was determined using BMP test, where the test sample was taken from the pilot scale landfill reactor (without leachate recirculation). After 24 months, the potential methane

produced was 117 L/kg dry waste, which is partially comparable with the methane produced in this study, when the fraction organic material was 44%.

However, the efficiency of AD is directly linked to Total solid (TS) of MSW, as TS is an indicator of the organic and inorganic matters of MSW (Jingura and Kamusoko, 2017). Abbassi-Guendouz et al. (2012) studied the total production of methane from cardboard with differing TS content, ranging from 10% to 35% using batch AD. They found that the higher methane production rate was 197 mL/g VS at 10% TS, which decreased to 24 mL/g VS when TS was 35%. This also agrees with the results reported by Forster-Carneiro et al. (2008) who studied the biogas produced from food waste with varying TS content of 20%, 25% and 30% using anaerobic digester. The authors concluded that the cumulative biogas produced decreased from 7136, 6308 and 6135 mL, as TS increased from 20%, 25% and 30%, respectively. The trend of the results in this study is similar to those obtained from other related studies. Table A-2 illustrates that the higher fraction of organic content has lower values of TS, which lead to high production of biogas.

Table A-2: TS and VS of different high organic content waste types

% of organic matter	TS%	VS%
Case 1 (73)	44	70
Case 2 (58)	56	58
Case 3 (43)	62	44
Case 4 (29)	78	31

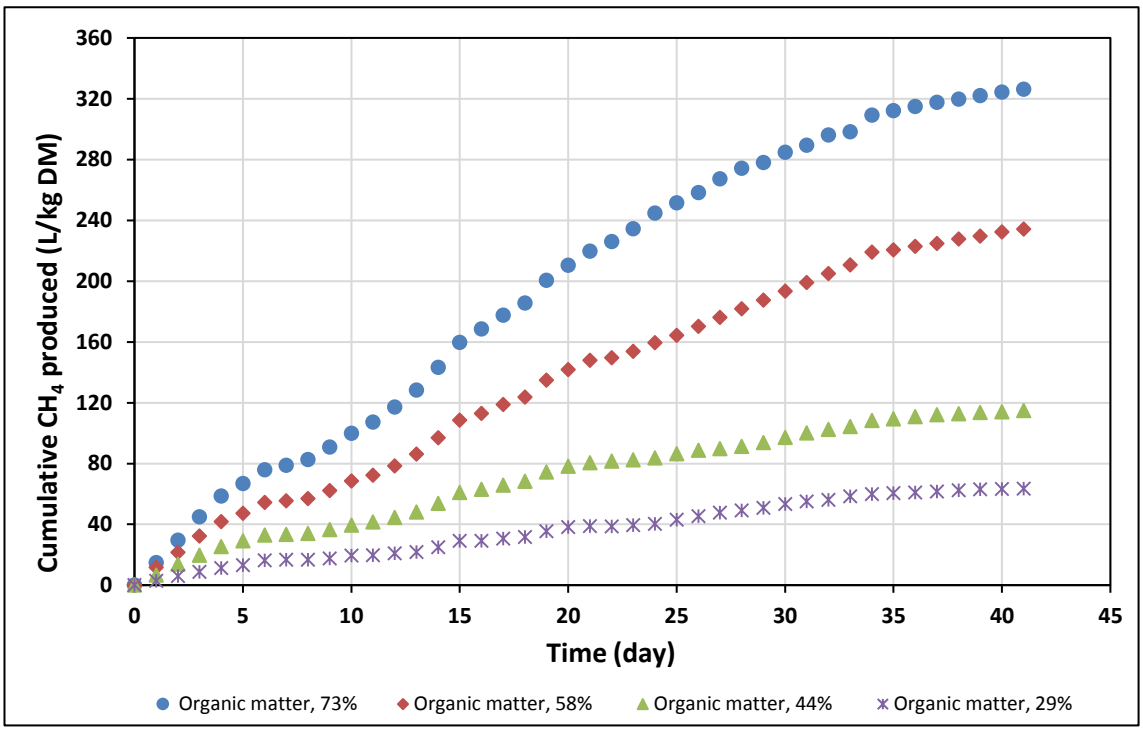

Figure A-2: Cumulative methane produced over time

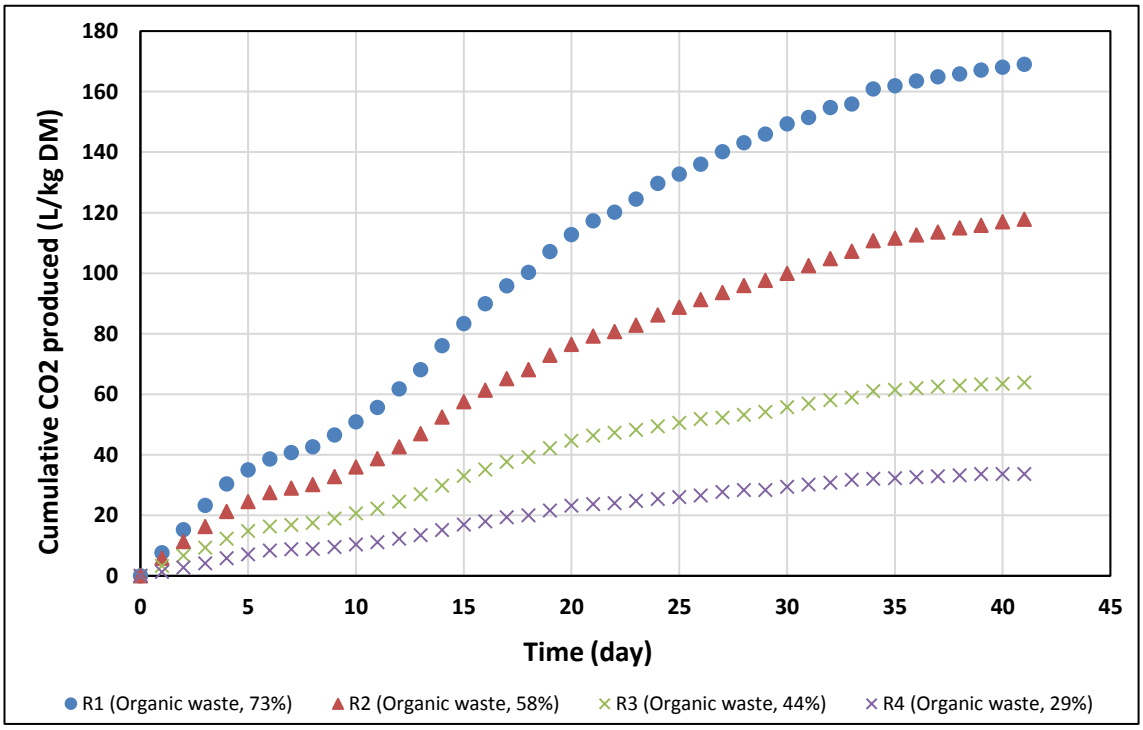

Figure A-3: Cumulative carbon dioxide produced over time.

REFERENCES

A. Vaclavik, C.., 2008. Essentials of Food Science, THIRD EDIT. ed, Food Science Texts Series. Springer New York, New York, NY.

Abbassi-Guendouz, A., Brockmann, D., Trably, E., Dumas, C., Delgenès, J.P., Steyer, J.P., Escudié, R., 2012. Total solids content drives high solid anaerobic digestion via mass transfer limitation. Bioresource Technology 111, 55–61.

Abdul, S., Al, H., Sulaiman, H., Suliman, F.E., Abdallah, O., 2014. Assessment of Heavy Metals in Leachate of an Unlined Landfill in the Sultanate of Oman. International Journal of Environmental Science and Development 5, 10–13.

Agrahari, R., Tiwari, G.N., 2013. The Production of Biogas Using Kitchen Waste. International Journal of Energy Science 3, 408.

Ahmadifar, M., Sartaj, M., Abdallah, M., 2015. Investigating the performance of aerobic, semi-aerobic, and anaerobic bioreactor landfills for MSW management in developing countries. Journal of Material Cycles and Waste Management 18, 703–714.

Al-arifi, N.S., Al-agha, M.R., El-nahhal, Y.Z., 2013. Environmental Impact of Landfill on Groundwater, South East of Riyadh, Saudi Arabia. Jornal of Natural sciences Reserach 3, 118–128.

Alkaabi, S., Van Geel, P.J., Warith, M. a, 2009. Effect of saline water and sludge addition on biodegradation of municipal solid waste in bioreactor landfills. Waste management & research : the journal of the International Solid Wastes and Public Cleansing Association, ISWA 27, 59–69.

Altan, A., Maskan, M., 2005. Microwave assisted drying of short-cut (ditalini) macaroni : Drying characteristics and effect of drying processes on starch properties 38, 787–796.

Alvarez-Vazquez, H., Jefferson, B., Judd, S.J., 2004. Membrane bioreactors vs conventional biological treatment of landfill leachate: a brief review. Journal of Chemical Technology & Biotechnology 79, 1043–1049.

Al-Wabel, M.I., Al Yehya, W.S., AL-Farraj, A.S., El-Maghraby, S.E., 2011. Characteristics of landfill leachates and bio-solids of municipal solid waste (MSW) in Riyadh City, Saudi Arabia. Journal

of the Saudi Society of Agricultural Sciences 10, 65–70.

Al-Yaqout, a. F., Hamoda, M.F., 2003. Evaluation of landfill leachate in arid climate - A case study. Environment International 29, 593–600.

Al-Yaqout, a. F., Hamoda, M.F., Zafar, M., 2005. Characteristics of Wastes, Leachate, and Gas at Landfills Operated in Arid Climate. Practice Periodical of Hazardous, Toxic, and Radioactive Waste Management 9, 97–102.

Ashebir, D., Jezik, K., Weingartemann, H., Gretzmacher, R., 2009. Change in color and other fruit quality characteristics of tomato cultivars after hot-air drying at low final-moisture content. International Journal of Food Sciences and Nutrition 60, 308–315.

Aziz, S.Q., Aziz, H.A., Yusoff, M.S., Bashir, M.J.K., Umar, M., 2010. Leachate characterization in semi-aerobic and anaerobic sanitary landfills: A comparative study. Journal of Environmental Management 91, 2608–2614.

Baawain, M.S., Al-futaisi, A.M., 2013. Identification of Possible Migration of Contaminants in Groundwater at a Landfill – A Case Study of Oman. Journal of Environment and Earth Science 3, 86–98.

Bae, W., Kwon, Y., 2017. Consolidation settlement properties of seashore landfills for municipal solid wastes in Korea. Marine Georesources & Geotechnology 35, 216–225.

Barth, M., Hankinson, T.R., Zhuang, H., Breidt, F., 2009. Microbiological Spoilage of Fruits and Vegetables. In: Sperber, W.H., Doyle, M.P. (Eds.), Compendium of the Microbiological Spoilage of Foods and Beverages. Springer New York, New York, NY, pp. 135–183.

Basha, B.M., Parakalla, N., Reddy, K.R., 2016. Experimental and statistical evaluation of compressibility of fresh and landfilled municipal solid waste under elevated moisture contents Experimental and statistical evaluation of compressibility of fresh and landfilled municipal solid waste under elevat. International Journal of Geotechnical Engineering 10, 86–98.

Beaven, R.P., 2000. The hydrogeological and geotechnical properties of household waste in relation to sustainable landfilling. University of London.

Beaven, R.P., 2008. Review of responses to a landfill modelling challenge. Proceedings of the Institution of Civil Engineers - Waste and Resource Management 161, 155–166.

Benbelkacem, H.E. of leachate injection modes on municipal solid waste degradation in anaerobic bioreactor, Bayard, R., Abdelhay, A., Zhang, Y., Gourdon, R., 2010. Effect of leachate injection modes on municipal solid waste degradation in anaerobic bioreactor. Bioresource Technology 101, 5206–5212.

Benson, C.H., Barlaz, M. a., Lane, D.T., Rawe, J.M., 2007. Practice review of five bioreactor/recirculation landfills. Waste Management 27, 13–29.

Bilgili, M.S., Demir, A., Varank, G., 2009. Evaluation and modeling of biochemical methane potential (BMP) of landfilled solid waste: A pilot scale study. Bioresource Technology 100, 4976–4980.

Bleiker, D.E., Farquhar, G., McBean, E., 1995. Landfill settlement and the impact on site capacity and refuse hydraulic conductivity. Waste Management and Research 13, 533–554.

Bovi, G.G., Caleb, O.J., Ilte, K., Rauh, C., Mahajan, P. V., 2018. Impact of modified atmosphere and humidity packaging on the quality, off-odour development and volatiles of “Elsanta” strawberries. Food Packaging and Shelf Life 16, 204–210.

Britz, T.J., Van Der Merwe, M., Riedel, K.-H.J., 1992. Influence of phenol additions on the efficiency of an anaerobic hybrid digester treating landfill leachate. Biotechnology Letters 19, 323–328.

Britz, T.J., Venter, C. a., Tracey, R.P., 1990. Anaerobic treatment of municipal landfill leachate using an anaerobic hybrid digester. Biological Wastes 32, 181–191.

BS 1377-2:1990, n.d. Methods of test for Soils for civil engineering purposes - Part 2: Classification tests.

BS 1377-6: 1990, n.d. Methods of test for Soils for civil engineering purposes— Part 6: Consolidation and permeability tests in hydraulic cells and with pore pressure measurement.

Burnley, S.J., 2007. A review of municipal solid waste composition in the United Kingdom. Waste Management 27, 1274–1285.

Cesaro, A., Russo, L., Farina, A., Belgiorno, V., 2016. Organic fraction of municipal solid waste from mechanical selection: biological stabilization and recovery options. Environmental Science and Pollution Research 23, 1565–1575.

Chandra, D., Lee, J.-S., Choi, H.J., Kim, J.G., 2018. Effects of Packaging on Shelf Life and Postharvest

Qualities of Radish Roots during Storage at Low Temperature for an Extended Period. Journal of Food Quality 2018, 1–12.

Chen, R.H., Chen, K.S., Liu, C.N., 2010. Study of the mechanical compression behavior of municipal solid waste by temperature-controlled compression tests. Environmental Earth Sciences 61, 1677–1690.

Chiemchaisri, C., Chiemchaisri, W., Nonthapund, N., Sittichoktam, S., 2002. Acceleration of Solid Waste Biodegradation in Tropical Landfill Using Bioreactor Landfill Concept. In: 5th Asian Symposium on Academic Activities for Waste Management. p. 10.

Chu, L.M., Cheung, K.C., Wong, M.H., 1994. Variations in the chemical properties of landfill leachate. Environmental Management 18, 105–117.

Council Directive 1999/31/EC of 26 April 1999 on the landfill of waste, 1999. . Official Journal of the European Communities.

D'Aquino, S., Mistriotis, A., Briassoulis, D., Di Lorenzo, M.L., Malinconico, M., Palma, A., 2016. Influence of modified atmosphere packaging on postharvest quality of cherry tomatoes held at 20 °C. Postharvest Biology and Technology 115, 103–112.

Datta, A.K., 2006. Hydraulic Permeability of Food Tissues. International Journal of Food Properties 9, 767–780.

Deepanraj, B., Sivasubramanian, V., Jayaraj, S., 2017. Multi-response optimization of process parameters in biogas production from food waste using Taguchi – Grey relational analysis. Energy Conversion and Management 141, 429–438.

deMan, J.M., Finley, J.W., Hurst, W.J., Lee, C.Y., 2018. Principles of Food Chemistry, Fourth Edi. ed, Food Science Text Series. Springer International Publishing, Cham.

Devine, C., Wells, R., Lowe, T., Waller, J., 2014. Pre-rigor temperature and the relationship between lamb tenderisation, free water production, bound water and dry matter. Meat Science 96, 321–326.

Di Bella, G., Di Trapani, D., Mannina, G., Viviani, G., 2012. Modeling of perched leachate zone formation in municipal solid waste landfills. Waste Management 32, 456–462.

Dixon, N., Jones, D.R. V, 2005. Engineering properties of municipal solid waste. Geotextiles and Geomembranes 23, 205–233.

Durmusoglu, E., Sanchez, I.M., Corapcioglu, M.Y., 2006. Permeability and compression characteristics of municipal solid waste samples. Environmental Geology 50, 773–786.

Elagroudy, S., 2013. Predicting Bioreactor Landfill Air Space by Estimating Geotechnical Properties of Waste. Int. J. of Thermal & Environmental Engineering 5, 129–134.

Elagroudy, S. a., Abdel-Razik, M.H., Warith, M. a., Ghobrial, F.H., 2008. Waste settlement in bioreactor landfill models. Waste Management 28, 2366–2374.

Eleazer, W.E., Odle, W.S., Wang, Y.S., Barlaz, M. a., 1997. Biodegradability of municipal solid waste components in laboratory- scale landfills. Environmental Science and Technology 31, 911–917.

El-Fadel, M., Khoury, R., 2000. Modeling settlement in MSW landfills: a critical review 37–41.

El-Fadel, M., Shazbak, S., Saliby, E., Leckie, J., 1999. Comparative assessment of settlement models for municipal solid waste landfill applications. Waste Management & Research 17, 347–368.

Erses, a. S., Onay, T.T., Yenigun, O., 2008. Comparison of aerobic and anaerobic degradation of municipal solid waste in bioreactor landfills. Bioresource Technology 99, 5418–5426.

Fagundes, C., Moraes, K., Pérez-Gago, M.B., Palou, L., Maraschin, M., Monteiro, A.R., 2015. Effect of active modified atmosphere and cold storage on the postharvest quality of cherry tomatoes. Postharvest Biology and Technology 109, 73–81.

Feng, G.J., 2013. Research on the Properties of Municipal Solid Waste of Chongqing. Applied Mechanics and Materials 295-298, 1816–1819.

Feng, S., Gao, K., Chen, Y., Li, Y., Zhang, L.M., Chen, H.X., 2016. Geotechnical properties of municipal solid waste at Laogang Landfill , China. Waste Management.

Feng, S.-J., Gao, K.-W., Chen, Y.-X., Li, Y., Zhang, L.M., Chen, H.X., 2017. Geotechnical properties of municipal solid waste at Laogang Landfill, China. Waste Management 63, 354–365.

Forster-Carneiro, T., Pérez, M., Romero, L.I., 2008. Influence of total solid and inoculum contents on performance of anaerobic reactors treating food waste. Bioresource Technology 99, 6994–

7002.

Fourie, a. B., Blight, G.E., 1999. Leachate generation in landfills in semi-arid climates. Proceedings of the ICE - Geotechnical Engineering 137, 181–188.

Gao, W., Chen, Y., Zhan, L., Bian, X., 2015. Journal of Rock Mechanics and Geotechnical Engineering Engineering properties for high kitchen waste content municipal solid waste. Journal of Rock Mechanics and Geotechnical Engineering 7, 646–658.

Gavelyte, S., Baziene, K., Woodman, N., Stringfellow, A., 2015. Permeability of different size waste particles. MOKSLAS LIETUVOS ATEITIS SCIENCE 7, 407–412.

Gavelyte, S., Dace, E., Baziene, K., 2016. The Effect of Particle size Distribution on Hydraulic Permeability in a Waste Mass. Energy Procedia 95, 140–144.

Gawande, N. a., Reinhart, D.R., Thomas, P. a., McCreanor, P.T., Townsend, T.G., 2003. Municipal solid waste in situ moisture content measurement using an electrical resistance sensor. Waste Management 23, 667–674.

Gurijala, K.R., Suflita, J.M., 1993. Environmental Factors Influencing Methanogenesis from Refuse in Landfill Samples. Environmental Science & Technology 27, 1176–1181.

Halder, A., Datta, A.K., Spanswick, R.M., 2011. Water transport in cellular tissues during thermal processing. AIChE Journal 57, 2574–2588.

Hammond, S.T., Brown, J.H., Burger, J.R., Flanagan, T.P., Fristoe, T.S., Mercado-Silva, N., Nekola, J.C., Okie, J.G., 2015. Food Spoilage, Storage, and Transport: Implications for a Sustainable Future. BioScience 65, 758–768.

HE Pin-jing, QU Xianl, S Li-ming, L.D., 2006. Landfill leachate treatment in assisted landfill bioreactor. Journal of Environmental Sciences 18, 176–179.

Heshmati R, A.A., Mokhtari, M., Shakiba Rad, S., 2014. Prediction of the compression ratio for municipal solid waste using decision tree. Waste Management & Research 32, 64–69.

Hii, C.L., Itam, C.E., Ong, S.P., 2014. Convective Air Drying of Raw and Cooked Chicken Meats. Drying Technology 32, 1304–1309.

Holcroft, D., 2015. Water Relations in Harvested Fresh Produce. The Postharvest Education

Foundation 1–16.

Hoornweg, D., Bhada-Tata, P., 2012. What a waste: a global review of solid waste management.

Hossain, M.S., Gabr, M. a., Barlaz, M. a., 2003. Relationship of Compressibility Parameters to Municipal Solid Waste Decomposition. Journal of Geotechnical and Geoenvironmental Engineering 129, 1151–1158.

Hossain, M.S., Penmethsa, K.K., Hoyos, L., 2009. Permeability of municipal solid waste in bioreactor landfill with degradation. Geotechnical and Geological Engineering 27, 43–51.

Hoy, M.K.& C., 2014. High Commission For the Development of Arriyadh Comprehensive Waste Management Strategy for Arriyadh City Municipal Solid Waste Composition Analysis : Final Report.

Hudson, A.P., 2007. Evaluation of the vertical and horizontal hydraulic conductivities of household wastes. University of Southampton.

Hudson, A.P., White, J.K., Beaven, R.P., Powrie, W., 2004. Modelling the compression behaviour of landfilled domestic waste. Waste Management 24, 259–269.

Indraratna, B., Chu, J., Rujikiatkamjorn, C., 2015. Ground Improvement Case Histories. Butterworth-Heinemann.

Ivanova, L.K., 2007. Quantification of Factors Affecting Rate and Magnitude of Secondary Settlement of Landfills, PhD Thesis. University of Southampton.

Ivanova, L.K., 2007. Quantification of Factors Affecting Rate and Magnitude of Secondary Settlement of Landfills, PhD Thesis, University of Southampton.

Jingura, R.M., Kamusoko, R., 2017. Methods for determination of biomethane potential of feedstocks: a review. Biofuel Research Journal 4, 573–586.

Joardder, M.U.H., Karim, M.A., Kumar, C., 2013. Better Understanding of Food Material on the Basis of Water Distribution Using Thermogravimetric Analysis. In: International Conference on Mechanical, Industrial and Materials Engineering. Rajshahi, Bangladesh, pp. 1–3.

Joardder, M.U.H., Kumar, C., Karim, M. a., 2017. Food structure: Its formation and relationships with other properties. Critical Reviews in Food Science and Nutrition 57, 1190–1205.

Karak, T., Bhagat, R.M., Bhattacharyya, P., 2012. Municipal Solid Waste Generation, Composition, and Management: The World Scenario. Critical Reviews in Environmental Science and Technology 42, 1509–1630.

Khan, M.I.., Wellard, M., Pham, N.D., Karim, M.A., 2016. INVESTIGATION OF CELLULAR LEVEL WATER IN PLANT-BASED FOOD MATERIAL. In: The 20th International Drying Symposium (IDS 2016) Gifu, JAPAN, 7-10 August 2016. pp. 7–10.

Khan, M.I.H., Joardder, M.U.H., Kumar, C., Karim, M.A., 2018. Multiphase porous media modelling: A novel approach to predicting food processing performance. Critical Reviews in Food Science and Nutrition 58, 528–546.

Khan, M.I.H., Karim, M.A., 2017. Cellular water distribution, transport, and its investigation methods for plant-based food material. Food Research International 99, 1–14.

Khan, M.I.H., Wellard, R.M., Nagy, S.A., Joardder, M.U.H., Karim, M.A., 2016. Investigation of bound and free water in plant-based food material using NMR T2 relaxometry. Innovative Food Science & Emerging Technologies 38, 252–261.

Kjeldsen, P., Barlaz, M. a., Rooker, A.P., Baun, A., Ledin, A., Christensen, T.H., 2002a. Present and Long-Term Composition of MSW Landfill Leachate: A Review. Critical Reviews in Environmental Science and Technology 32, 297–336.

Kjeldsen, P., Barlaz, M. a., Rooker, A.P., Baun, A., Ledin, A., Christensen, T.H., 2002b. Landfill leachate treatment: Review and opportunity. Critical Reviews in Environmental Science and Technology.

Kumar, C., Karim, A., Joardder, M.U.H., Miller, G.J., 2012. Modeling Heat and Mass Transfer Process during Convection Drying of Fruit. The 4th international conference on computational methods, Gold Coast, Australia. 9.

Landva, a O., Valsangkar, a J., Pelkey, S.G., 2000. Lateral earth pressure at rest and compressibility of municipal solid waste. Canadian Geotechnical Journal 37, 1157–1165.

Landva, A., Clark, G., 1990. Geotechnics of Waste Fills-Theory and Practice. ASTM Internationa.

Liu, L., Xue, Q., Wan, Y., Tian, Y., 2015. Evaluation of Dual Permeability of Gas Flow in Municipal Solid Waste: Experiment and Modeling. Environmental Progress & Sustainable Energy 35, 41–

47.

Machado, S.L., Carvalho, M.F., Vilar, O.M., 2002. Constitutive Model for Municipal Solid Waste. Journal of Geotechnical and Geoenvironmental Engineering 128, 940–951.

Machado, S.L., Carvalho, M.F., Vilar, O.M., 2002. Constitutive Model for Municipal Solid Waste 128, 940–951.

Machado, S.L., Karimpour-Fard, M., Shariatmadari, N., Carvalho, M.F., Nascimento, J.C.F. do, 2010. Evaluation of the geotechnical properties of MSW in two Brazilian landfills. Waste Management 30, 2579–2591.

Machado, S.L., Vilar, O.M., Carvalho, M.F., 2008. Constitutive model for long term municipal solid waste mechanical behavior. Computers and Geotechnics 35, 775–790.

Mehta, R., Barlaz, M. a., Yazdani, R., Augenstein, D., Bryars, M., Sinderson, L., 2002. Refuse Decomposition in the Presence and Absence of Leachate Recirculation. Journal of Environmental Engineering 128, 228–236.

Morris, D.V. and Woods, C.., 1990. Settlement and Engineering Considerations in Lanfill Cover Design. Geotechnics of Waste Fills-Theory and Practice. ASTM STP 1070, Philadelphia, Pennsylvania, USA.

Nadu, T., Nadu, T., 2017. Operational Conditions of Anaerobic Digestion and their Optimization for Enhanced Biogas Production – A Review. International Journal of Scientific and Research Publications 7, 49–54.

Nakhaei, M., Amiri, V., Rezaei, K., Moosaei, F., 2014. An investigation of the potential environmental contamination from the leachate of the Rasht waste disposal site in Iran. Bulletin of Engineering Geology and the Environment 74, 233–246.

Nas, S.S., Nas, E., 2014. Assessing the Impacts of Seasonal Variations on Predicting Leachate Generation in Gumushane Open Dump Using Water Balance Method. Polish Journal of Environmental Studies 23, 1659–1668.

Nunes, C., Emond, J., 2007. Relationship between weight loss and visual quality of fruits and vegetables. Proceedings of the Florida State Horticultural Society 120, 235–245.

Ojuri, O.O., 2012. Permeability and Compressibility Characteristics of Municipal Solid Waste Samples Using a Fabricated Intermediate Scale Oedometer 17, 2713–2720.

Olivier, F., Gourc, J.P., 2007. Hydro-mechanical behavior of Municipal Solid Waste subject to leachate recirculation in a large-scale compression reactor cell. Waste Management 27, 44–58.

Ouda, O.K.M., Engineering, C., Mohamed, P., 2013. POTENTIAL VALUE OF WASTE-TO-ENERGY FACILITY IN RIYADH CITY - SAUDI ARABIA. POTENTIAL VALUE OF WASTE-TO-ENERGY FACILITY IN RIYADH CITY - SAUDI ARABIA BY Rafat Al-Waked ,Omar K. M. Ouda, AND Syed A. Raza.

Pandey, R.R., Tiwari, R.P., 2015. Physical Characterization and Geotechnical Properties of Municipal Solid Waste. IOSR Journal of Mechanical and Civil Engineering (IOSR-JMCE) 12, 15–21.

Park, H.I., Lee, S.R., 2002. Long-term settlement behaviour of MSW landfills with various fill ages. Waste Management and Research 20, 259–268.

Piwińska, M., Wyrwisz, J., Kurek, M., Wierzbicka, A., 2015. Hydration and physical properties of vacuum-dried durum wheat semolina pasta with high-fiber oat powder. LWT - Food Science and Technology 63, 647–653.

Powrie, W., Beaven, R.P., 1999. Hydraulic properties of household waste and implications for landfills. Proceedings of the ICE - Geotechnical Engineering 137, 235–247.

Powrie, W., Beaven, R.P., Hudson, A.P., 2005. Factors affecting the hydraulic conductivity of waste, In: International Workshop “Hydro-physico-mechanics of landfills.” France.

Prothon, F., Ahrné, L., Sjöholm, I., 2003. Mechanisms and Prevention of Plant Tissue Collapse during Dehydration : A Critical Review. Critical Review in Food Science and Nutrition 43, 447–479.

R. Campuzano, S.G.-M., 2016. Characteristics of the organic fraction of municipal solid waste and methane production: A review. Waste Management 54, 3–12.

Rahman, S.M., 2007. Food preservation, Second edi. ed. Taylor & Francis, Boca Rotan, London, New York.

Raponi, F., Moscetti, R., Monarca, D., Colantoni, A., Massantini, R., 2017. Monitoring and Optimization of the Process of Drying Fruits and Vegetables Using Computer Vision: A Review.

Sustainability 9, 1–27.

Rastogi, M., Hooda, R., Nandal, M., 2014. Review on Anaerobic Treatment of Municipal Solid Waste With Leachate Recirculation. International Journal of Plant, Animal and Environmental Sciences 4, 110–117.

Rawat, S., 2015. Food Spoilage : Microorganisms and their prevention. Asian journal of plant ascience and research 5, 47–56.

Reddy, K.R., Hettiarachchi, H., Gangathulasi, J., Bogner, J.E., 2011. Geotechnical properties of municipal solid waste at different phases of biodegradation. Waste Management 31, 2275–2286.

Reddy, K.R., Hettiarachchi, H., Parakalla, N., Gangathulasi, J., Bogner, J., Lagier, T., 2009a. Hydraulic Conductivity of MSW in Landfills. Journal of Environmental Engineering 135, 677–683.

Reddy, K.R., Hettiarachchi, H., Parakalla, N.S., Gangathulasi, J., Bogner, J.E., 2009b. Geotechnical properties of fresh municipal solid waste at Orchard Hills Landfill, USA. Waste Management 29, 952–959.

Rickman, J.C., Barrett, D.M., Bruhn, C.M., 2007. Nutritional comparison of fresh, frozen and canned fruits and vegetables. Part 1. Vitamins C and B and phenolic compounds. Journal of the Science of Food and Agriculture 87, 930–944.

Robinson, H.D., Grantham, G., 1988. THE T R E A T M E N T OF L A N D F I L L LEACHATES IN ON-SITE AERATED LAGOON PLANTS : EXPERIENCE IN BRITAIN AND I R E L A N D. Water Research 22, 733–747.

Safari, E., Ghazizade, M.J., Shokouh, a, Nabi Bidhendi, G.R., 2011. Anaerobic removal of COD from high strength fresh and partially stabilized leachates and application of multi stage kinetic model. International Journal of Environmental Research 5, 255–270.

Sang, N.N., Soda, S., Ishigaki, T., Ike, M., 2012. Microorganisms in landfill bioreactors for accelerated stabilization of solid wastes. Journal of Bioscience and Bioengineering 114, 243–250.

Sanphoti, N., Towprayoon, S., Chaiprasert, P., Nopharatana, a., 2006. The effects of leachate recirculation with supplemental water addition on methane production and waste decomposition in a simulated tropical landfill. Journal of Environmental Management 81, 27–

35.

Siddiqui, a. a., Richards, D.J., Powrie, W., 2012. Investigations into the landfill behaviour of pretreated wastes. Waste Management 32, 1420–1426.

Siddiqui, A.A., 2011. Biodegradation and Settlement Behaviour of Mechanically Biologically Treated (MBT) Waste. Thesis for the degree of Doctor of Philosophy. UNIVERSITY OF SOUTHAMPTON FACULTY.

Srikiatden, J., Roberts, J.S., 2007. Moisture Transfer in Solid Food Materials: A Review of Mechanisms, Models, and Measurements. International Journal of Food Properties 10, 739–777.

Staub, M., Galietti, B., Oxarango, L., Khire, M. V, Gourc, J.-P., 2009a. Porosity and Hydraulic Conductivity of MSW Using Laboratory-Scale Tests. The International Workshop "Hydro-Physico-Mechanics of Landfills" 1–9.

Staub, M., Galietti, B., Oxarango, L., Khire, M. V, Gourc, J.-P., 2009b. Porosity and Hydraulic Conductivity of MSW Using Laboratory-Scale Tests, The International Workshop "Hydro-Physico-Mechanics of Landfills."

Stoltz, G., Gourc, J.P., Oxarango, L., 2010. Liquid and gas permeabilities of unsaturated municipal solid waste under compression. Journal of Contaminant Hydrology 118, 27–42.

Sutthasil, N., Chiemchaisri, C., Chiemchaisri, W., Wangyao, K., 2014. Comparison of Solid Waste Stabilization and Methane Emission from Anaerobic and Semi-Aerobic Landfills Operated in Tropical Condition. Environmental Engineering research 19, 261–268.

Swati, M., Joseph, K., 2008. Settlement analysis of fresh and partially stabilised municipal solid waste in simulated controlled dumps and bioreactor landfills. Waste Management 28, 1355–1363.

Tchobanoglous, G., Theisen, H., Vigil, S., 1993. Integrated solid waste management: engineering principles and management issues., 2, illustr. ed. McGraw-Hill, New York.

Thompson, F., James, F., Mitchell, G., RumsayR, 2008. Commercial cooling of fruits, vegetables, and flowers. University of California, Agriculture and Natural Resources, Oakland.

Tiwari, D., 2014. Estimation of Optimum Compaction Level for Bioreactor Landfill Operation. THE UNIVERSITY OF TEXAS AT ARLINGTON.

Valentinuzzi, F., Pii, Y., Mimmo, T., Savini, G., Curzel, S., Cesco, S., 2018. Fertilization strategies as a tool to modify the organoleptic properties of raspberry (Rubus idaeus L.) fruits. Scientia Horticulturae 240, 205–212.

Warith, M., Li, X., Jin, H., 2005. Bioreactor Landfills : State-of-the-Art Review. Emirates Journal for Engineering Research 10, 1–14.

White, J., Robinson, J., Ren, Q., 2004. Modelling the biochemical degradation of solid waste in landfills. Waste Management 24, 227–240.

White, J.K., 2008. The application of LDAT to the HPM2 challenge. Proceedings of the ICE - Waste and Resource Management 161, 137–146.

White, J.K., Beaven, R.P., 2013. Developments to a landfill processes model following its application to two landfill modelling challenges. Waste Management 33, 1969–1981.

White, J.K., Nayagum, D., Beaven, R.P., 2014. A multi-component two-phase flow algorithm for use in landfill processes modelling. Waste Management 34, 1644–1656.

Woodman, N.D., Rees-White, T.C., Stringfellow, a. M., Beaven, R.P., Hudson, a. P., 2014. Investigating the effect of compression on solute transport through degrading municipal solid waste. Waste Management 34, 2196–2208.

Yesiller, N., Hanson, J.L., Cox, J.T., Noce, D.E., 2014. Determination of specific gravity of municipal solid waste. Waste Management 34, 848–858.

Yigit, S., Akgul, D., Demir, G., Mertoglu, B., 2012. Solidification/stabilization of landfill leachate concentrate using different aggregate materials. Waste Management 32, 1394–1400.

Zanetti, M.C., 2008. Aerobic Biostabilization of Old MSW Landfills. American Journal of Engineering and Applied Sciences 1, 393–398.

Zeiss, D.K.W. and C., 1995. Municipal Landfill Biodegradation 121, 214–224.

Zeng, G., Liu, L., Xue, Q., Wan, Y., Ma, J., Zhao, Y., 2017. Experimental study of the porosity and permeability of municipal solid waste. Environmental Progress & Sustainable Energy 36,

1694–1699.

Zhang, C., Feng, J., Zhao, T., Rong, L., 2017. Physical, Chemical, and Engineering Properties of Landfill Stabilized Waste. Landfill Degradation & Development 28, 1113–1121.

Zhao, Y., Yang, C., Liu, L., 2012. Experimental Study on the Effect of Organic Content on the Compression Properties of Municipal Solid Waste. Electronic Journal of Geotechnical Engineering 17, 2335–2342.

Zhao, Y.R., Liu, T.J., Chen, X.S., Xie, Q., Huang, L.P., 2016. The effect of temperature on the biodegradation properties of municipal solid waste. Waste Management & Research 34, 265–274.

Ziyang, L., Luochun, W., Nanwen, Z., Youcai, Z., 2015. Martial recycling from renewable landfill and associated risks: A review. Chemosphere 131, 91–103.